8-2013

Scale-dependent heterogeneity in fracture data sets and grayscale images

Ankur Roy
aroy1@utk.edu

To the Graduate Council:

I am submitting herewith a dissertation written by Ankur Roy entitled "Scale-dependent heterogeneity in fracture data sets and grayscale images." I have examined the final electronic copy of this dissertation for form and content and recommend that it be accepted in partial fulfillment of the requirements for the degree of Doctor of Philosophy, with a major in Geology.

Edmund Perfect, Major Professor

We have read this dissertation and recommend its acceptance:

William M. Dunne; Larry D. McKay; John S. Tyner

Accepted for the Council:

Carolyn R. Hodges

Vice Provost and Dean of the Graduate School

(Original signatures are on file with official student records.)

SCALE-DEPENDENT HETEROGENEITY IN FRACTURE DATA SETS AND GRAYSCALE IMAGES

A Dissertation Presented for the
Doctor of Philosophy
Degree

THE UNIVERSITY OF TENNESSEE, KNOXVILLE

Ankur Roy
August 2013

ACKNOWLEDGEMENTS

There are several people without whose inspiration, help and support this dissertation would have been impossible. I would like to begin by mentioning the name of Sakshi Gopal Saha, scientist at Indian Jute Industries' Research Association, India, who for the very first time introduced me to the wonderful world of science and mathematics during my high school years. Prof. Gouri Sankar Ghatak, former Head of the Department of Geology, Presidency College, India (presently known as Presidency University) and Dr. Amitabha Chakrabarti, former Head of the Department of Geology and Geophysics, Indian Institute of Technology, Kharagpur, India are those two most prominent people in my life who inspired me to build a career in scientific research. However, had it not been for my MS and PhD advisor Dr. Edmund Perfect, I'd have largely remained ignorant about fractals and the usefulness of mathematical principals for solving problems in geology. I do hereby also express my gratitude to my committee members Dr. Bill Dunne, Dr. Larry McKay and Dr. John Tyner for spending their time and providing ample guidance during the course of my PhD research. I'd also like to thank my research collaborator Dr. Noelle Odling at the University of Leeds, UK and my friend Dr. Leonel Gomez who have provided me with data that have been used in this dissertation. Finally, this statement would remain incomplete if I do not mention my very good friend Mr. Avik Mukherjee and my wife Mrs. Pubali Roy without whose untiring help and support I would not have sailed through all the ups and downs of my life and career over the past four years.

ABSTRACT

Lacunarity is a technique developed for multiscale analysis of spatial data and can quantify scale-dependent heterogeneity in a dataset. The present research is based on characterizing fracture data of various types by invoking lacunarity as a concept that can not only be applied to both fractal and non-fractal binary data but can also be extended to analyzing non-binary data sets comprising a spectrum of values between 0 and 1. Lacunarity has been variously modified in characterizing fracture data from *maps* and *scanlines* in tackling five different problems. In Chapter 2, it is shown that normalized lacunarity curves can differentiate between maps (2-dimensional binary data) belonging to the same fractal-fracture system and that clustering increases with decreasing spatial scale. Chapter 4 analyzes spacing data from scanlines (1-dimensional binary data) and employs log-transformed lacunarity curves along with their 1st derivatives in identifying the presence of fracture clusters and their spatial organization. This technique is extended to 1-dimensional non-binary data in chapter 5 where spacing is integrated with aperture values and a lacunarity ratio is invoked in addressing the question of whether large fractures occur within clusters. Finally, it is investigated in chapter 6 if lacunarity can find differences in clustering along various directions of a fracture network thus identifying differentially-clustered fracture sets. In addition to fracture data, chapter 3 employs lacunarity in identifying clustering and multifractal behavior in synthetic and natural 2-dimensional non-binary patterns in the form of soil thin sections. Future avenues for research include estimation of 2-dimensional clustering from 1-dimensional samples (e.g., scanlines and well-data), forward modeling of fracture networks using lacunarity, and the possible application of lacunarity in delineating shapes of other geologic patterns such as channel beds.

TABLE OF CONTENTS

Chapters **Page**

LIST OF TABLES

LIST OF FIGURES

Introduction
&
General Information

Chapter I

Ankur Roy

Fractures are developed by brittle failure and are defined as discrete breaks within a rock mass across which cohesion is lost. They have important impact on rock strength and the flow properties of aquifers and reservoirs. Not surprisingly, there have been numerous studies on the scaling properties of fracture data from well-bores, scanlines and maps. Such research is key to understanding fracture geometry and serves as a preliminary step towards stochastic modeling. Characterization techniques have ranged from geostatistical analyses (LaPointe and Hudson, 1985; Chiles, 1988) and other standard statistical approaches like finding cumulative frequencies of fracture length (deJossineau and Aydin, 2007) and aperture (Marrett at al., 1999) to fractal descriptors (Berkowitz and Hadad, 1997; Roy et al., 2007).

Since the heterogeneity of fractures exists over a wide range of scales, from microns (in thin sections) to hundreds of kilometers (as in transform faults), fractal modeling has become a popular tool in studying fracture patterns (Bonnet et al., 2001; Roy et al., 2007; Kruhl, 2013). These models however, can be applied for characterizing self-similar behavior only in binary patterns i.e. patterns that are made up of only two values (0 and 1). While this isn't a problem for fracture networks or scanline data with spacing values, it may be limited in its application to say, fracture intensity maps and scanline data that record fracture aperture and/or length along with spacing values. Multifractal analysis is a more general tool that may be applied for quantifying scale-independent behavior in non-binary patterns that comprise a spectrum of values between zero and one. This technique has been applied to fractures by Belfield (1994), Chen (1999), and Cowie et al. (1995). However, these approaches are applicable only to a limited number of fracture data sets that are strictly fractal or multifractal.

Lacunarity as a concept was initially developed for studying clustering in fractal patterns (Mandelbrot, 1983). This approach is based on a multi-scale analysis of spatial dispersion (Plotnick, 1996) and can quantify scale-dependent heterogeneity in a dataset. In simple terms, lacunarity characterizes the distribution of spaces or gaps in a pattern as a function of scale. The biggest advantage of this technique is that not only is it applicable to both fractal and non-fractal binary data alike but can also be extended to analyze multifractals and other non-binary datasets. This dissertation is an attempt to capture the

scale-dependent heterogeneity of fracture data in the form of networks (2-dimensional binary data), scanline spacing values (1-dimensional binary data) and scanline aperture values along with spacing (1-dimensional non-binary). Chapter 3 is slightly different from the rest of this dissertation in that it essentially deals with 2-dimensional non-binary synthetic data and briefly attempts to identify multifractal behavior in soil thin-sections using lacunarity.

A concept takes root if the user is able to customize it to the ever changing needs of his projects (Journel, 1989). Therefore, in an endeavor to best capture the essence of lacunarity as a concept it has been variously "customized" in the different chapters of this dissertation each of which addresses a separate problem. Chapter 2 is modified from Roy et al. (2010) and deals with the clustering of fractures in 2-dimensional networks. Since lacunarity values are influenced by the overall fracture intensity of a network, a normalization scheme for the lacunarity parameter was devised to remove this effect. It was proved that not only fracture networks with same fractal dimension have different clustering but also, at larger scales fractures tend to become less clustered. Chapter 3 is modified from a manuscript in review that empirically tests the theory of Allain and Cloitre (1991) on the relationship between lacunarity and correlation dimension in multifractals. It demonstrates how lacunarity can be employed to identify the multifractal nature of grayscale patterns. For this purpose, lacunarity values were log-transformed and plotted against the log-transformed scale values.

Chapters 4 through 6 deal with lacunarity analyses of 1-dimensional scanline data. Chapter 4 builds on the concept that distinct breaks in the slope of lacunarity curves in log-log space correspond to distinct scales within a pattern (Plotnick et al., 1996). In order to better identify these "breaks" the 1st derivative of the lacunarity curves was plotted against the scale. It was demonstrated that such plots can pick up "patterns within patterns" in that they could identify both the inter-cluster distance and the organization of fractures within the clusters. Chapter 5 is based on devising a test that finds if large fractures statistically occur within clusters, or if they are mostly found within the inter-cluster regions. For this purpose, the ratio of lacunarity of a dataset to the lacunarity of its random counterpart was plotted against the scale. Chapter 6 focusses on the anisotropy of fracture clustering and

thus has a directional aspect to it. It simply analyzes scanlines that are taken at different orientations from a fracture network. In order to offset the differences in length and fracture intensity (number of fractures per unit length) of the scanline samples, the scale was normalized. Finally, for finding a single clustering parameter at each orientation, a weighted mean of the log-transformed lacunarity values was calculated, the weights being determined by the log-transformed normalized scale.

REFERENCES

Allain, C. and Cloitre, M., 1991, Characterizing the lacunarity of random and deterministic fractal sets, *Phys. Rev. A.* vol. 44, no. 6, 3552-3558

Belfield, W.C., 1994, Multifractal characteristics of natural fracture apertures, *Geophysical Research Letters,* vol. 21, no. 24, 2641-2644

Belfield, W.C., 1998, Incorporating spatial distribution into stochastic modeling of fractures: multifractals and Levy-stable statistics, *Journal of Structural Geology,* vol. 20, no. 4, 473-486

Berkowitz B., Hadad, A., 1997, Fractal and multifractal measures of natural and synthetic fracture networks, *Journal of Geophysical Research,* vol. 102, no. B6, 12,205-12,218.

Bonnet E., Bour, O., Odling, N. E., Davy, P., Main, I., Cowie, P., Berkowitz, B, 2001, Scaling of fracture systems in Geological Media, *Reviews in Geophysics,* vol. 39, no. 3, 347-383.

Chen, Q., 1999, The gliding box method for multifractal modeling, *Computers & Geosciences*, vol. 25, 1073–1079.

Chiles, J.P., 1988, Fractal and geostatistical methods for modeling of a fracture network, *Mathematical Geol*ogy, vol. 20, 631–654.

Cowie, P.A., Sornette, D., Vanneste, C., 1995, Multifractal scaling properties of a growing fault population, *Geophysical J. Int.,*, vol. 122, 457–469.

de Joussineau, G., and Aydin, A., 2007, The evolution of damage zones with fault growth in sandstones and its multifractal characteristics, *Journal of Geophysical Research*, B12401, doi:10.1029/2006JB0045711

Gillespie, P., Johnston, J.D., Loriga, M.A., McCaffrey, K.J., Walsh, J.J. and Watterson, J., 1999, Influence of layering in vein systematics in line samples; in *Fractures, Fluid Flow and Mineralization*

Journel, A. G., 1989, Fundamentals of Geostatistics in Five Lessons, *Short Course Geol. Ser.*, vol. 8, 40 pp., AGU, Washington, D. C., doi:10.1029/SC008

Kruhl, J.H, 2013, Fractal-geometry techniques in the quantification of complex rock structures: A special view on scaling regimes, inhomogeneity and anisotropy, *Journal of Structural Geology*, vol. 46, 2-21

LaPointe, P.R. and Hudson, J.A., 1995, Characterization and interpretation of rock mass joint patterns, *Geological Society of America*, Special Paper 199

Mandelbrot, B.B., 1983, *The Fractal Geometry of Nature*, Freeman, New York, NY, 468pp.

Marrett, R., Ortega, O., and Kelsey, C., 1999. Extent of power-law scaling for natural fractures in rock, *Geology* vol. 27, 799-802

Plotnick, R.E., Gardner, R.H., Hargrove, W.W., Prestegaard, K., Perlmutter, M., 1996, Lacunarity analysis: A general technique for the analysis of spatial patterns, *Phys. Rev. E.* vol. 53, no. 5, 5461-5468

Roy, A., Perfect, E., Dunne, W.M., and McKay, L.D., 2007, Fractal characteristics of fracture networks: An improved box-counting technique, *Journal of Geophysical Research*, B12201, doi:10.1029/2006JB004582

Roy, A., Perfect, E., Dunne, W.M., Odling, N. and Kim, J., 2010, Lacunarity analysis of fracture networks: Evidence for scale-dependent clustering, *Journal of Structural Geology*, vol. 32, 1444-1449

Lacunarity Analysis of Fracture Networks: Evidence for Scale-Dependent Clustering

Chapter II: A reformatted version of the paper originally published in Journal of Structural Geology by Roy et al*., 2010

***Ankur Roy, Edmund Perfect, William M. Dunne, Noelle E. Odling & Jung-Woo Kim**

Ankur Roy contributed by performing data analysis and writing the paper. He also helped in developing some of the concepts and model building. Others contributed by revising the manuscript, providing data & help with coding

ABSTRACT

Previous studies on fracture networks have shown that fractures contained within distinct mechanical units ("stratabound") are regularly spaced while those that terminate within the rock mass are clustered ("non-stratabound"). Lacunarity is a parameter which can quantify the distribution of spaces between rock fractures. When normalized to account for differences in fracture abundance, lacunarity characterizes the distribution of spaces as the degree of clustering in the fracture network. Normalized lacunarity curves, $L^*(r)$, computed using the gliding-box algorithm and plotted as a function of box-size, r, were constructed for natural fracture patterns from Telpyn Point, Wales and the Hornelen Basin, Norway. The results from analysis of the Telpyn Point fractures indicate that such curves are sensitive to differences in the clustering of different fracture sets at the same scale. For fracture networks mapped at different scales from the Hornelen basin, our analysis shows that clustering increases with decreasing spatial scale. This trend is attributed to the transition from a "stratabound" system at the scale of sedimentary cycles (100-200m) that act as distinct mechanical units to a "non-stratabound" fracture system geometry at the finer 10's of meters thick bedding scale.

1. INTRODUCTION

Fractures control or influence important behaviors in geological systems such as fluid storage, contaminant transport, seismicity, and rock strength. In the context of joints, a key attribute that influences these characteristics is the geometry of the fracture network. To better understand joint geometry it is necessary to consider fractures from the perspective of mechanical stratigraphy. Joints in sedimentary rocks fall in two categories, those that terminate randomly within the rock mass and those that terminate at distinct mechanical layer boundaries (Gross et al., 1995). Lithologic contacts, as well as pre-existing fractures, can serve as mechanical layer boundaries, thereby dividing the rock mass into discreet mechanical units (Gross, 1993). For our study, only lithologic contacts are considered as mechanical layer boundaries. Fractures that that terminate at lithologic contacts are termed as "stratabound" while the ones that randomly terminate within the rock mass are "non-stratabound" (Odling et al., 1999; Gillespie et al., 1999). The former often display a log-normal distribution for length (Narr and Suppe, 1991) or other non-power law type distribution and appear to be regularly spaced as seen in the siliceous layers of the Monterey Formation (Gross et al., 1995). The "non-stratabound" fractures, however, have a wide range of length distribution (e.g. joint patterns at the Oliana anticline, Schakleton et al., 2005), sometimes yielding a power-law, and are typically clustered (Odling et al., 1999; Gillespie et al., 1999).

Interface strength and the contrast between the rheology of layers control the ability of joints to propagate through lithologic contacts. Analog and numerical experiments suggest that weak interfaces inhibit joint propagation by sliding or opening, and similarly cracks terminate at contacts with soft and ductile layers (Schakleton et al., 2005 and references therein). In this case, the joints developed are "stratabound" and their spacing is proportional to the bed thickness (Narr and Suppe, 1991; Wu and Pollard, 1995 and references therein; Gross et al., 1995; Gillespie et al., 1999; Odling et al., 1999; Cooke et al., 2006). The driving condition for such joint formation is the result of either remote extension or possibly thermal relaxation (Hobbs, 1967; Engelder & Fischer, 1996; Bai & Pollard, 2000). In contrast, for stratabound joints the driving condition for fracture

formation relates to fluid pressure (Gillespie et al., 1999; Odling et al., 1999, Engelder and Fischer, 1996).

Joint spacing distributions can be measured from 1D scanlines (LaPointe & Hudson, 1985). Semi-variograms constructed from such measurements have been independently employed by LaPointe and Hudson (1985) and Chiles (1988) for quantifying the spatial heterogeneity of fracture networks. The ratio of the standard deviation to the mean of the spaces along a scanline has also been used by Gillespie et al. (1999) to discern between clustered and anticlustered veins. Given that rock properties can vary with direction, if possible it is more useful, although certainly more time consuming, to characterize joint spacing distribution in two dimensions using an area or map approach (Wu & Pollard, 1995; Rohrbaugh et al., 2002). In this paper, we present a technique modified from Plotnick et al. (1996) for analyzing clustering of joint populations in a 2-dimensional representation.

To quantify the clustering of fractures, we use the concept of lacunarity (Mandelbrot, 1983). This approach is based on a multiscale analysis of spatial or temporal dispersion (Plotnick et al., 1996). Stated simply, lacunarity characterizes the distribution of spaces or gaps in a pattern as a function of scale. For a fracture pattern, therefore, it can be employed to quantify the degree of fracture clustering at a given spatial resolution. To implement lacunarity as a tool for our purpose, we have introduced a new normalization of this parameter. It is distinct from that of Plotnick et al. (1996) and completely removes the effect of fracture abundance on the lacunarity values. We use a set of three maps from Wales, U.K (Rohrbaugh et al., 2002) to demonstrate the usefulness of our normalized lacunarity measure over that proposed by Plotnick et al. (1996) and show its effectiveness in discerning between different sets of fractures within the same network. We then use normalized lacunarity to analyze a set of four maps from the Devonian sandstones of Hornelen basin, Norway (Odling, 1997) to investigate clustering of fractures at different scales. Finally, we interpret our observations from this sedimentary package in terms of mechanical stratigraphy as a function of scale.

2. LACUNARITY AND ITS QUANTIFICATION

A useful conceptual perspective for understanding lacunarity is to evoke the idea of translational invariance. Consider a uniform sequence of alternating 0's and 1's like 101010101... and so on. This sequence will map onto itself if a copy is made and moved over by two digits so that the original cannot be distinguished from the translated copy. This property is called translational invariance. In terms of lacunarity, a translationally-invariant pattern exhibits no clustering, because all of the gap sizes (denoted by zeroes in our example) are the same. This behavior is not observed in the case of a slightly more heterogeneous sequence, such as 101000101... where the gaps have a range of sizes, including a cluster of three gaps in the middle. The greater the degree of gap clustering, the greater the lacunarity. Lacunarity is a scale dependent parameter because sets that are uniform at a coarse scale might be heterogeneous at a finer scale, and vice-versa. Lacunarity can thus be considered a scale-dependent measure of textural heterogeneity (Allan and Cloitre, 1991; Plotnick et al., 1993).

Quantifying lacunarity as a function of scale can be achieved by using the gliding-box algorithm (Allan and Cloitre, 1991; Plotnick et al., 1996). This algorithm slides a window or box of a given length, r, translated in increments of a chosen unit length across the pattern. In the case of all our analyses, this unit length is chosen to be at the pixel scale (size of the smallest dot that can be drawn on a computer screen). The box-size, r, is generally a multiple of this assigned unit length. The interrogator box searches for occupied sites in the pattern at each step and counts them as $s(r)$. The total number of steps, $N(r)$, required to cover the entire pattern is given by:

$$N(r) = (r_t - r + 1)^E \quad \text{(1)}$$

Here, E is the Euclidean dimension of the pattern (for fracture maps, $E = 2$) and r_t is the total length of the set. The first and second moments of the distribution of the number of occupied sites at each step, $Z_1(r)$, and $Z_2(r)$ respectively, are given by (Plotnick et al., 1996):

$$Z_1(r) = \overline{s(r)} \quad \text{(2a)}$$

$$Z_2(r) = s_s^2(r) + [\overline{s(r)}]^2 \quad \text{(2b)}$$

Here $\overline{s(r)}$ and $s_s^2(r)$ are the arithmetic mean and variance of $s(r)$, respectively. The lacunarity is then defined as a function of box-size, $L(r)$, by (Allan and Cloitre, 1991):

$$L(r) \equiv Z_2(r)/[\,Z_1(r)]^2 \quad \ldots\ldots(3)$$

In terms of the mean and variance of $s(r)$ the lacunarity can also be expressed as:

$$L(r) = s_s^2(r)/\,[\overline{s(r)}]^2 + 1 \quad \ldots\ldots(4)$$

Lacunarity is thus the dimensionless ratio of the dispersion (variance) to the square of the central tendency (mean) at a given scale, r (Plotnick et al., 1996). An alternative derivation of lacunarity may be found in Turcotte (1997).

Typically, lacunarity, $L(r)$, is calculated for a range of box-sizes r, and is plotted as a "lacunarity curve." For any given pattern, this curve will have upper and lower bounding values. Let ϕ be the fraction of sites that are occupied. It may then be proved that for $r = 1$, $Z_1(1) = \phi$ and $Z_2(1) = \phi$ in all cases (Plotnick et al., 1996). As a result, the lacunarity $L(1) = Z_2(1)/[\,Z_1(1)]^2 = \phi/\phi^2 = 1/\phi$. For $r = r_t$, there is only one box that covers the entire pattern and hence there the distribution of occupied sites, $s(r_t)$ consists of just one value. This implies that the variance, $s_s^2(r_t) = 0$. The lacunarity therefore is $L(r_t) = 1$. To summarize, the upper and lower bounds of the lacunarity curve are $L_{max} = L(1) = 1/\phi$ and $L_{min} = L(r_t) = 1$, respectively. The upper bound indicates that differences in ϕ will result in different values of L_{max}, and thus different lacunarity curves, even in the case of fracture patterns with similar clustering characteristics. The lacunarity parameter therefore needs to be normalized in order to overcome this effect.

3. NORMALIZATION OF LACUNARITY: THE TELPYN POINT FRACTURES

The fracture network at Telpyn Point, UK, (Rohrbaugh et al.; 2002) is comprised primarily of two orthogonal sets of vein-filled joints (striking 200° (NS-trending) and 290° (EW-trending)) that occur in Carboniferous sandstone (Dunne and North, 1990, Rohrbaugh et al., 2002) (Fig. 2.1a). The pattern was sampled over an area of 247.6m^2. The NS-trending

joints occur mainly in clusters (Fig. 2.1b), while the EW-trending set consists of somewhat clustered, large joints (Fig. 2.1c).

The original fracture map from Rohrbaugh et al. (2002) was converted into three different maps (Fig. 2.1) each being a 545 X 578 pixels bitmap. The gliding-box technique, as outlined in section 2, was applied to each map using a Matlab program (Roy, 2006) to generate the lacunarity curves (Fig. 2.2a). As seen in Fig. 2.2a, the EW fracture set yields much greater lacunarity values as compared to the NS set. This result is quite contrary to what is expected because visual inspection of the NS fractures (Fig. 2.1a) clearly indicates they are more clustered than the EW set (Fig. 2.1b). This apparent discrepancy arises because the lacunarity values are controlled both by clustering and by the ϕ value, which correlates to the fracture abundance. Thus, patterns with a small fracture abundance (i.e. low ϕ–value) and therefore a high L_{max}, will tend to have a greater lacunarity as the size of the gliding box (r) goes to smaller values close to the size of a pixel. Clearly, the NS fractures (Fig. 2.1c) are more abundant than the EW fractures (Fig. 2.1b). Since the EW pattern has a ϕ–value that is seven times smaller than the NS pattern, the effect of the ϕ–value overrides the effect of clustering in the calculation of the lacunarity values.

In an attempt to eliminate the abundance effect, Plotnick et al. (1996) used the quotient of the log-transformed values of $L(r)$ and L_{max} to normalize the lacunarity function. We implemented their normalization approach for the Telpyn Point fracture maps and the results are plotted as $\log[L(r)]/\log[L_{\max}]$ versus r in Fig. 2.2b. It can be seen that while this approach reduces the overall discrepancy, it does not eliminate it altogether; the EW fracture set still has the higher curve, again suggesting greater clustering. Therefore, we propose an alternative approach, widely used in the physical sciences, for normalizing the lacunarity parameter as:

$$L^*(r) = \frac{L(r) - L_{min}}{L_{max} - L_{min}} = \frac{L(r) - 1}{1/\phi - 1} \quad \text{.....(5)}$$

where $L^*(r)$ is the normalized lacunarity. This normalization has two advantages. Firstly, the lacunarity does not need to be log-transformed because its values now range between

unity at $r = 1$ to zero at $r = r_t$. Secondly, it completely removes the effect of the ϕ–value since the normalized lacunarity values reflect the effects of clustering alone rather than both clustering and fracture abundance. Compared to the curves for lacunarity in Figs. 2.2a and 2b, the curves for normalized lacunarity in Fig. 2.2c do show that the more clustered NS set has much higher normalized lacunarity values as compared to the sparsely-spaced EW set.

Figure 2.2 also includes lacunarity results for the NS and EW sets combined into a single network. Regardless of the technique employed, it is obvious that the lacunarity of the combined set is always dominated by the contribution of the NS set. In the case of our newly proposed normalization, the $L^*(r)$ curve for both sets combined is only slightly less than that for the single NS set. This result is because the NS fractures are very tightly clustered and, when combined with the sparsely-spaced EW set, the character of the entire pattern is essentially controlled by the NS set.

4. SCALE-DEPENDENT CLUSTERING: HORNELEN BASIN FRACTURES, NORWAY

4.1 Normalized Lacunarity Results

The Hornelen Basin fractures of Odling (1997) were chosen to delineate clustering within a fracture network at different scales. The four maps (Fig. 2.3) from this data set share two characteristics. They are all based on imagery gathered with a helicopter and they are a nested set of data where the sampling resolution changed with the change in map scale by varying the height of the helicopter. This approach is quite unlike collecting all data at one scale and then segmenting them to create maps at different scales. As a result, this pattern can be considered at a variety of scales in terms of the resolution of data at each scale, which is not the usual situation for the analysis of natural fracture patterns. The maps cover areas of sizes 90m x 90 m (Map 4), 180m x 180m (Map 5), 360m x 360m (Map6) and 720m x 720m (Map 7). Each map is a window on the fracture system and contains a range of fracture lengths, the shortest being dictated by the resolution of the image and the longest by the area mapped. When analyzed as fractal networks (Roy et al.,

2007), the box-counting fractal dimensions, D_b, for each map were not statistically different (Table 2.1).

For lacunarity analysis, the original fracture maps of Odling (1997) were converted to 1042 x 1042 pixel bitmaps. Normalized lacunarity curves were computed for each of the four maps for five different *r*-values (Fig. 2.4). The lacunarity values for box-sizes of 10 and 500 pixels along with the ϕ-values of each map are documented in Table 2.1. Paired (two-tailed) t-tests performed between the $L^*(r)$ values of maps 4 and 5, 5 and 6, and 6 and 7 respectively, indicated that, when considered over all scales, the normalized lacunarities were significantly different at the 95% confidence level in each case. The trend revealed is: the greater the resolution (the smaller the map scale), the greater the lacunarity. This result implies that fractures are more clustered at small scales and more uniformly distributed at large scales.

4.2 Geologic Interpretation

To geologically interpret the above results we need to return to a consideration of the differences between stratabound and non-stratabound joint networks. The former are ones that terminate at lithologic contacts while the latter terminate randomly within the rock mass and their geometries are not controlled by mechanical layer boundaries. Odling et al. (1999) cite the Hornelen fracture system as a good example of a "non-stratabound" fracture system, displaying joints with a power-law length distribution and qualitatively observed clustered fractures with a lack of regular spacing. Our $L^*(r)$ curves quantitatively show that the Hornelen fracture system has evidence of decreasing clustering with increasing scale (Fig. 2.4). Each map represents a subset of the fracture system with respect to fracture length, implying that the fractures become less clustered with respect to each other as their length increases. This relationship suggests that the Hornelen fracture system tends towards a more "stratabound" type system as fractures approach the scale of the entire basin. Visual inspection of an aerial photograph of the Hornelen Basin, with long fractures (400m – 1500m) and regular spacing (50m -100m), supports the tendency toward less clustering at larger scales (Fig. 2.5).

As discussed earlier, interface strength and the contrast between rheology of layers control the ability of joints to propagate through lithologic contacts. So, if the fracture system of the Hornelen Basin trends towards a smaller lacunarity (i.e. more "stratabound" system type), as scale increases and resolution decreases, the question of the nature of the layering that would control the fracture system at this greater scale arises. For map sizes of 90m x 90m to 720m x 720 m, Odling (1997), Odling et al. (1999) and our results show that the fracture system is clustered. This condition implies that at these scales, the fractures are likely not stratabound and during formation likely propagated across bedding surfaces that had cohesion and lacked sufficient differences in mechanical properties between beds. Therefore, at the scale of bedding (10's of metres or less), the layers do not constitute distinct mechanical units which results in "non-stratabound" systems and noticeable lacunarity.

However, at the scale of sedimentary cycles, the lithological packages of the Hornelen Basin do have characteristic changes at the scale of 100 m-200 m of sequence. These packages are characterized by finer-grained material at their base (Steel, 1976), which results in a high rigidity contrast between the cycles. Therefore, as opposed to the bedding-scale layering, these cycles can be considered as distinct mechanical units that can house "stratabound" fractures. The cycles exert a strong control on the topography of the area which is clearly seen in the aerial photograph image (Fig. 2.5). From the aerial photograph, it seems that composite fractures large enough to penetrate the thickness of an individual cycle (lengths of 400-1,500 m), tend to develop a more "stratabound" fracture system geometry with regular spacings of 50 to 100 m. The natural fracture patterns analyzed here (maps 4 to 7) were mapped from the well exposed surface of one of these cycles. The smallest map of 90 m x 90 m (map 4) shows a fracture length mode of around 1.7 m and a range of fracture lengths from 0.15 to 52 m. The majority of fractures in this map therefore have lengths comparable with the thickness of individual beds. Because the beds do not act as distinct mechanical units, this map shows a greater degree of clustering with a corresponding large lacunarity value. In the 720 by 720 m map (map 7), the fracture length mode is 11.7 m with a length range from 1.4 to 281 m. Thus, only the very largest fractures imaged by this map will penetrate an entire cycle which, as opposed to a single

bed (10's of m's), acts as a distinct mechanical unit. The progressive decrease in lacunarity as the scale increases (from map 4 to map 7), may therefore reflect an increasing influence of cycle thickness on the fracture system geometry. As the fracture lengths in the observed subset of the fracture system increase, the influence of cycle thickness (distinct mechanical unit) on fracture system geometry increases and the fracture system evolves from a "non-stratabound" type toward a more "stratabound" system. This change corresponds to a progressive reduction in lacunarity reflecting the transition from a clustered ("non-stratabound") to a more regularly-spaced ("stratabound") fracture system.

5. CONCLUSIONS

Plotnick et al. (1996) have shown that lacunarity is an effective means of characterizing spatial dispersion. Our present study shows that lacunarity can be used to quantify clustering in two dimensional fracture networks. Procedurally, it refines the normalization technique of Plotnick et al. (1996) to account for differences in the fraction of occupied sites in fracture maps with varying fracture abundance.

Separate analyses of two different sets of fractures within the same network (Telpyn Point), as well as that for the combined sets, show that normalized lacunarity is more sensitive to clustering than either the non-normalized lacunarity or Plotnick et al's (1996) previous normalization. We also demonstrated that the normalized lacunarity can quantify the degree of clustering so as to reveal that the most tightly clustered set controls the lacunarity curve of the pattern as a whole.

The normalized lacunarity for the complex, multi-generational pattern of Hornelen basin fractures clearly indicates that fractures become more clustered (like "non-stratabound" type) as the spatial scale of observation is decreased. Additional observations at the aerial-photograph scale show that fractures, which possibly penetrate the entire thickness of major sedimentary cycles (100m to 200m), are regularly spaced at 50m to 100m like "stratabound" fractures. This observation implies that these cycles behave like distinct mechanical units as opposed to the beds (10's of meters thick) that are contained

within them. It is argued that this trend reflects a gradual evolution from a "non-stratabound" fracture network, with greater clustering at the bed scale, towards a more "stratabound" system, with lesser clustering as fracture size perpendicular to bedding approaches the thickness of major sedimentary cycles.

Since fracture patterns can generally only be examined over a limited range of scales, such as with seismic reflection data, our results could be economically important for the mining and petroleum industries. Any scale-dependency in the clustering of fractures will also likely have significant implications for rock strength and flow processes that depend upon fracture connectivity. Thus, in terms of potential consequences, the nature of the relationship between lacunarity and fracture connectivity deserves to be elucidated in future studies.

REFERENCES

Allain, C. and Cloitre, M., 1991, Characterizing the lacunarity of random and deterministic fractal sets, *Phys. Rev. A.* vol. 44, no. 6, 3552-3558

Bai, T. and Pollard, D.D., 2000, Fractue spacing in layered rocks: a new explanation based on the stress transition, *Journal of Structural Geology,* vol. 22, 43-57.

Bour O., Davy, P., Darcel, C., Odling, N. E., 2002, A statistical scaling model for fracture network geometry, with validation on a multiscale mapping of a joint network (Hornelen Basin, Norway), *Journal of Geophysical Research*, vol. 107, no. B6, ETG 4-1 – 4-12.

Chiles, J. P., 1988, Fractal and geostatistical methods for modeling of a fracture network, *Math. Geol*., vol. 20, no. 6, 631–654.

Cooke, M.L., Simo, J.A., Underwood, C.A., Rijken, P., 2006, Mechanical stratigraphic control on fracture patterns within carbonates and implications for groundwater flow, *Sedimentary Geology*, vol. 184, 225-239.

Dunne, W. M. and North, C.P., 1990, Orhogonal fracture systems at the limits of thrusting: an example from southwestern Wales, *Journal of Structural Geology,* vol. 12, no. 2, 205-215.

Engelder, T. and Fischer, M.P., 1996, Loading configurations and driving mechanisms for joints based on Griffith energy-balance concept, *Tectonophysics,* vol. 256, 253-277.

Gillespie, P., Johnston, J.D., Loriga, M.A., McCaffrey, K.J., Walsh, J.J. and Watterson, J., 1999, Influence of layering in vein systematics in line samples; in *Fractures, Fluid Flow and Mineralization*,

Gross, M.R., 1993, The origin and spacing of cross joints: example from the Monterey Formation, Santa Barbra Coastline, California, *Journal of Structural Geology*, vol. 15, 737-751.

Gross, M.R., Fischer, M.P, Engelder, T., Greenfield, R.J., 1995, Factors controlling joint spacing in interbedded sedimentary rocks: interpreting numerical models with field observations from the Monterey Formation, USA; in: Ameen, M.S., (Ed.), *Fractography: Fracture Topography as a Tool in Fracture Mechanics and Stress Analysis* Geological Society, America, Special Publication, vol. 93, p. 215-233.

Hobbs, D.W., 1967, The formation of tension joints in sedimentary rocks: an explanation, *Geological Magazine,* vol. 104, 550-556.

La Pointe, P.R., Hudson, J.A., 1985, Characterization and interpretation of rock mass joint patterns, *Geological Society of America*, Special Paper 199.

Narr, W. and Suppe, J., 1991, Joints spacing in sedimentary rocks, *Journal of Structural Geology*, vol. 13, no. 9, 1037-1048.

Mandelbrot, B.B., 1983, *The Fractal Geometry of Nature*, Freeman, New York, NY, 468 pp.

Odling, N. E., 1997, Scaling and connectivity of joint systems in sandstones from western Norway, *Journal of Structural Geology,* vol. 19, no. 10, 1257-1271.

Odling, N.E., Gillespie, P., Bourgine, B., Castaing, C., Chiles, J.P., Christensen, N.P., Fillion, E., Genter, A., Olsen, C., Thrane, L., Trice, R., Aarseth, E., Walsh, J.J., Watterson, J., 1999, Variations in fracture system geometry and their implications for fluid flow in fractured hydrocarbon reservoirs, *Petroleum Geoscience*, vol. 5, p.373-384.

Plotnick, R.E., Gardner, R.H., Hargrove, W.W., Prestegaard, K., Perlmutter, M., 1996, Lacunarity analysis: A general technique for the analysis of spatial patterns, *Phys. Rev. E.* vol. 53, no. 5, 5461-5468.

Rohrbaugh, M.B., Dunne, W.M. and Mauldon, M., 2002. Estimating fracture trace intensity, density and mean length using circular scan lines and windows, *AAPG Bulletein,* v. 86, no. 12, 2089-2104.

Roy, A., Perfect, E., Dunne, W.M. and McKay, L.D. 2007. Fractal characterization of fracture networks: An improved box-counting technique. *J. Geophys. Res.* 112: B12201, doi:10.1029/2006JB004582

Sammis, G. C., Osborne, R.H., Anderson, J. L., Banerdt, M, White, P., 1986, Self-Similar Cataclasis in the Formation of Fault Gouge, *Pure Appl. Geophysics*, vol. 124, nos. 1/2, 53-78

Shackleton, R., Cooke, M. L., and Sussman, A. J., 2005. Evidence for temporally changing mechanical stratigraphy and effects on joint network architecture, *Geology* , vol. 33, pp. 101-104.

Steel, R. 1976. Devonian basins of western Norway – sedimentary response to tectonism and to varying tectonic context. *Tectonophysics* Vol. 36, pp. 207-224.

Turcotte, D. L., 1997, *Fractals and Chaos in Geology and Geophysics*, 2nd edition, Cambridge U. Press, New York, 398 pp.

Wu, H. and Pollard, D.D., 1995, An experimental study of relationship between joints spacing and layer thickness, *Journal of Structural Geology*, vol. 17, no. 6, 887-905.

APPENDIX I-A: TABLES

Table 2.1. Areas, scales, box-counting fractal dimensions, D_b, from Roy et al. (2007), fraction of sites occupied by fractures (ϕ), and non-normalized lacunarities L (10) and L (500) for Odling's (1997) fracture maps

Map no.	Area (m^2)	Scale	D_b	ϕ	$L(10)$	$L(500)$
4	8,100	1:511	1.81±0.05	7.95	2.023	1.021
5	32,400	1:1023	1.82±0.04	7.93	1.936	1.015
6	129,600	1:2045	1.84±0.04	10.09	1.641	1.006
7	518,400	1:4091	1.84±0.04	9.84	1.608	1.004

Appendix I-B: FIGURES

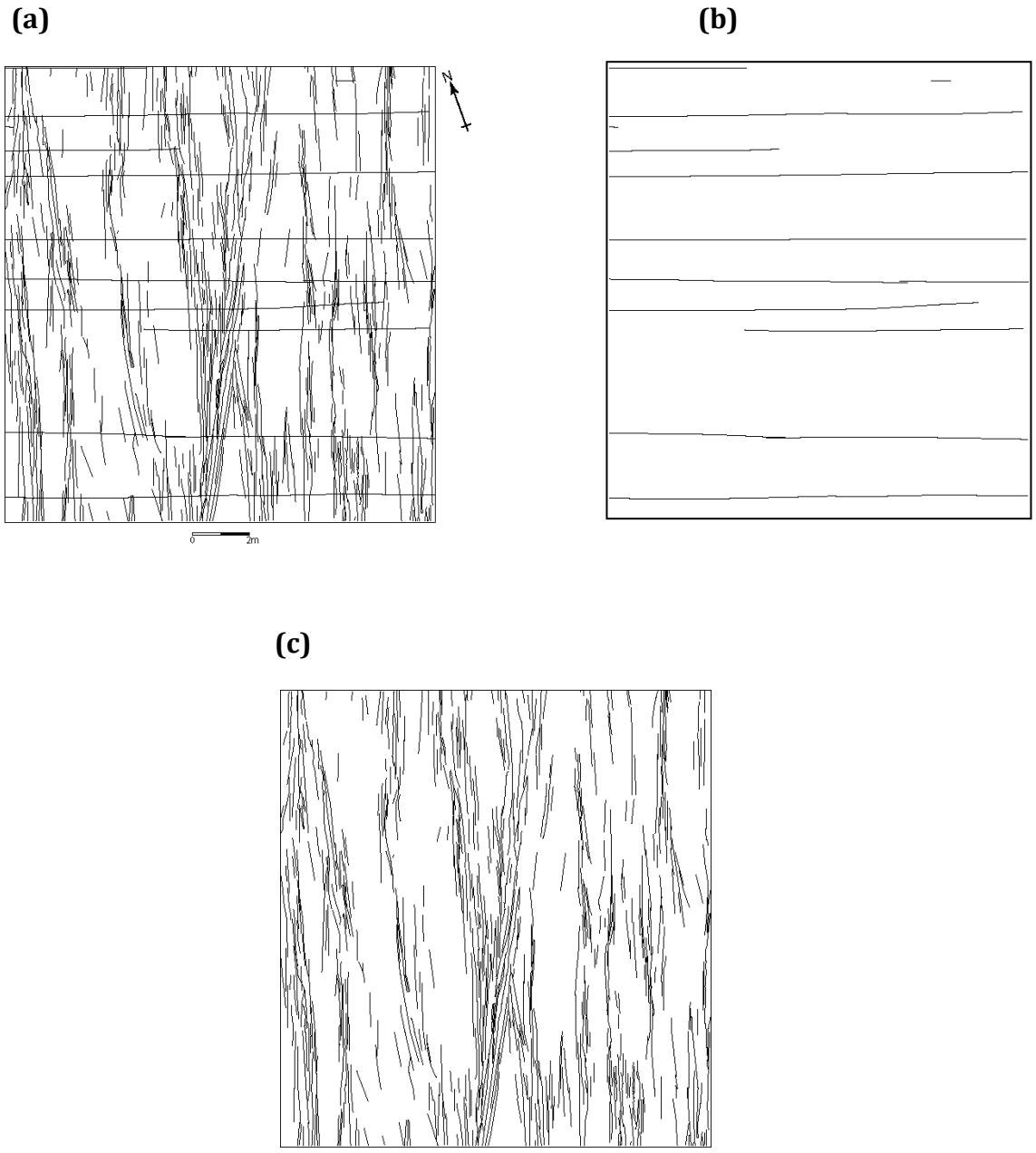

Figure 2. 1. Telpyn Point, Wales, fracture maps (Rohrbaug et al., 2002): (a) NS trending fractures (b) EW trending fractures (c) both EW and NS trending fracture sets

Figure 2.2. (a) Non-normalized lacunarity curves for Telpyn Point fractures (b) same set of curves using Plotnick's (1996) normalization of lacunarity (c) same set of curves using new normalization, L*

2.2(a)

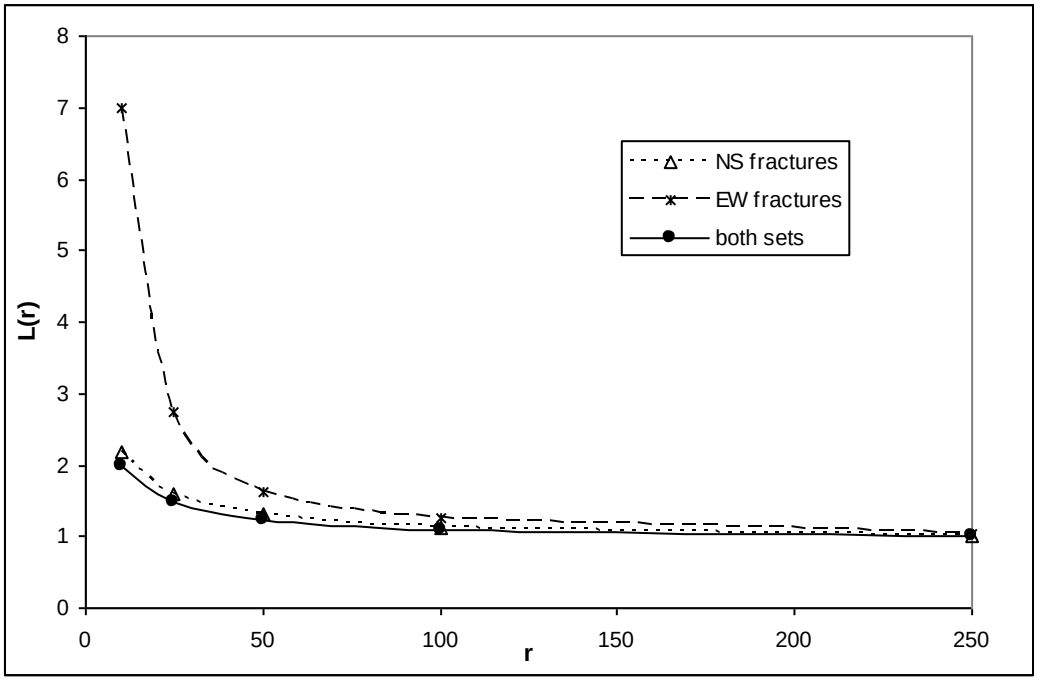
8
7
6
5
4
3
2
1
0
L(r)
0
50
100
150
200
250
r
NS fractures
EW fractures
both sets

2.2 (b)

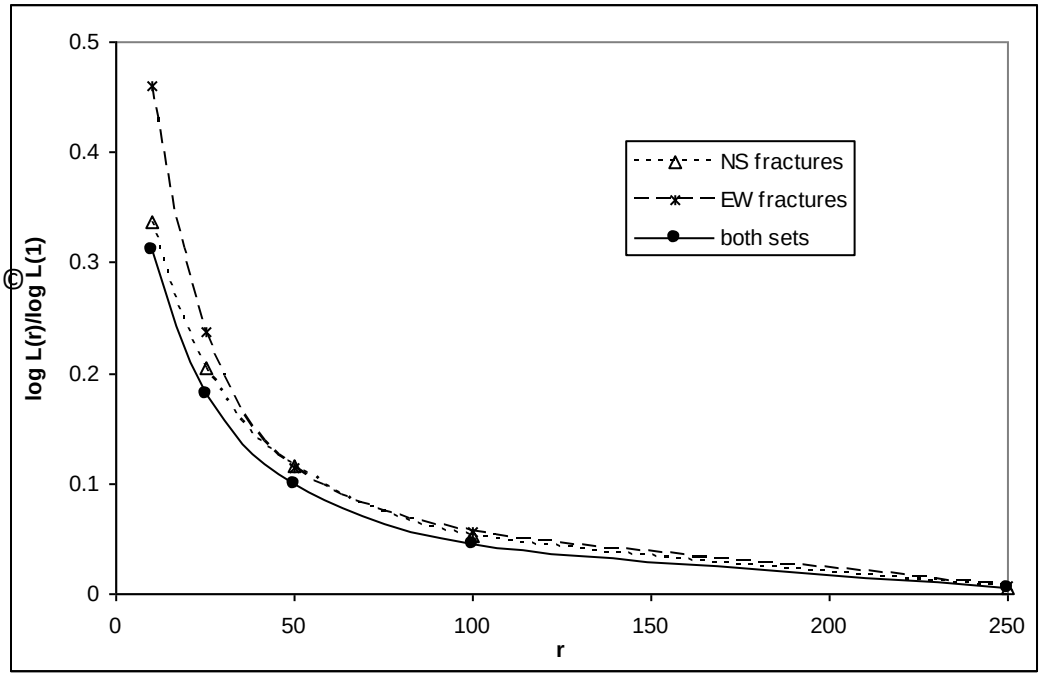
0.5
0.4
0.3
0.2
0.1
0
log L(r)/log L(1)
0
50
100
150
200
250
r
NS fractures
EW fractures
both sets

2.2 (c)

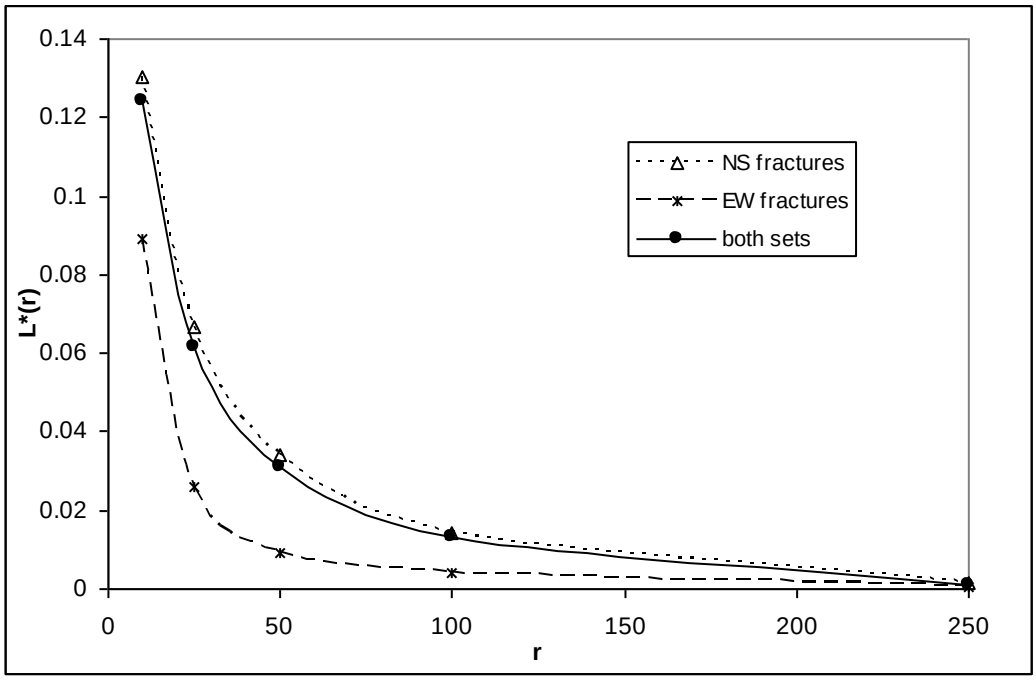
0.14
0.12
0.1
0.08
0.06
0.04
0.02
0
L*(r)
0
50
100
150
200
250
r
NS fractures
EW fractures
both sets

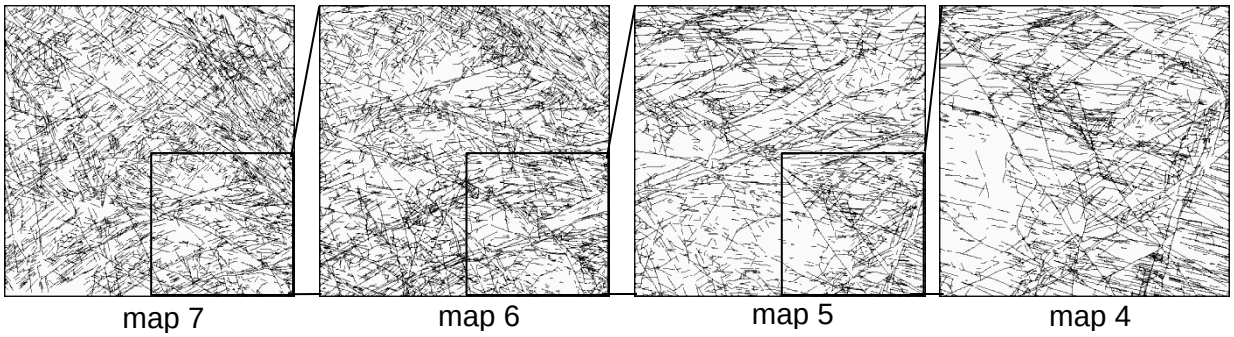

Figure 2.3. Hornelen basin fracture network mapped from a helicopter (Odling 1997): map 7 (720m x 720m), map 6 (360m x 360m), map 5 (180m x 180m) and map 4 (90m x 90m)

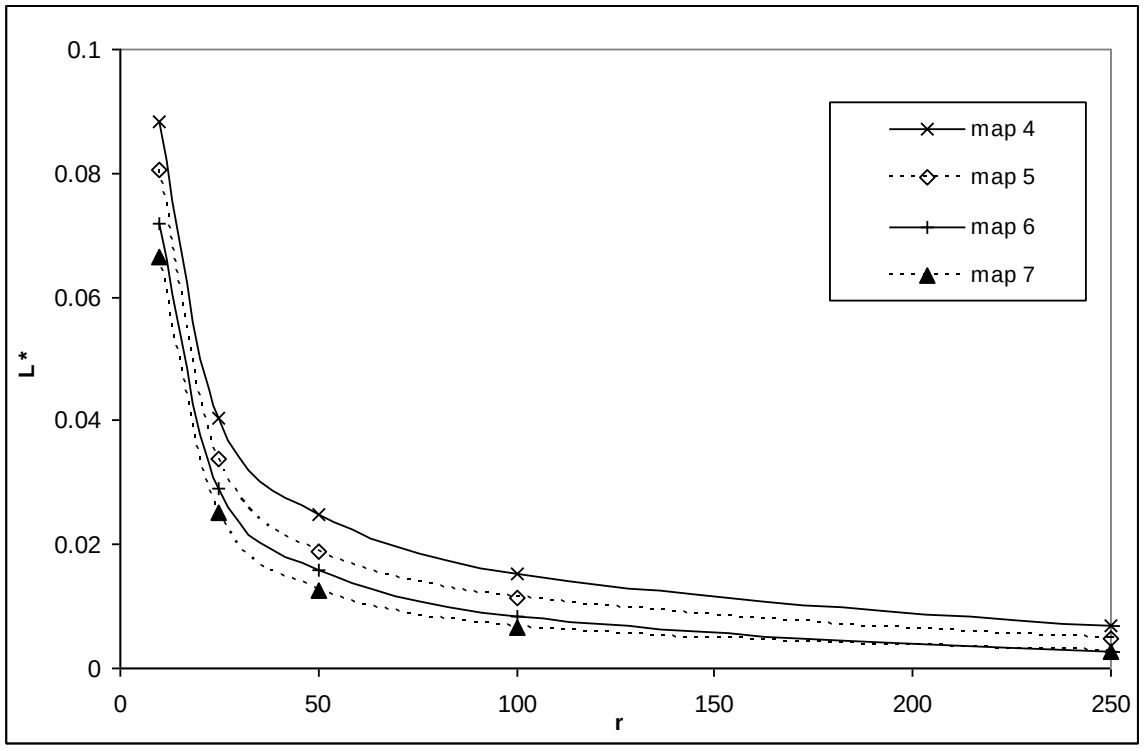

Figure 2.4. Normalized lacunarity curves for Hornelen basin fracture maps 4,5,6 and 7 depicting scale dependent clustering

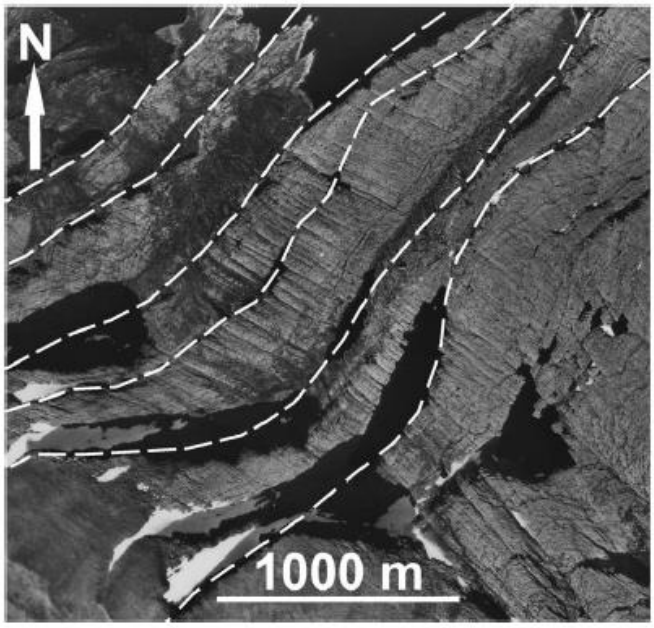

Figure 2.5. Section of an aerial photograph from Hornelen showing typical regularly spaced fractures with lengths of 400-1500m

Lacunarity Analyses of Multifractal & Natural Grayscale Patterns

Chapter III: A modified version of the manuscript submitted to FRACTALS by Roy et al*., 2012

***Ankur Roy & Edmund Perfect**

Ankur Roy contributed by performing data analysis, writing MATLAB codes and drafting the manuscript.

ABSTRACT

Lacunarity is a parameter that can distinguish between spatiotemporal patterns, fractal, multifractal or otherwise, for differences in texture. Previous studies have theoretically established that lacunarity analysis can delineate multifractal behavior in grayscale patterns. A set of multifractal grayscale patterns was generated with known correlation dimensions, D_2, and analyzed for lacunarity by employing the gliding-box algorithm. The log-transformed values thus obtained, log $L(r)$, were plotted as a function of the log-transformed box-size, log r. The slopes of these linear relations, estimated using regression analysis, were then used to calculate D_2. The calculated D_2 values gave approximately a1:1 relationship with the known D_2 values thus empirically demonstrating the usefulness of lacunarity analysis in establishing multifractal behavior. This approach was further used to evaluate the multifractal nature of natural grayscale images in the form of soil thin sections that had been previously classified as multifractals based on the more standard box counting (BC) analysis. Our results indicate that lacunarity analysis is a more sensitive indicator of multifractal behavior in natural grayscale patterns than the BC approach. A weighted mean of the log-transformed lacunarity values at different scales was also employed in differentiating between grayscale patterns with various degrees of scale-dependent clustering attributes. This new lacunarity measure, which expresses the lacunarity versus box size curve as a single number, should be useful to researchers who want to explore the correlative influence of texture on, for instance, flow and transport parameters.

1. INTRODUCTION

Lacunarity is a parameter that characterizes the distribution of spaces or gaps in a pattern as a function of scale. Originally proposed for distinguishing between patterns having the same fractal dimension but different textures (Mandelbrot, 1983) lacunarity has since been used for analyzing textures of various other fractal and non-fractal data. Examples include natural fracture networks (Roy et al., 2010), binary ecological data (Plotnick et al., 1996) and natural non-binary (grayscale) data (Mynt & Lam, 2005; Du & Yeo, 2009 and Manikka-Baudge & Dougherty, 2009). The gliding-box algorithm is generally used for measuring lacunarity at various scales (or box-sizes) and the resulting values, $L(r)$, are plotted against the box-size, r. It has been theoretically established that when log-transformed values of $L(r)$ and r are plotted, both fractals and multifractals result in straight lines such that the slope plus the known embedding dimension equals the box or correlation dimension, respectively (Allain & Cloitre, 1991).

Although there have been a few studies on lacunarity of both synthetic and natural multifractal patterns (Plotnick et al., 1996 and Chen, 1997) there is not enough evidence to unequivocally establish that lacunarity analysis can delineate multifractal behavior of non-binary data, and that the true correlation dimension, D_2 of a multifractal can be found by employing this technique. In the present paper, we test the theory of Allain and Cloitre (1991) on multifractal grayscale patterns with known correlation dimensions. We also propose a novel technique for expressing lacunarity as a single number that takes into account the clustering of elements in a pattern at different scales thus differentiating it from other patterns having the same correlation dimension but different textures. We finally use natural grayscale images in the form of soil thin sections that have been previously analyzed as multifractals using the standard box counting method, BC by Zhou et al. (2011) and show that lacunarity analysis is a more reliable technique for establishing multifractal behavior.

2. LACUNARITY AS AN INDICATOR OF MULTIFRACTAL BEHAVIOR

2.1. Multifractal Grayscale Patterns

A set of 2-dimensional multifractal grayscale patterns were constructed following the steps outlined in Perfect et al. (2006) and subsequently employed by other researchers (Koirala et al., 2008 and Zhou et al., 2010). The process is akin to generating a Sierpinski carpet, only the zeros and ones in the pattern are replaced with fractional values. The algorithm involves normalizing mass-fractions calculated from the truncated binomial distribution for an average probability, p, of retaining a cell in the generator with a scale factor, b, in successive iterations. As described in Koirala et al. (2008) the locations of the normalized mass fractions can be spatially randomized so as to create a random multifractal grayscale pattern (Fig. 3.1). Eight different patterns were created from a generator with a scale factor of b = 3 and probability values corresponding to p = 1/9, 2/9, 3/9, 4/9, 5/9, 6/9, 7/9, and 8/9 by iterating the system 5 times to produce grayscale fields of size $3^5 \times 3^5$ pixels. For each of the 8 models (as seen in Fig. 1 in Koirala at al., 2010), 3 random realizations were constructed amounting to a total of 24 random multifractal patterns. These were named using the following scheme: p # r ## where # corresponds to the numerator of the p-value (1-8) and ## to the realization (r) number (1-3). For example, a pattern from the model p = 3/9 and random realization 2 will be named $p3r2$. Figure 3.1 corresponds to the pattern $p8r3$.

2.2. Lacunarity of Grayscale Patterns

Lacunarity is a scale-dependent measure of textural heterogeneity that can be quantified by employing the gliding-box algorithm (Allain & Cloitre, 1991; Plotnick et al., 1993). Essentially, this method involves sliding a window or an interrogator box of a given length, r, translated in increments of a chosen unit length (usually that of a pixel) across the whole pattern such that the total number of steps is given by $(r_t - r + 1)^2$, r_t being the length of the entire pattern. The details of this technique employed in analyzing binary patterns can be found in Roy et al. (2010). In the case of grayscale patterns, the mass of all pixels, $s(r)$, contained within the interrogator box at each step is calculated and a distribution of this mass at the scale r is obtained by gliding the box through all the steps. Finally, the

mean, $\overline{s(r)}$, and variance, $s_s^2(r)$ of this distribution are used in calculating the lacunarity, $L(r)$, at the scale r as:

$$L(r) = s_s^2(r) / [\overline{s(r)}]^2 + 1 \quad \ldots\ldots(1)$$

Typically, $L(r)$ is calculated for a range of box-sizes, and for any given pattern, this curve will have upper and lower bounding values. It can be easily perceived that at $r = 1$, the interrogator box contains only 1 pixel and it moves r_t^2 steps equal to the total number of pixels (each associated with a mass number) in the pattern. It then follows that $L(1)$ is the same for patterns with the same set of mass numbers but distributed differently in space. In other words, all random realizations of a model corresponding to a specific p-value will have the same maximum lacunarity, $L(1)$. At $r = r_t$, there is only one box that covers the entire pattern and hence the distribution of masses, $s(r_t)$ consists of just one value. This implies that the variance, $s_s^2(r_t) = 0$ such that the lacunarity is $L(r_t) = 1$. It may be noted that uniform patterns have no variance and hence they furnish, $L(r) = 1$ for all r values.

2.3. Lacunarity and the Correlation Dimension

It has been theoretically demonstrated by Allain & Cloitre (1991) that in the case of multifractals, lacunarity, $L(r)$ is related to the size of the interrogator box, r by a power-law such that the power-term equals $D_2 - E$, where D_2 is the correlation dimension and E the Euclidean embedding dimension. Based on this result, it is expected that the log-transformed lacunarity functions for the 2-dimensional multifractal patterns described in section IA can be fitted with a straight line of the form, $y = mx + c$, such that the slope is:

$$m = D_2 - 2 \quad \ldots\ldots(2)$$

For each of the 24 multifractal patterns, the log $L(r)$ vs. log r values were calculated and a subset of the array of points thus obtained was fitted with a straight line. Figure 3.2a shows one such plot for the pattern $p8r3$. Figure 3.2b shows the local slope of the log $L(r)$ vs. log r curve calculated at each r with the dashed line describing the slope of the fitted line from Fig. 3.2a. In order to meet the condition of multifractality in Allain and Cloitre (1991), and to estimate the proper correlation dimension for the pattern, only the relatively "flat" segment of the curve in Fig. 3.2b was considered for fitting a linear model to the points in

Fig. 3.2a. Also, it is important to realize here that patterns that do not furnish such "flat" segments are thus not multifractals. We'll come back to a detailed discussion on this in a later section. For large r values it is seen from Fig. 3.2b that the local slope starts to fluctuate and increases abruptly. Therefore, the points corresponding to box-sizes r > r_t /2 were not included in the fitting. For smaller r values, the coefficient of determination, R^2, of the fit improved when points were sequentially excluded from the left in Fig. 3.2a. However, it is the first point at r = 1 that mostly influences the change in slope such that there was a difference of ~4% in the estimated slope if this point was excluded from the fit. If two or more additional points were excluded from the fitting there was no more than ~1% difference. This is mainly because the first few points on the left hand side of the log $L(r)$ vs. log r plot were always sparsely distributed. Therefore from the lower end, only the first point in the plot was excluded from the fitting. The points thus excluded from both ends are shown in grey in Fig 3.2.

Correlation dimensions for all 24 patterns were calculated from their log $L(r)$ vs. log r plots by employing the above protocol. An average estimated D_2 value from all three realizations of each model corresponding to a particular p-value was computed and compared to the theoretical D_2 value (Perfect et al., 2006). The results are graphed in Fig. 3.3. The 95% confidence intervals in the computed D_2 values arising from the 3 random realizations for each model are shown as vertical bars. As can be seen from the figure, the computed D_2 values overlap the 1:1 line (45˚ slope) and are thus are statistically equal to their theoretical counterparts. This analysis demonstrates empirically that an almost exact value of the correlation dimension for multifractals can be found from lacunarity analysis. It may therefore be concluded that lacunarity analysis can detect if a grayscale pattern exhibits multifractal behavior (on the basis of log-log linearity) and, if it does, provide an accurate estimate its correlation dimension (from the slope of this relation).

3. LACUNARITY AS A MEASURE OF CLUSTERING IN MULTIFRACTALS

Lacunarity analysis has been used as a measure of clustering in monofractals and other binary patterns. Examples include those of simulated landscape maps (Plotnick et al.,

1993) and fracture networks (Roy et al., 2010). Lacunarity has also been used for textural analysis of grayscale patterns (Du & Yeo, 2009 and Manikka-Baudge & Dougherty, 2009). This section extends the previous research by implementing lacunarity as a measure of clustering in multifractal grayscale patterns.

A set of three deterministic (Fig. 3.4 A-C) and one random (Fig. 3.4 D) multifractal grayscale patterns of size 343×343 pixels were constructed using the following parameters: $b = 7$, $p = 40/49$, and 3 iterations. These patterns will henceforth be referred to as models A, B, C and D, respectively. The random multifractal grayscale pattern D was generated using exactly the same approach as described in section 2.1. The deterministic patterns (A-C) were generated by placing nine of the largest mass-fractions obtained from the truncated binomial distribution (Perfect et al., 2006) in different predetermined locations within the generator and the rest of the 40 mass-fraction numbers in random locations around them, and then iterating the system 3 times. Of these four patterns, A and C are the least and most clustered, respectively, and may be thought of as multifractal counterparts of Figures 3-7(B) and 3-7(A) respectively in Perfect & Sukop (2001). Patterns B and D are intermediately clustered. A fifth model, designated E (Fig. 3.4 E), was constructed by completely randomizing the spatial locations of the mass fractions produced by the $b = 7$, $p = 40/49$, and 3 iterations multifractal model; it is thus a true random grayscale pattern. As such, it should have minimal clustering, and negligible lacunarity.

Models A through E were analyzed for their lacunarity using the gliding box method and the resulting log $L(r)$ versus log r values plotted as before (Fig. 3.5). All of the multifractal models produced a straight line trend that was very different from that of model E, which is not a multifractal. Being a truly random pattern, the lacunarity values for model E follow a non-linear curve and quickly converge to a value of zero which shows that at larger scales ($r > 30$) it behaves like a uniform pattern with $L(r) = 1$ (since $\log L(r) = 0$) at all r values. Despite some kinks in the linearity of the log-log plots for the three deterministic multifractal grayscale patterns, created by the non-random geometric arrangement of the generator mass fractions, regression analysis still yielded estimates of D_2 (Table 3.1) that were within 1% of the theoretical value of 1.914. As expected, the

random multifractal grayscale pattern D produced the most linear relationship between log $L(r)$ and log r resulting in the best estimate of D_2 (within 0.5% of theoretical value).

Amongst the multifractals, model A always had the lowest lacunarity values while model C had the highest (Fig. 3.5). Models B and D had intermediate lacunarity values at all scales. These results are consistent with the different degrees of clustering imposed on the patterns by the choice of the locations of mass fractions in the different generators (Fig. 3.4). For purposes of comparison between patterns with different clustering, it can be advantageous to report lacunarity as a single number rather than a log $L(r)$ vs. log r plot. In such plots, $L(r)$ is high at small values of r, while for large values of r, $L(r)$ is low and, as seen in Fig. 3.5, the differences in lacunarity between variously clustered grayscale multifractals are most pronounced in the middle order r values. A log-weighted mean of the log-transformed values of lacunarity, $<L>$, will best describe these differences while taking into account the variability in $L(r)$ with r. This weighted mean can be calculated with the following equation:

$$< L >= \frac{\sum [\log L(r)][\log r]}{\sum \log r} \quad \text{.....(3)}$$

The values of $<L>$ for models A through E are given in Table 3.1. It may be noted that the different patterns rank as E << A < D ~ B < C in terms of $<L>$ as expected from visual inspection of the different degrees of clustering in Fig. 3.4.

4. LACUNARITY ANALYSIS OF NATURAL GRAYSCALE IMAGES

In this final section we apply the lacunarity technique developed above to a set of natural grayscale patterns that have been previously characterized as multifractals based on the box counting method (BC) by Zhou et al. (2011). These patterns comprise a set of three soil thin sections photographed in plane polarized light with a Nikon DS-Fi1 digital camera at an 8-bit depth resolution (Fig. 3.6). Each image is 1024×1024 pixels, the length of a pixel being 1.9 μm. As described in Zhou et al. (2011), Soil 1 (Fig. 3.6a) has a relatively homogenous structure, soil 2 (Fig. 3.6b) has medium-sized aggregates with evenly

distributed pores, while soil 3 (Fig. 3.6c) has well-developed aggregates with large pores. Visual inspection of these patterns suggests that soil 1 is comparable to model E from the previous section, while soil 3 compares to most closely to models B or D.

The log $L(r)$ vs. log r plots for these soils are shown in Figure 3.7. The inset shows the local slopes of the log $L(r)$ vs. log r curves calculated at each r and denoted by d(log L)/d(log r). It is clearly seen from this figure that only soil 3 behaves like the multifractal pattern $p8r3$ in Fig. 3.2b and displays somewhat of a "flat segment" in the d(log L)/d(log r) vs. log r plot. It therefore meets the condition of multifractality as stated in Allain & Cloitre (1991) over the corresponding range of r values and can thus be classified as a true multifractal pattern. Soil 2 clearly does not have any "flat segments" and is therefore not a multifractal. Soil 1 reaches a constant $L(r)$ of one (i.e., log $L(r) = 0$) around $r = 100$. Therefore at larger scales, soil 1 behaves like the pure random pattern, model E, which is expected due to its "relatively homogenous structure."

Based on standard box counting analyses, it was concluded that all three soil thin section images were multifractal (Zhou, et al., 2011). It is evident from the above results, however, that only soil 3 can be considered truly multifractal in nature, with a linear $L(r)$ vs. log r plot covering ~2 orders of magnitude. Thus, compared to the BC method, lacunarity analysis is more reliable when it comes to establishing multifractal behavior of natural grayscale patterns. A similar conclusion was arrived at by Grau et al. (2006) when comparing the BC and gliding box approaches for conducting full multifractal analyses. The gliding box algorithm, which forms the basis of lacunarity analysis, produces more continuous coverage with a large number of r values as compared to BC, which relies on fewer discrete step increments.

The weighted mean log-transformed lacunarities, $\langle L \rangle$, of the three soils, along with the correlation dimension, D_2, for soil 3 as computed from the log $L(r)$ vs. log r plot, are reported in Table 3.2. This D_2 value is within ~ 2% of the value reported in Zhou et al. (2011) based on BC. The $\langle L \rangle$ values show that soil 3 is the most clustered amongst the three thin sections and this is no surprise since it has was previously reported as having

"relatively well developed aggregates with large pores." Also, the <*L*> value for soil 3 compares favorably with that of models B and D in Table 3.1.

5. CONCLUSIONS

The results from our research on lacunarity analysis of natural and multifractal grayscale patterns bring forth two main points. First, it empirically tests the equation of Allain and Cloitre (1991) that relates lacunarity to the correlation dimension in grayscale patterns. Thus, it demonstrates that by running a lacunarity analysis on grayscale patterns one can check for possible multifractal behavior and hence find the correlation dimension. Second, it shows that lacunarity analysis can delineate clustering in synthetic and natural grayscale images regardless of their multifractal nature. More importantly, this work introduces the novel concept of expressing lacunarity as a single number which takes into account the clustering in a pattern at different scales. This is particularly helpful when comparing different grayscale patterns or images for their clustering attributes. This new lacunarity parameter will likely prove useful in future research exploring the influence of texture on flow and transport processes within greyscale fields.

REFERENCES

Allain, C. and Cloitre, M., 1991, Characterizing the lacunarity of random and deterministic fractal sets, *Phys. Rev. A.* vol. 44, no. 6, 3552-3558

Chen, Q., 1997, Multifractal Modeling and Lacunarity Analysis, *Mathenatical Geology,* vol. 29, no. 7, 919-932

Du, G. and Yeo, T.S, 2009, A novel lacunarity estimation method applied to SAR image segmentation, *IEEE Transactions on Geoscience & Remote Sensing*, vol. 40, no .12, 2687-2691

Grau, J., Méndez, V., Tarquis, A.M., Díaz, M.C. and Saa, A., 2006, Comparison of gliding box and box-counting methods in soil image analysis. Geoderma 134: 349–359

Koirala, S.R., Perfect, E., Gentry, R.W., Kim J.W., 2008, Effective saturated hydraulic conductivity of two-dimensional random multifractal fields, *Water Resources Research,* vol. 48, W08410, 1-9

Mandelbrot, B.B., 1983, *The Fractal Geometry of Nature*, Freeman, New York, NY, 468 pp.

Manikka-Baudge, D. C. and Dougherty, G., 2009, Texture analysis using lacunarity and average local variance, *Medical Imaging 2009: Image Processing*, vol. 7259, 1-12

Myint, S. W. and Lam, N., 2005, A study of lacunarity based texture analysis approaches to improve urban image classification, *Computers, Envir. Urban Syst.*, vol. 29, 501-523

Perfect, E., and Sukop M.C., 2001, Models relating solute dispersion to pore space geometry: A review, *Soil Science Society of America,* sp. pub no. 56, 77-145

Perfect, E., Gentry, R.W., Sukop M.C., Lawson, J.E., 2006, Multifractal Sierpinski carpets: Theory and application to upscaling effective saturated hydraulic conductivity, *Geoderma,* vol. 134, 240-252

Plotnick, R.E., Gardner, R.H., O'Neill, R.V., 1993, Lacunarity indices as measures of landscape texture, *Landscape Ecology*, vol. 8, no. 3, 201-2011

Plotnick, R.E., Gardner, R.H., Hargrove, W.W., Prestegaard, K., Perlmutter, M., 1996, Lacunarity analysis: A general technique for the analysis of spatial patterns, *Phys. Rev. E.* vol. 53, no. 5, 5461-5468.

Roy, A., Perfect, E., Dunne, W.M., Odling, N. and Kim, J.W., 2010, Lacunarity analysis of fracture networks: Evidence for scale-dependent clustering, *J. Structural Geology,* vol. 32, 1444-1449.

Zhou, H., Perfect, E., Li, B.G. and Lu, Y.Z., 2010, Effects of bit depth on the multifractal analysis of grayscale images, *Fractals,* vol. 18, 127-138

Zhou, H., Perfect, E., Lu, Y.Z., Li, B.G., Peng, X.H., 2011, Multifractal analyses of grayscale and binary soil thin section images, *Fractals,* vol. 19, no. 3, 1-11

APPENDIX II-A: TABLES

Table 3.1. Correlation dimensions (D_2), associated coefficients of determination (R^2), and weighted mean log-transformed lacunarities, <*L*>, for the five synthetic grayscale fields illustrated in Fig. 4

Model	D_2	R^2	<*L*>†
A	1.932	0.947	6.1
B	1.928	0.996	12.6
C	1.928	0.915	25.7
D	1.922	0.995	11.1
E	n.a.	n.a.	0.1

† <*L*> values reported as × 10^3
n.a. = not applicable (log $L(r)$ vs. log r plot not linear)

Table 3.2. Correlation dimensions (D_2), associated coefficients of determination (R^2), and weighted mean log-transformed lacunarities, <*L*>, for the three natural grayscale fields illustrated in Fig. 6

Soil	D_2	R^2	<*L*>†
1	n.a.	n.a.	1.2
2	n.a.	n.a.	8.4
3	1.924	0.999	15.5

† <*L*> values reported as × 10^3
n.a. = not applicable (log $L(r)$ vs. log r plot not linear)

APPENDIX II-B: FIGURES

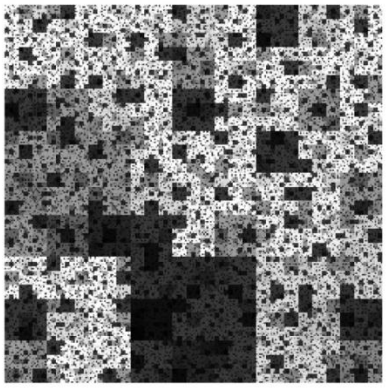

Figure 3.1. A grayscale random multifractal pattern: p8r3. Lighter phases have higher mass fractions

(a)

(b)

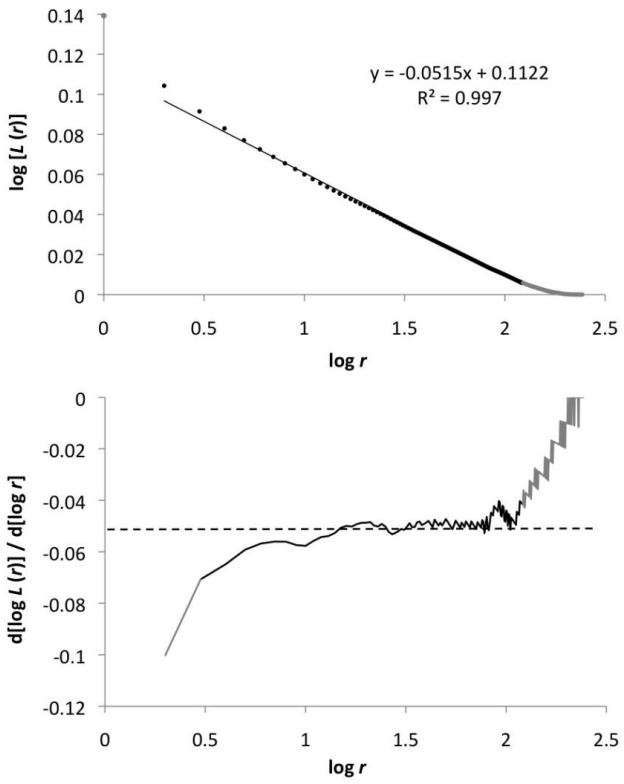

Figure 3.2. (a) log L(r) vs. log r plot for pattern p8r3: points not included in the linear fit are shown in grey. (b) Local slope of (a) plotted as d[log $L(r)$]/d[log r] against log r: dashed line shows slope of linear fit from (a), the "flat segment" used for fitting the linear model is shown in black

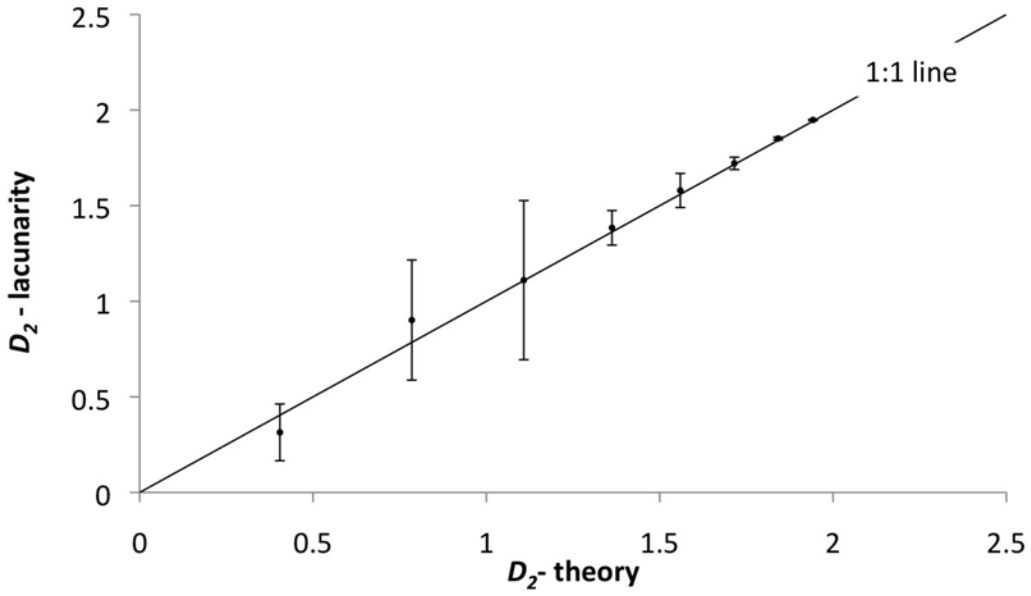

Figure 3.3. Correlation dimension, $D_{2,}$ estimated from lacunarity analysis compared to theoretical D_2 values for random multifractal fields with scaling factor b=2, and probability of occupied cells, p = 1/9 to 8/9 (three realizations for each of the eight fields); average values of 3 realizations with bars corresponding to the 95% confidence intervals

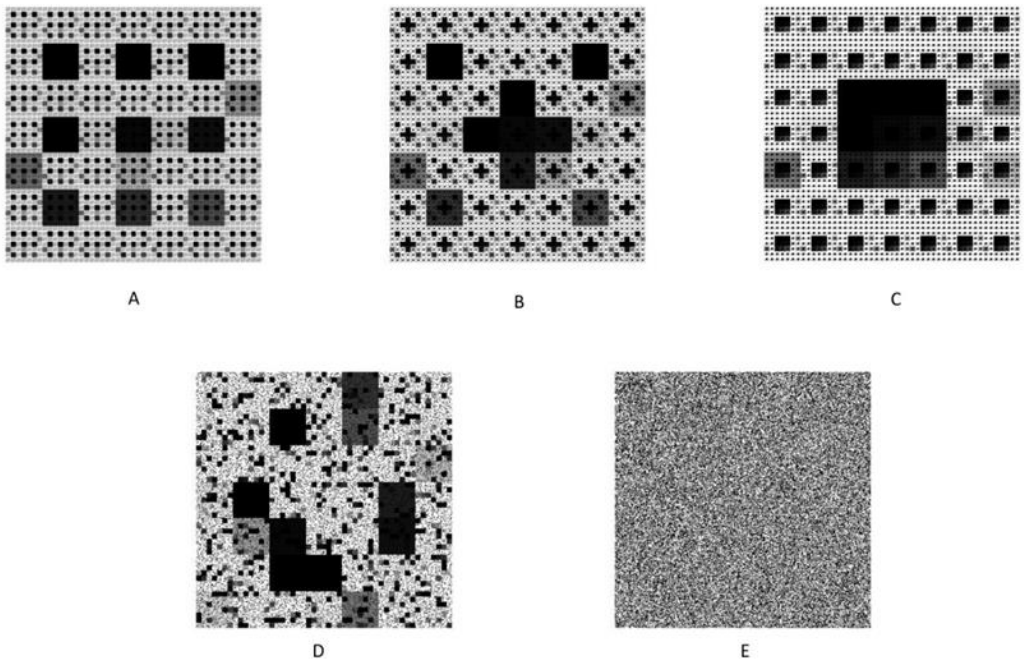

Figure 3.4. Grayscale multifractal models with b=7 and p = 40/49, and 3 iterations; models A, B, C: deterministic multifractals showing low, medium and high clustering, respectively; model D: random multifractal; model E: non-multifractal random grayscale pattern with same mass fractions as the others models

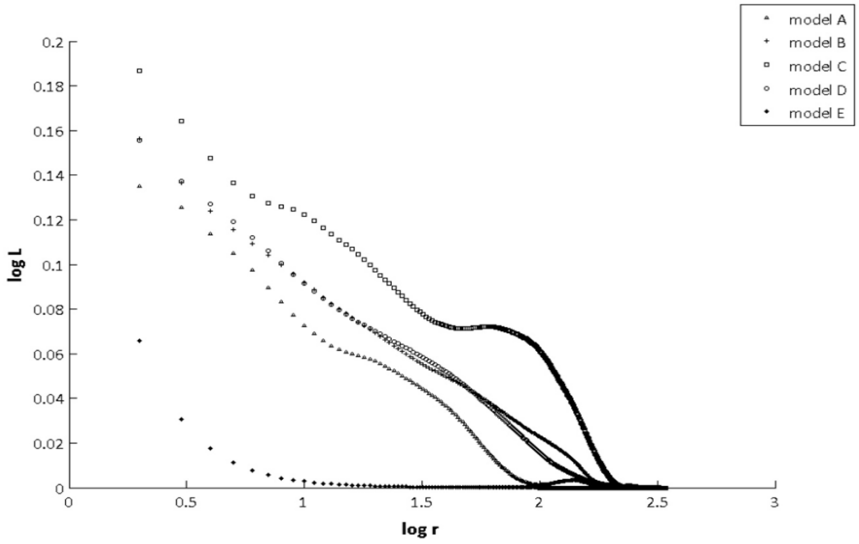

Figure 3.5. log L(r) vs. log r plots for models A-E. Note curvilinear behavior of model E (random), as compared to the other (multifractal) models

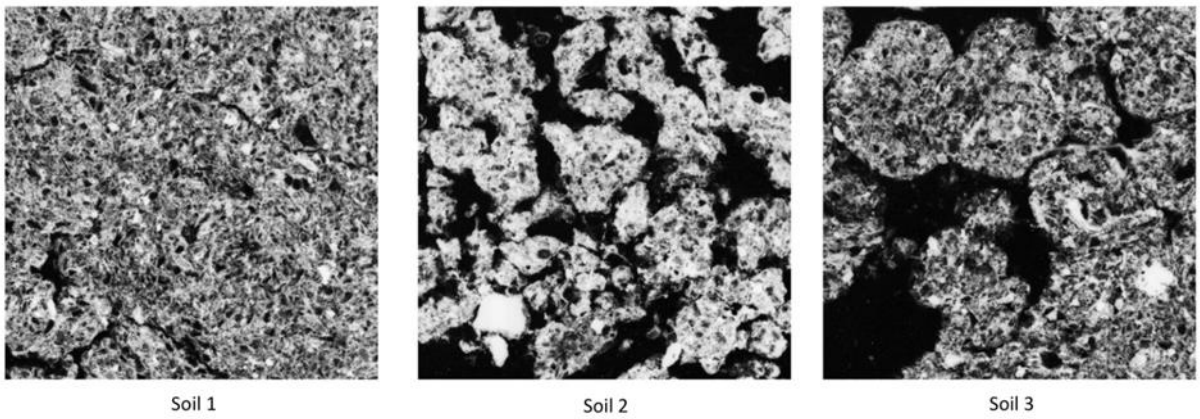

Figure 3.6. Natural grayscale images of soil thin sections from Zhou et. al. (2011); note: soil 1 compares to model E in Fig. 4, while soil 3 compares to models B or D

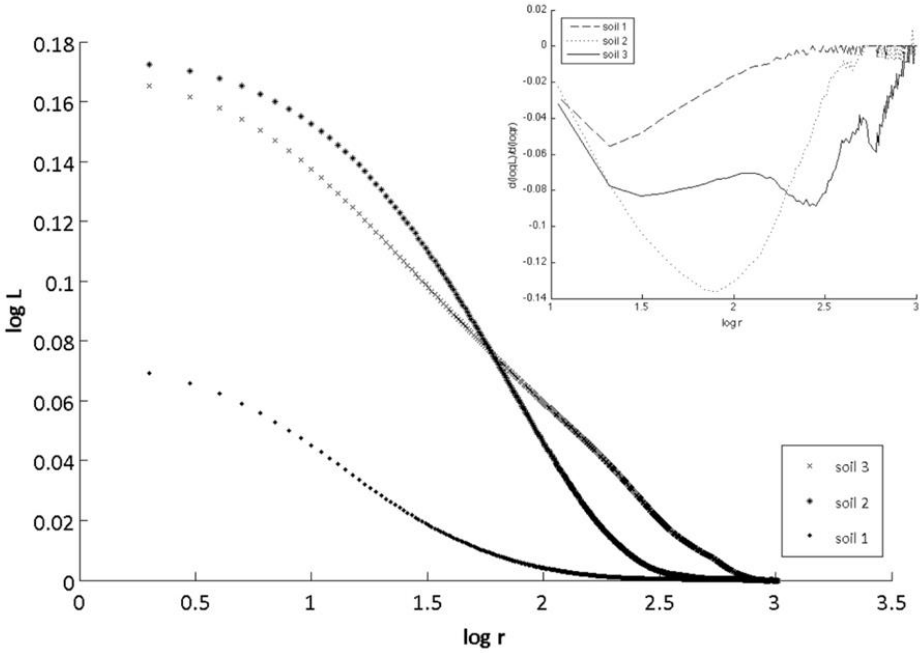

Figure 3.7. log $L(r)$ vs. log r plots for natural grayscale images. Note: soil 3 exhibits straight line behavior over ~2 orders of magnitude (multifractal); soil 1 compares to the $L(r)$ vs. log r plot for model E (random) in Fig. 5; soil 2 is intermediate. Figure in inset shows the local slopes plotted as d[log $L(r)$]/d[log r] vs. log r

A Technique for Revealing Scale-dependent Patterns in Scanline Data: I. Fracture Spacing

Chapter IV: A manuscript for submission to the Journal of Geophysical Research

Ankur Roy & Edmund Perfect
Potential Co-authors: William M. Dunne & Larry D. McKay

ABSTRACT

Data on fracture spacing along scanlines have been widely analyzed for the purposes of characterization. Most of these studies however, either consider the cumulative frequency of spacing data without regard to the actual sequence of the spacing values or compute an average spacing that may not work for clustered fractures. The coefficient of variation parameter is used to differentiate between clustered, random and anticlustered fractures in a scanline but does not address the issue of scale-dependent variations in spacing. Lacunarity is a parameter that has been previously used for delineating scale-dependent clustering in fracture networks with similar fractal dimensions. This technique has the further capability of identifying scales at which different patterns emerge within the same dataset. Lacunarity can also delineate possible fractal behavior. This paper tests the capability of lacunarity to find patterns (fractal/uniform/random) within synthetic and natural fracture clusters. A set of four model scanlines: uniformly-spaced fractures, periodically-spaced fracture clusters, fractal fracture clusters, and random fractures were considered. The 1st derivative of the lacunarity curves of these models was used to find the inter-cluster distance and organization of fractures within the clusters. The same technique was then applied to a set of two natural fracture scanline data, one with fracture clusters with fractal organization within, and the other with randomly spaced fractures. It was found that this technique can discriminate the random pattern from the clustered one, find the intercluster distance, and identify the organization within the clusters.

1. INTRODUCTION

Quantifying fracture spacing is the key to understanding the spatial organization of fracture networks and serves as a preliminary step towards stochastic modeling. Previous researchers have employed various parameters for studying fracture spacing that include the coefficient of variation (Gillespie et. al., 1999) and fracture spacing index (Narr and Suppe, 1991). However, these descriptors fail to capture the entire range of heterogeneity mainly because they look at data sets only at a single scale. For example, the coefficient of variation determines whether fractures are clustered on the entire length scale of a scanline while the fracture spacing index focuses on the average fracture spacing. Many naturally occurring fractures however, display heterogeneity such that not only do they occur as clusters but may have a different organization (e.g. random or fractal) within the clusters. Therefore, while a simple parameter like average spacing is sufficient for predicting the presence of evenly-spaced fractures in a well-bore it will not work where fractures are present in clusters. Also, while a single-scale clustering index may help determine if a fracture set is clustered it cannot quantify the inter-cluster distance or find the organization within such clusters.

Semivariograms (LaPointe and Hudson, 1985; Chiles, 1988) and, more recently, Lacunarity (Roy et al., 2010) and the correlation dimension and Lyapunov exponent (Riley, et al., 2011), have been introduced as mathematically rigorous parameters that can determine the heterogeneity of fracture data sets at different scales. The focus of the present study is on the quantification of scale-dependent clustering in scanline data using lacunarity. Lacunarity is a parameter developed for multiscale analysis of spatial data and allows for the determination of scale-dependent changes in spatial structure. Stated simply, lacunarity characterizes the distribution of spaces or gaps in a pattern as a function of scale and can thus quantify scale-dependent clustering in a dataset. It has been demonstrated by Plotnick et al. (1996) that lacunarity versus scale curves of one-dimensional sets will have distinct breaks in slope corresponding to distinct scales within the sets. This technique is therefore well suited for capturing the entire range of heterogeneity in fracture spacing data that may be clustered at one scale while random or even fractal at another.

Our present research focusses on the application of this technique in revealing changes in scale-dependent patterns in 1-d fracture spacing data. We consider four model scanlines with differences in scale-dependent patterns and generate their lacunarity curves in log-log space to test if the curves can delineate the differences. We further introduce the concept of the 1st derivative of the log-transformed lacunarity and demonstrate that this function can determine the inter-cluster spacing and find possible fractal behavior over certain scales. Finally, we test the technique on a set of two natural scanlines, one that comprises fractures occurring in regularly-spaced fractal clusters and another that has randomly-spaced fractures.

2. METHOD DEVELOPMENT

2.1 Synthetic Scanlines

Four synthetic scanlines with spacing data (fig 4.1and, table 4.1) were constructed representing different types of heterogeneities encountered in nature. Model A is a set of fractures spaced equally at 22 length units and representing a homogeneous distribution in space which is typical of "stratabound" fractures found in mechanically-layered rock units (Odling et al., 1999; Riley et al., 2011). Model B is set of five 73 unit-wide fracture clusters spaced at 162 units with fractures within each cluster spaced at 8 units. The NS trending fractures in the map from Telphyn Point, Wales, (Rohrbaugh et al., 2002) and subsequently analyzed by Roy et al (2010) display similar regularly-spaced clusters with somewhat uniformly-spaced fractures within the clusters. Model C is also a set of five 81 unit-wide fracture clusters with inter-cluster spacings of 172, 142, 182 and 152 units (average inter-cluster spacing 162 units). The fractures within each cluster however, are modeled by a randomized Cantor-bar, a fractal model with theoretical fractal dimension of 0.63. Cantor bars have been used in modeling fractures by numerous researchers including Velde et al. (1990), Gillespie et al. (1993), Barton (1995), Chiles (1998) and Kruhl (2013). Model C was created by integrating properties of this fractal and that of model B and serves as an example of a scanline with "clusters of fractures within clusters" (Boadu and Long, 1994). Finally, model D is a set of fractures whose spacing values were picked at random from a

uniform distribution and represents a set of random fractures. Models B, C and D are typically found in mechanically non-layered rocks and are examples of non-stratabound fractures (Gillespie et al., 1999).

Gillespie et al. (1999, 2001) studied the spacings of veins and used the coefficient of variation, C_v, for detecting clustering. This parameter is defined as the ratio of the standard deviation to the mean value of the spaces such that $C_v = 0$ for perfectly periodic fractures, $C_v = 1$ for a random distribution, $C_v > 1$ for clustered fractures, and $C_v < 1$ for anticlustered fractures. Models A and D which are periodic and random patterns yielded C_v values of 0 and 1.2, respectively. Models B and C have C_v values of 2.04 and 2.43 respectively, which are consistent with clustered fractures, however the exact form of the clustering is not revealed by these values.

2.2 Lacunarity and its 1st Derivative

A useful conceptual perspective for understanding lacunarity is to evoke the idea of homogeneity. Consider a uniform sequence of alternating 0's and 1's like 101010101... and so on. This sequence will map onto itself if a copy is made and moved over by two digits so that the original cannot be distinguished from the translated copy. Another pattern like 1000100010001….and so on, will similarly map onto itself if its copy is moved over by four digits. Such homogenous sequences have minimal values in terms of lacunarity because all of the gap sizes (denoted by zeroes in our example) are the same. This behavior is not observed in the case of a slightly more heterogeneous sequence, such as 101000101... where the gaps have a range of sizes including a cluster of three gaps in the middle. Lacunarity quantifies this deviation of a pattern from homogeneity. It is a scale-dependent parameter because sets that are uniform at a coarse scale might be heterogeneous at a finer scale, and vice-versa. Lacunarity can thus be considered a scale dependent measure of textural heterogeneity (Allan and Cloitre, 1991; Plotnick et al., 1993).

Quantifying lacunarity as a function of scale can be achieved by using the gliding-box algorithm (Allan and Cloitre, 1991; Plotnick et al., 1996). For a 1-dimensional sequence of 0's and 1's, this algorithm slides a ruler of a given length, r, translated in increments of a unit length such that the total number of steps is given by $(r_t - r + 1)$, r_t being the length of

the entire sequence. The number of occupied sites, $s(r)$, denoted by 1's and contained within the interrogator box at each step is calculated and a distribution of this parameter at the scale r is obtained by sliding the ruler through all the steps. Finally, the mean, $\overline{s}(r)$, and variance, $ss^2(r)$ of this distribution are used for calculating the lacunarity, $L(r)$, at scale, r as:

$$L(r) = ss^2(r)/\,[\overline{s}(r)]^2 + 1 \quad \ldots\ldots(1)$$

Log-transformed values of lacunarity, log $L(r)$ plotted against log-transformed values of the scale, log r yields a curve that is characteristic of the heterogeneity of the sequence under investigation. If ϕ is the fracture intensity, defined by number of fractures per unit length of a scanline (Ortega et al., 2006), it may easily be proved that L (1) = $1/\phi$ and L (r_t) = 1, such that scanlines with different fracture intensities will have different L (1) values. A uniform sequence like 101010…and so on will have $L(r)$ = 1 at all r values. As pointed out by Plotnick et al. (1996), distinct breaks in the slope of this curve correspond to distinct scale-dependent changes within the sequence. Since fractal patterns are scale-independent, they appear to have the same pattern at all scales they produce straight-lines in the log $L(r)$ vs. log r space.

Plotnick et al. (1995, 1996) cited the example of a sequence of randomly-spaced clusters and how changes in the slope of the lacunarity curve corresponded to changes in the pattern with scale. A visual inspection of the lacunarity curve however, is not sufficient for identifying these breaks in scale. In this paper, we therefore, introduce the concept of the 1st derivative of the lacunarity curve. At each point i, the local slope of the log $L(r)$ vs. log r curve is found by:

$$d[log\ L(r_i)]\ /d[log\ r_i] \ = \ \frac{log\ L(r_{i+1}) - log\ L(r_{i-1})}{log\ r_{i+1} - log\ r_{i-1}} \quad \ldots\ldots(2)$$

This value plotted against log r yields a curve that is easier to interpret because breaks in the slope of the log $L(r)$ vs. log r curve appear as distinct peaks and troughs along a line parallel to the x-axis.

From the equation established by Allain and Cloitre (1991) it can be shown that the lacunarity $L(r)$ at a scale, r and fractal dimension, D of a 1-dimensional fractal sequence are related as:

$$L(r) = k(r)^{D-1} \quad \text{.....(3a)}$$

Here k is any constant. Taking the logs of both sides, Eq. (3a) can be transformed to:

$$\log L(r) = \log k + (D-1)\log(r) \quad \text{.....(3b)}$$

Finally, differentiating Eq. (3b) as in equation (2) will yield:

$$\frac{d[log\ L(r)]}{d[log\ r]} = D - 1 \quad \text{.....(3c)}$$

For a fractal sequence therefore, the local slope in equation (3c) when plotted against log r will yield a straight line parallel to the x-axis with a constant value of D – 1. Figure 3.2 in chapter III illustrates a similar example for the case of a 2-dimenisonal multifractal pattern. A uniform pattern on the other hand, like 101010…and so on, will also plot as a straight line along x-axis but with slope equal to zero, such that D is actually the embedding Euclidean dimension in this case.

3. APPLICATION TO MODEL SCANLINES

Figure 4.2 shows the lacunarity curves for models A-D. The lacunarity curve of model A drops to zero at log $r \sim 1.35$, i.e. $r \sim 22$ and continues along the x-axis thereafter. This behavior is indicative of the fact that the fractures in model A are uniformly-spaced at 22 units. Model B follows model A up to $r \sim 8$ units and then diverges and follows the lacunarity curve of model C. This is happens because at that scale model B behaves as a uniform sequence (like model A) with a constant fracture spacing of 8 units while at a larger scale it appears somewhat similar to model C with its uniformly-spaced fracture clusters as seen in fig 4.1. Model C is linear within the range of the fractal clusters (i.e., between 1 and 81 units), Fitting Eq. (3b) to the lacunarity data over this range of r values using linear regression yielded an estimate of D = 0.6 with an R-square = 0.99. The curve

for model D (random sequence) divides the x-y space into two regions: clustered sequences plot above it while anti-clustered ones plot below. For example, while the curve for model A (uniformly-spaced fractures) lie below that of model D models B and C (evenly-spaced fracture clusters) lie above it.

While the lacunarity curves as described above can delineate overall differences between the models, the subtle breaks in these curves that potentially correspond to major breaks within the sequences are not easy to locate. Hence, it is important to consider their 1st order derivatives that amplify such breaks and can identify finer details of the scale-dependent patterns in the scanlines (Fig. 4.3). The 1st order derivative curve for the uniform model A (fig. 4.3a) breaks at r = 22 units that exactly matches the constant fracture spacing value and thereafter, oscillates about the homogenous line (slope = 0) denoting that the sequence is a uniform one throughout its entire length. The curve for model B has two main slope breaks: the first abrupt jump at r = 8, and the largest trough at r = 161 (Fig. 4.3b). The 1st break is equal to the fracture spacing within the clusters while the 2nd break closely approximates the inter-cluster spacing of 162 units.

Model C breaks at r = 171 which is a large trough as seen in fig. 4.3c. This value matches with the 1st intercluster spacing which is 172 units. To the left of this trough the curve is sub-parallel to the x-axis with only minor peaks and troughs about a line that represents the known fractal dimension of 0.63 for the Cantor-bars used in modeling the clusters. At scales larger than r = 171, the sequence oscillates about the homogenous line (slope $\sim$ 0) like in model B indicating that at these scales (larger than the inter-cluster distance) the sequence is a uniform one. This happens because the fractal clusters are spaced-evenly along the scanline. Model D being random, does not show any specific trend (fig. 4.3d). It can therefore be concluded from our models that lacunarity curves and their slopes can delineate scale-dependent pattern changes within the same scanline as well as the scales at which these changes take place. Patterns that appear clustered at one scale and fractal or uniform over another can be identified. All of the fracture organization parameters extracted from the lacunarity analyses of the synthetic scanlines are summarized in Table 4.1.

4. APPLICATION TO NATURAL DATA

The lacunarity derivative curve for detecting changes in spatial clustering with scale as developed in the last section was applied to two scanline datasets collected from the Monterrey salient, Sierra Madre Oriental, NE Mexico by Gomez (2007). These fracture data constitute veins in carbonate layers of the Lower Cretaceous Cupido Formation. The data were obtained from layers 11 and 13 in the Palmas canyon and are henceforth referred to as P11 and P13 respectively (fig. 4.4a and b). The former is a 21m long scanline with fourteen 220mm wide fractal clusters spaced at about 1.1m. The clusters have a fractal dimension of 0.42 (Gomez, 2007; table 7.2 therein). P13 is a 5.5m long scanline with randomly arranged fractures (Gomez, 2007). The data were discretized on the millimeter scale following the scheme of Priest and Hudson (1976). A unit length is 1mm such that 1mm spacing is represented by a 0 and a fracture by 1 thus yielding a sequence of zeros and ones, essentially, a 1-dimensional binary data set. The coefficient of variation parameter (Gillespie et al., 1999) yielded a value of C_v = 1.7 for P11 which indicates a clustered sequence. For P13, C_v = 0.9 indicating a near random arrangement.

Figure 4.5 shows the lacunarity curves of P11 and P13. The former has 257 recorded fractures along a 21m line (fracture intensity, ϕ = 0.012) while the latter has 459 fractures along a 5.5m line (ϕ = 0.083). This difference in fracture intensities (which is clearly apparent visually in fig. 4.4) leads to the offset in L-values at r = 1 given by $1/\phi$, such that log L (1) of P11 is 1.92 and that of P13 is 1.08. The straight line segment of the P11 lacunarity curve indicates a constant slope and as seen from equation (3b). This behavior implies a fractal organization over the scale of the segment in question. This is comparable to model C (fig. 4.2) which is comprised of fracture clusters with fractal organization within. It may be noted here that the coefficient of variation parameter for P11 (C_v = 1.7) and model C (C_v = 2.43) are very different and fails to recognize this similarity. P13 has a concave-up lacunarity curve similar to that for the random population of fractures in model D (fig. 4). This is consistent with the findings of Gomez (2007) that P13 is populated by randomly distributed fractures.

Fig. 4.6a is the 1st order derivative of the lacunarity curve of P11 and is comparable to that of model C in the previous section. Between scales of $r \sim 25$ mm and 740 mm (i.e., log $r \sim 1.4$ and 2.87) the pattern shows a relatively flat line thus indicating a fractal organization. These bounds are similar to the bounds of 12 mm and 664 mm found by Gomez (2007). The fractal dimension, D of fractures within the clusters was found from fitting a linear model to this segment between $r \sim 25$mm and 740mm in the log $L(r)$ vs. log r curve that yielded an $R^2 = 0.99$ and applying equation (3b). The resulting value of $D \sim 0.52$ is slightly higher than the value of $D = 0.44$ found by Gomez (2007). Beyond $r \sim 740$ mm the sequence starts to approach uniform behavior indicating that the clusters themselves are spaced at regular intervals just as in model C. A major difference being that P11 has fractures in the inter-cluster regions. This is the reason that the transition from fractal to uniform behavior is more continuous and there is no distinct trough as seen in fig. 4.3c. The different fracture organization parameters extracted by lacunarity analyses of the P11 scanline data are summarized in Table 4.1.

Fig. 4.6b is the 1st order derivative of the lacunarity curve of P13 and is very unlike those of models A, B or C in fig 4.3. Also, it has no sharp breaks in its slope indicating that it behaves the same way at all scales. Although there seems to be some differences between P13 and random model D in terms of their lacunarity derivative curves, their lacunarity curves look similar as discussed in the last paragraph and it may therefore be concluded that P13 is indistinguishable from a random distribution at all scales.

5. DISCUSSION

The 1st order derivative of lacunarity curves can be used to detect breaks in the slope of the lacunarity curve in order to find scales at which a pattern changes its spatial distribution. For clustered populations, plotting the slope against the scale can reveal the inter-cluster spacing and possible fractal or random organization within the clusters. Further, where fractures within a cluster are periodically spaced, the spacing at that scale can also be found as with model B. This kind of analysis is important where wells in a fractured formation need to be perforated to target fractures that conduct flow. For

example, model B (uniform clusters) has an average fracture spacing of 22 units, the same as that of model A, but the former has an inter-cluster spacing of 162 units. Likewise, natural scanline P11 has an average fracture spacing of 78 mm but the fracture actually present in clusters that are uniformly spaced when observed at scales larger than r = 740 mm. It can be clearly seen that information on the spacing of clusters and their spatial organization obtained from lacunarity analysis will prove to be more useful than data on the average spacing and C_v parameter when drilling exploration/production wells in formations that house clusters of fractures.

Consequently, the use of lacunarity derivative curves can find changes in spatial distributions at different length scales within the same scanline, including the type of cluster (fractal vs. uniform vs. random). Our technique, like most others, considers only fracture spacing in determining scale-dependent heterogeneity. As such, fracture clusters and intercluster distances may be determined for situations such as perforating well-casings the technique does not include a consideration of the individual fractures in terms of parameters such as aperture and length. It would be useful to be able to add fracture aperture to the analysis because it is the widest fractures that contribute to most of the flow within a system. Additionally, wide fractures are important because they account for most of the strain accommodated. Therefore, a further improvement to this new technique would be to include data about fracture widths together with spacing in order to test if large fractures occur inside clusters. This topic is discussed in the next chapter of this dissertation.

REFERENCES

Allain, C. and Cloitre, M., 1991, Characterizing the lacunarity of random and deterministic fractal sets, *Phys. Rev. A.* vol. 44, no. 6, 3552-3558

Barton, C.C., 1995, Fractal analysis of scaling and spatial clustering of fractures, p. 141-178 in Barton C. C., and La Pointe, P., eds., *Fractals in the Earth Sciences*, Plenum, New York, 265pp.

Boadu, F.K. and Long, L.T., 1994, The fractal character of fracture spacing and RQD, *Int. J. Rock Mech. Min. Sci. & Geomech. Abstr.*, vol. 31, no. 2, 127-134

Chiles, J. P., 1988, Fractal and geostatistical methods for modeling of a fracture network, *Math. Geol.*, vol. 20, no. 6, 631-654

Gillespie, P.A., Howard, C.B., Walsh, J.J., Watterson, J., 1993, Measurement and characterization of spatial distributions of fractures, *Tectonophysics,* vol. 226, 113-141

Gillespie, P., Johnston, J.D., Loriga, M.A., McCaffrey, K.J., Walsh, J.J. and Watterson, J., 1999, Influence of layering in vein systematics in line samples; in *Fractures, Fluid Flow and Mineralization*

Gillespie, P.A., Walsh, J.J., Watterson, J., Bonson, C.G., Manzocchi, T., 2001, Scaling relationships of joint and vein arrays from The Burren, Co. Clare, Ireland, *Journal of Structural Geology,* vol. 23, 183-201

Gomez, L., 2007, Characterization of the Spatial Alignment of Opening-mode Fractures, PhD Dissertation, The University of Texas at Austin, 844 pp.

Kruhl, J.H, 2013, Fractal-geometry techniques in the quantification of complex rock structures: A special view on scaling regimes, inhomogeneity and anisotropy, *Journal of Structural Geology*, vol. 46, 2-21.

La Pointe, P.R. and Hudson, J.A., 1985, Characterization and interpretation of rock mass joint patterns, *Geological Society of America*, Special Paper 199.

Narr, W. and Suppe, J., 1991, Joints spacing in sedimentary rocks, *Journal of Structural Geology*, vol. 13, no. 9, 1037-1048.

Odling, N.E., Gillespie, P., Bourgine, B., Castaing, C., Chiles, J.P., Christensen, N.P., Fillion, E., Genter, A., Olsen, C., Thrane, L., Trice, R., Aarseth, E., Walsh, J.J., Watterson, J., 1999, Variations in fracture system geometry and their implications for fluid flow in fractured hydrocarbon reservoirs, *Petroleum Geoscience*, vol. 5, p.373-384.

Ortega, O., Marrett, R. and Laubcah, S.E., 2006, A scale-independent approach to fracture intensity and average spacing measurement, *AAPG Bulletein,* vol. 90, no. 2, 193-208.

Plotnick, R.E., Gardner, R.H., O'Neill, R.V., 1993, Lacunarity indices as measures of landscape texture, *Landscape Ecology*, vol. 8, no. 3, 201-2011.

Plotnick, R.E., 1995, Introduction to fractals, p. 1-28, in Middleton, G.V., Plotnick, R.E, Rubin, D. eds., *Nonlinear Dynamics and Fractals: New Numerical Techniques in for Sedimentary Data. SEPM Short Course No. 36*, SEPM, Tulsa

Plotnick, R.E., Gardner, R.H., Hargrove, W.W., Prestegaard, K., Perlmutter, M., 1996, Lacunarity analysis: A general technique for the analysis of spatial patterns, *Phys. Rev. E.* vol. 53, no. 5, 5461-5468.

Priest, S.D. and Hudson, J.A., 1976, Discontinuity spacings in rock, *Int. J. Rock Mech. Min. Sci. & Geomech. Abstr.*, vol. 13, 135-148.

Riley, P., Tikoff, B and Murray, A.B., 2011, Quantification of fracture networks in non-layered, massive rock using synthetic and natural data sets, *Tectonophysics*, v. 505, 44-56.

Rohrbaugh, M.B., Dunne, W.M. and Mauldon, M., 2002. Estimating fracture trace intensity, density and mean length using circular scan lines and windows, *AAPG Bulletein,* vol. 86, no. 12, 2089-2104.

Roy, A., Perfect, E., Dunne, W.M., Odling, N. and Kim, J. (2010), Lacunarity analysis of fracture networks: Evidence for scale-dependent clustering, *Journal of Structural Geology*, vol. 32, 1444-1449.

Velde, B., Dubois, J., Touchard, G., Badri, A.,1990, Fractal analysis of fractures in rocks, *Tectonophysics,* v. 179, 345-352.

APPENDIX IIIA: TABLES

Table 4.1. Model and estimated (from lacunarity analyses) fracture organization parameters: fracture spacing, intercluster spacing, spacing within clusters, and fractal dimension (*D*)

Scanline	Organization	Parameter (model)	Parameter (estimated)
model A	periodic fractures	fracture spacing = 22	fracture spacing = 22
model B	periodic clusters (periodic within)	intercluster spacing = 162 spacing within clusters = 8	intercluster spacing = 161 spacing within clusters = 8
model C	periodic clusters (fractal within)	intercluster spacing = 162 *D* of clusters = 0.63	periodic @ scale > 170 *D* of clusters = 0.60
model D	random fractures	n/a	-
data P11	periodic clusters (fractal within)	n/a	periodic @ scale > 0.74m *D* of clusters = 0.52
data P13	random fractures	n/a	-

n/a: not applicable

APPENDIX IIIB: FIGURES

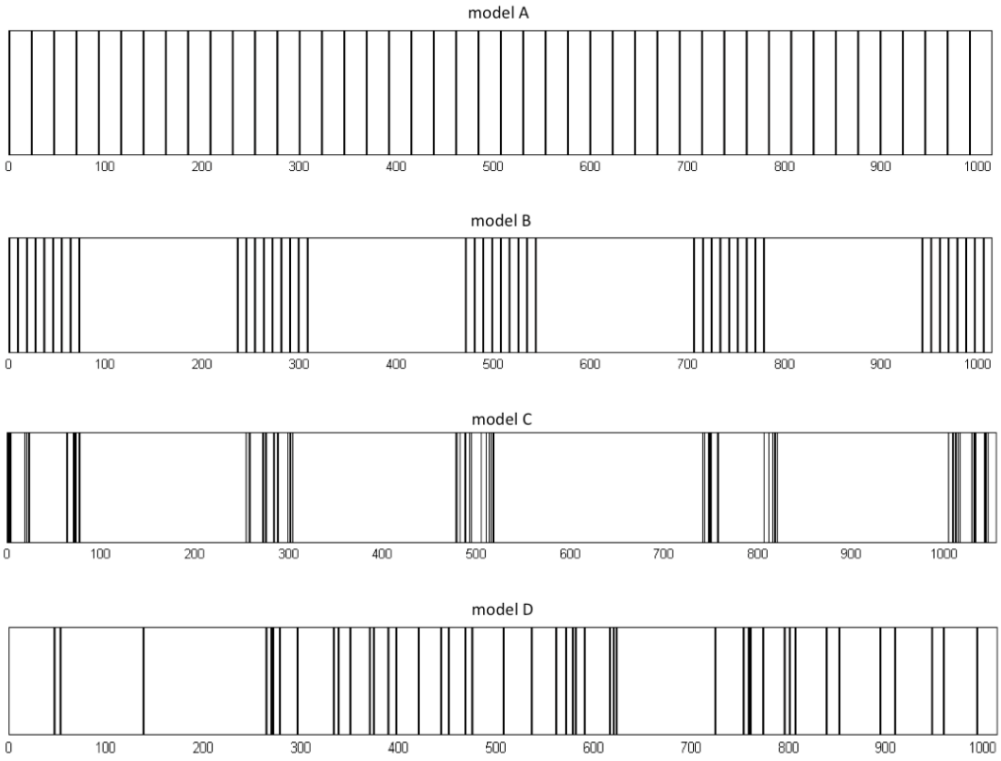

Figure 4.1. Model scanlines, x-axis denotes positions of fractures along a line (a) model A: uniformly spaced fractures, spacing = 22 units. (b) model B: equally spaced uniform (spacing = 8 units) clusters spaced at 162 units, cluster width = 73 units. (c) model C: regularly spaced fractal (cantor-bar, D = 0.63) clusters, avg. spacing = 162 units. (d) model D: randomly spaced fractures with avg. spacing = 21 units. y-axis = 0 for no fracture, 1 for a fracture.

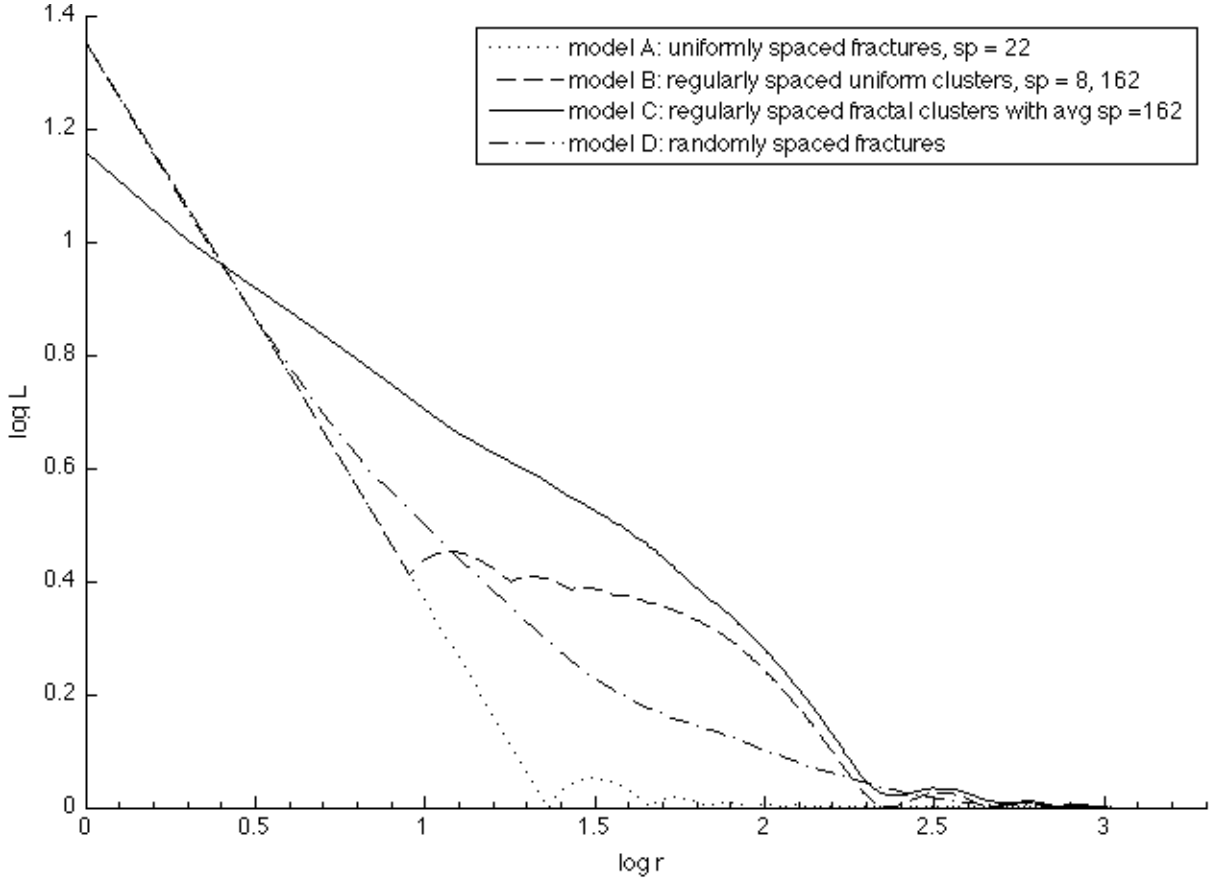

Figure 4.2. Lacunarity curves for model scanlines A, B, C and D. Note the range of scale over which model B coincides with model A showing that B is uniform over that range

Figure 4.3. Lacunarity slopes for models A, B, C and D. Breaks in slope correspond to spacings at given scales e.g. model B, breaks at log $r \sim 0.9$ ($r = 8$) and log $r \sim 1.35$ ($r = 22$) denotes spacing within clusters and spacing between clusters

4.3 (a)

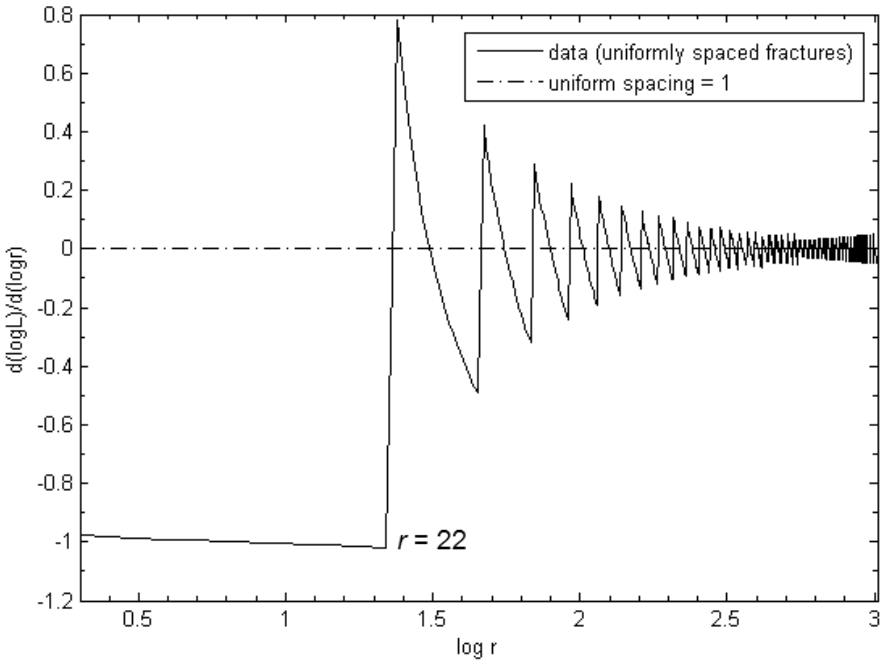
data (uniformly spaced fractures)
uniform spacing = 1
r = 22
d(logL)/d(logr)
log r

4.3 (b)

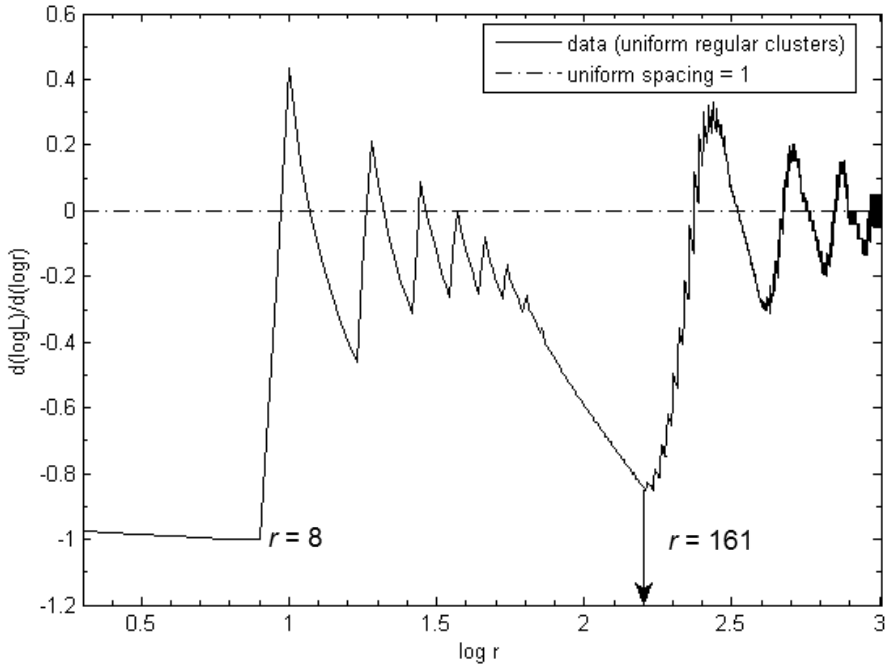
data (uniform regular clusters)
uniform spacing = 1
r = 8
r = 161
d(logL)/d(logr)
log r

4.3 (c)

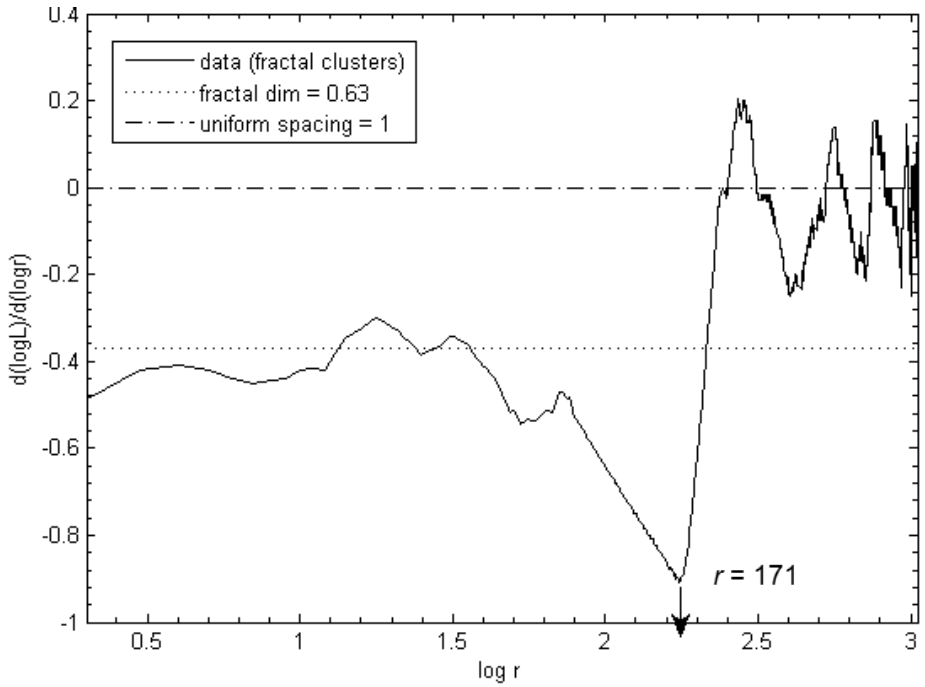
data (fractal clusters)
fractal dim = 0.63
uniform spacing = 1
r = 171
d(logL)/d(logr)
log r
0.4
0.2
0
-0.2
-0.4
-0.6
-0.8
-1
0.5
1
1.5
2
2.5
3

4.3 (d)

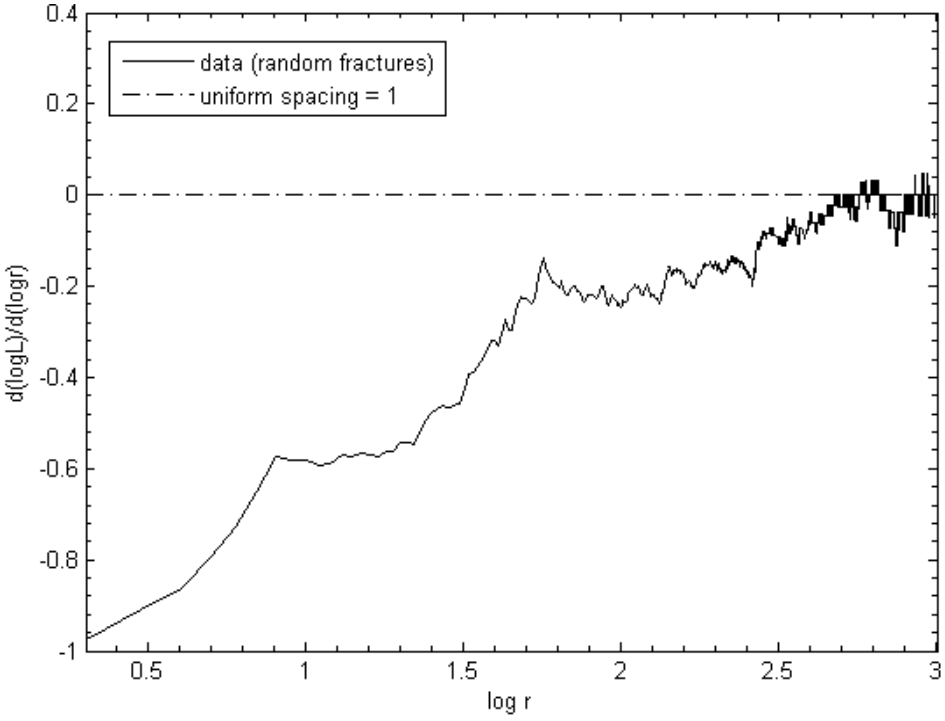
data (random fractures)
uniform spacing = 1
d(logL)/d(logr)
log r
0.4
0.2
0
-0.2
-0.4
-0.6
-0.8
-1
0.5
1
1.5
2
2.5
3

(a)

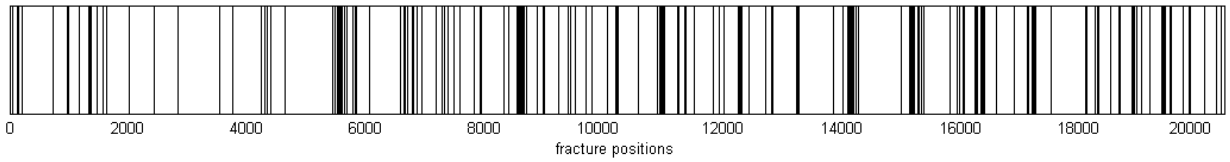

(b)

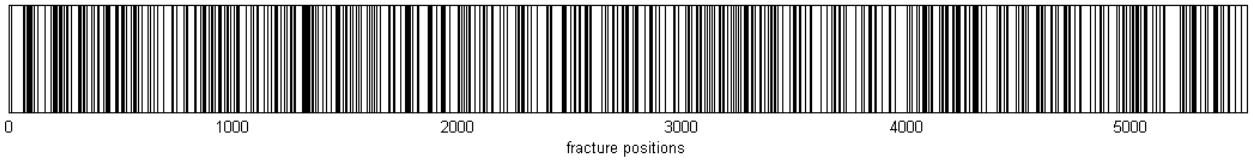

Figure 4.4. Natural scanlines from Gomez (2007) where fractures are shown by lines: (a) P11: fractal clusters and (b) P13: random fractures. Note differences in fracture intensity (ϕ). x-axis denotes positions of fractures. y-axis = 0 for no fracture, 1 for a fracture.

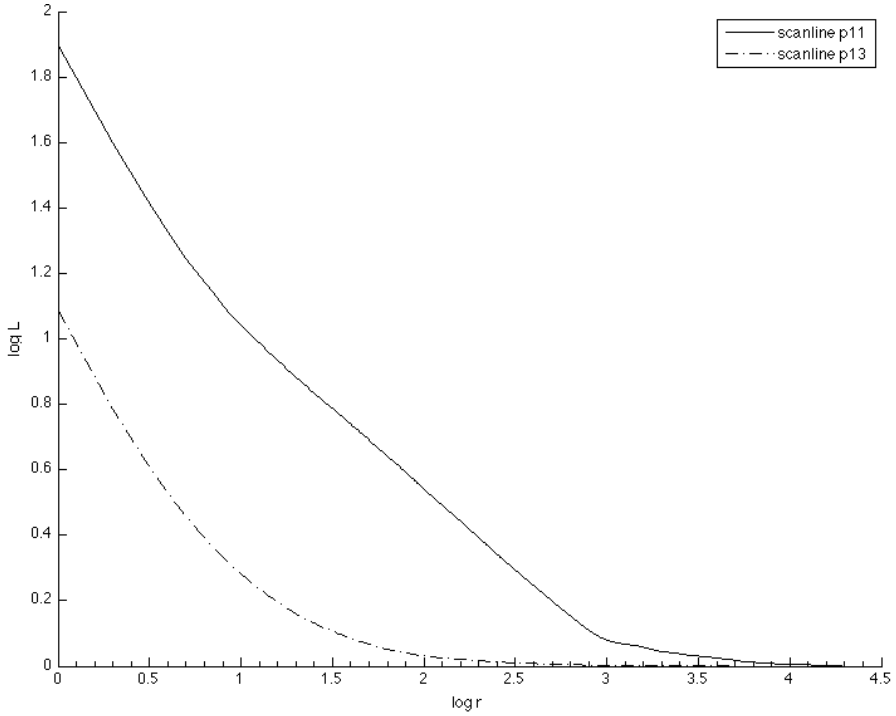

Figure 4.5. Lacunarity curves for natural scanlines P11 and P13. The two are offset because P11 has a lower intensity, hence higher lacunarity than P13.

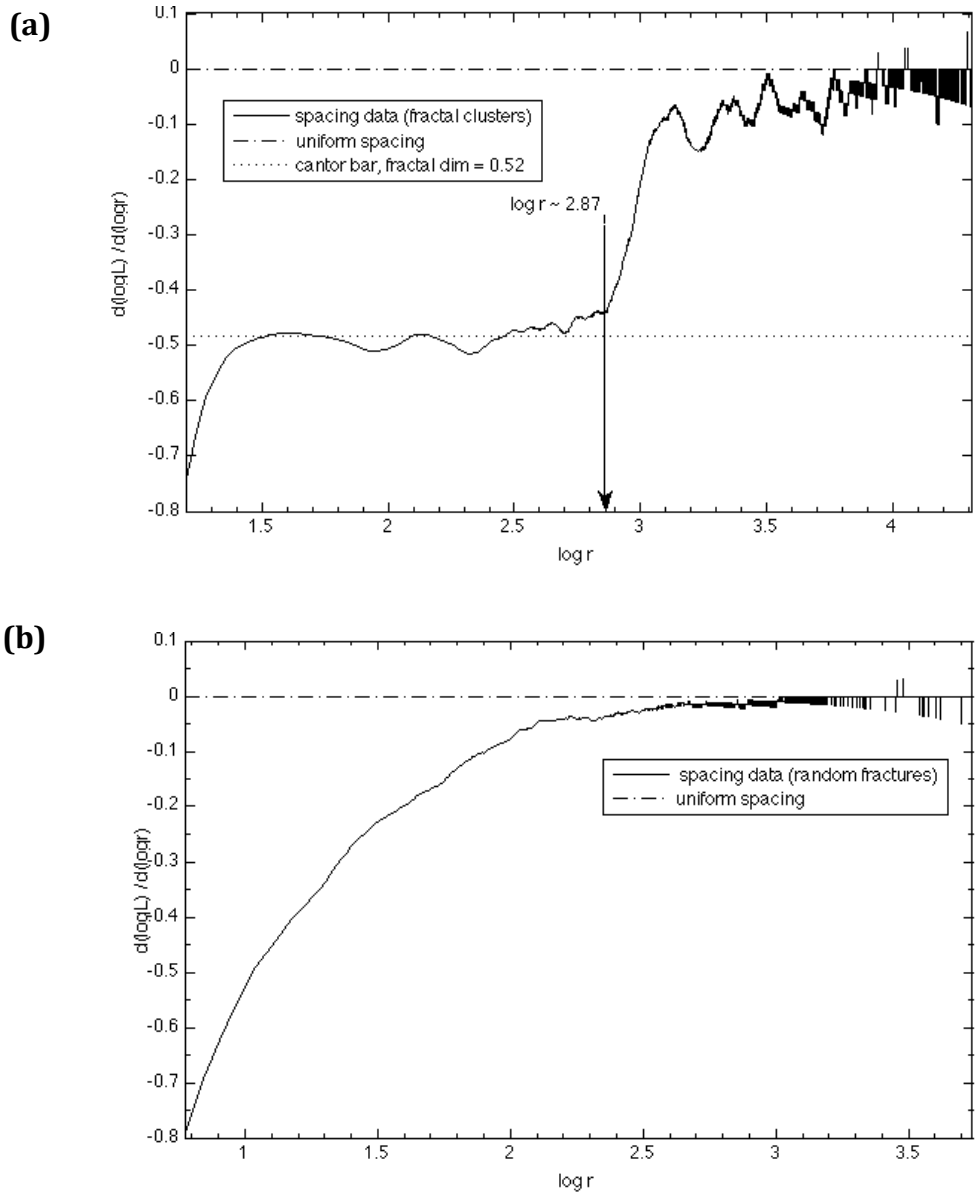

Figure 4.6. Lacunarity slopes for natural data. (a) P11 showing fractal (D = 0.52) and uniform behavior at different scales (b) P13 indistinguishable from random.

A Technique for Revealing Scale-dependent Patterns in Scanline Data: II. Fracture Aperture

Chapter V: A manuscript for submission to Journal of Geophysical Research

Ankur Roy & Edmund Perfect
Potential Co-authors: William M. Dunne

ABSTRACT

Scanline data about fracture spacing and size attributes such as aperture/length are mostly considered in separate studies that compute the cumulative frequency of these attributes without regard to their actual spatial sequence. In a previous study, we showed that spacing data can be analyzed using lacunarity to identify whether fractures occur in clusters. However, to determine if such clusters also contain the largest fractures in terms of a size attribute such as aperture, it is imperative that data about the size dimension be integrated with information about fracture spacing. While for example, some researchers have considered aperture in conjunction with spacing, their analyses were either applicable only to a specific type of data (e.g. multifractal) or failed to characterize the data at different scales. Lacunarity is a technique for analyzing multi-scale non-binary data and is ideally-suited for characterizing scanline data with spacing and aperture/length values. We present a technique that can statistically delineate the relationship between size attributes and spatial clustering. We begin by building a model scanline that has complete partitioning of fractures with small and large apertures between the intercluster regions and clusters. We demonstrate that the ratio of lacunarity for this model to that of its counterpart for a completely randomized sequence of apertures can be used to determine whether large-aperture fractures preferentially occur next to each other. The technique is then applied to two natural fracture scanline datasets, one with most of the large apertures occurring in fracture clusters, and the other with more randomly-spaced fractures, without any specific ordering of aperture values. The lacunarity ratio clearly discriminates between these two datasets and, in the case of the first example, it is also able to identify the range of scales over which the widest fractures are clustered. The technique thus developed can help in identifying the spatial distribution of fractures in terms of a size attribute such as aperture or length.

1. INTRODUCTION

Quantifying fracture spacing and attributes such as aperture, displacement and length is important for better understanding the geometric arrangement of fractures and their genesis. Research in this area has focused on the use of cumulative frequency plots (Gillespie et al., 1993; Manning, 1994) and parameters like the coefficient of variation (Gillespie et. al., 1999) and fracture spacing index (Narr and Suppe, 1991). Cumulative frequency analyses have also been independently reported for other fracture/fault attributes such as aperture, displacement, and length (Ouillon et al., 1996; Marrett et al., 1999; Gillespie et al., 2001; deJossineau and Aydin, 2007).

The applicability of the above approaches, however, is limited in two ways. First, cumulative frequency plots and parameters such as the coefficient of variation consider fractures at only the scale of the entire population. They do not provide any information about the spatial distribution of fractures. As a result, geostatistical and fractal analyses have been applied to quantify the heterogeneity of fracture networks with respect to these characteristics over various ranges of spatial scales. Semivariograms have been used to determine the spatial dependence of the variance in fracture density and frequency (LaPointe and Hudson, 1985; Chiles, 1988). Fractal analysis (La Pointe, 1988; Berkowitz and Hadad, 1997; Roy et al., 2007), on the other hand, has mostly focused on finding power-law behavior, i.e. it is strictly applicable to limited set of scale-invariant features.

The second limitation is that, although cumulative frequency studies of fracture length or aperture are helpful for determining their size-distributions, they do not tell us anything about their covariance. To address this issue, Belfield (1994) integrated fracture spacing along horizontal wellbores with their aperture values and showed that the data display multifractal behavior. However, it is unlikely that this approach will have general applicability, since all such data may or may not scale as a multifractal. More recently, Tran (2004) applied the cross-variogram from geostatistics to characterize the spatial relationship between fracture size and orientation.

Lacunarity analysis, which is a technique developed for multiscale analysis of spatial data, may also be employed for overcoming the limitations discussed above. The goal of

this paper is to develop and evaluate an alternative statistical characterization for the spatial co-variance of fracture attributes based on lacunarity. Lacunarity can be used to overcome the first limitation referred to above, and has been previously employed for characterizing clustering in binary fracture maps (Roy et al., 2010) and scanline data (Roy et al., 2013). Since lacunarity is applicable to both binary and non-binary data sets, we also apply the technique to overcome the second limitation by analyzing fracture spacing data that are integrated with their corresponding normalized aperture values, thus yielding a dataset comprised of zeros and fractions. In this research, we use the term non-binary to denote such data. The advantage of this approach is that both spacing and aperture values can be analyzed simultaneously.

We start by building a model scanline where fractures with large apertures are restricted to clusters and small apertures are present only in the inter-cluster regions. We then introduce the concept of the lacunarity ratio for demonstrating that this technique can statistically identify the spatial distribution of large fractures with respect to fracture clusters. It is worth noting that the technique developed here is applicable to data sets where spacing has been integrated with any other fracture attributes. Thus, it can analyze spatial variation in length, aperture or displacement in the case of faults. We test this technique on a set of two natural scanlines with spacing and aperture data, one that comprises fractures occurring in regularly-spaced clusters and another that has more randomly- spaced fractures with no particular organization of apertures.

2. METHOD DEVELOPMENT

2.1 Generation of Model Scanlines

Roy et al. (2013) document four synthetic scanlines comprised of only fracture spacing values of which model A is a set of fractures spaced equally at 22 length units and model C a set of five 81-unit wide fracture clusters with an average inter-cluster spacing of 162 units. Similar models were previously employed by Velde et al. (1990), Gillespie et al. (1993) and Chiles (1998) for analyzing fracture spacing. For the present study, two new

model scanlines, A1 and C1 (fig. 5.1), were constructed from models A and C respectively, by adding apertures drawn from a uniform distribution. The apertures were then normalized to sum to unity so that different datasets covering various aperture scales can be analyzed. Finally, a new model E (fig. 5.2a) was generated by populating the inter-cluster spaces of model C1 with model A1 after reducing the apertures of the latter by an order of magnitude. Model E thus represents an extreme case of large (wide) fractures occurring preferentially within clusters and small fractures present at regular intervals only in the inter-cluster spaces. Random versions of model E, denoted by E*, were also generated in which the sequence of aperture values was randomized while keeping the spaces between fractures unaltered. This was done so that the clustering in E arising from two different effects, the spatial distribution of fractures and presence of large aperture values next to each other, can be separated. One such random realization of E is illustrated in fig. 5.2b.

2.2 Lacunarity and its Quantification

Lacunarity is a parameter that characterizes the distribution of spaces or gaps in a binary pattern as a function of scale and quantifies the degree of clustering at a given spatial resolution. It is applicable to both binary (e.g., fracture spacing) and non-binary data (e.g., fracture spacing with aperture). We begin by considering binary data first. A uniform sequence of alternating 0's and 1's like 1001001001001... and so on, will map onto itself if a copy is made and moved over by three places so that the original cannot be distinguished from the translated copy because the gap sizes are same. This behavior is not observed in the case of a slightly more heterogeneous sequence, such as 101000101... where the gaps have a range of sizes, including a cluster of three gaps in the middle; the greater the degree of gap clustering, the greater the lacunarity. In the case of a non-binary pattern like (1/25) 0 0 (1/3) 0 0 (1/7)… where the ones are replaced by fractional values, there will still be some lacunarity. Even though the gap sizes in this case are same as in the first binary example, the non-zero values have a distribution such that the pattern will not map onto itself if a copy is made and moved over by three places as before. The pattern is therefore, heterogenous. In essence, lacunarity is a scale-dependent measure of this heterogeneity (Allan and Cloitre, 1991; Plotnick et al., 1993).

Quantifying lacunarity as a function of scale can be achieved by using the gliding-box algorithm (Allan and Cloitre, 1991; Plotnick et al., 1996). For a 1-dimensional sequence, this algorithm slides a ruler of a given length, r, translated in increments of a unit length such that the total number of steps is given by $(r_t - r + 1)$, where r_t is the length of the entire sequence. The total mass (i.e., the sum of the normalized aperture values in our case) contained within the interrogator box at each step, $s(r)$, is calculated and a distribution of this parameter at the scale r is obtained by sliding the ruler through all the steps. Finally, the mean, $\bar{s}(r)$, and variance, $s^2(r)$ of this distribution are used in calculating the lacunarity, $L(r)$, at scale, r as:

$$L(r) = [s^2(\mathrm{r}) / \{\bar{s}(r)\}^2] + 1 \quad \ldots\ldots(1)$$

Log-transformed values of the lacunarity, log $L(r)$, plotted against log-transformed values of the scale, log r, yield a curve that is characteristic of the heterogeneity of the sequence under investigation. It can easily be shown that sequences with the same set of aperture values, but with different spatial distributions, will have the same maximum lacunarity, $L(1)$, where $L(1)$ is the lacunarity evaluated at $r = 1$ (Roy et al., 2010). In other words, all random realizations of a scanline will have equal $L(1)$ values. Also, at $r = r_t$, where r_t is the total length of the scanline, the lacunarity is $L(r_t) = 1$ (Roy et al, 2010). As pointed out by Plotnick et al (1996), distinct breaks in the slope of the log $L(r)$ curve that occur between these limiting values correspond to distinct scale-dependent changes within the sequence.

2.3. The Lacunarity Ratio

To delineate the degree of scale-dependent clustering in a sequence of γ-ray peaks (binary data) from a well-log Plotnick et al (1996) analyzed its lacunarity and compared it with the lacunarity of a randomized version of the same data. Plotted in log-log space, greater scale-dependent lacunarity values of the dataset compared to its randomized counterpart implied greater clustering. In the case of non-binary data, higher lacunarity with respect to a randomized sequence can arise because of clustering in two different aspects of the data set. For the specific example of model E, these two aspects are fracture spacing and fracture aperture values. Even in a uniformly-spaced fracture sequence, wide

fractures occurring preferentially next to each other will generate greater lacunarity values. Examples of other non-binary sequences where such compound clustering may arise from two different aspects of the data can be found in various fields of science that investigate spatially- or temporally-distributed data like, for example, changes in the pH of precipitation with time.

Clustering arising from the spacing of such sequences may be identified by simply ignoring the values at each data point (i.e., the apertures in model E). Considering only the spacing values and finding the lacunarity of the binary sequence thus generated can help identify spatial (or temporal) clustering of the points (i.e., the fractures in model E). However, simply analyzing the values at each data point and ignoring the spacing in between would not help in delineating if large values are found in clusters next to each other in space or time. Therefore, to identify clustering arising from the ordering of the apertures in model E, the lacunarity should be compared to random sequences where the spacing's are left unaltered but the sequence of aperture values is randomized (e.g., model E* in Fig. 2b).

To better visualize this type of clustering, we compute the scale-dependent lacunarity ratio, *LR(r)*, of a dataset with respect to the average its randomized counterparts, $\langle L(r) \rangle$, such that at any given scale, *r*, the ratio is given by:

$$LR(r) = \frac{L(r)\ of\ original\ data}{\langle L(r) \rangle\ of\ randomized\ data} \quad \text{.....(2)}$$

Based on this definition, a random aperture data set compared to itself will plot as a horizontal line with $LR(r) = 1$ at all scales or values of *r*, where log *r* is plotted along the x-axis of the graph. Therefore, for comparing the clustering of the apertures in model E (Fig. 5.2a) to their random counterparts, such as model E* (Fig. 5.2b), we generated 10 random realizations of E and computed the scale-dependent lacunarity curves of each. An average random lacunarity curve $\langle L(r) \rangle$, was found by computing the arithmetic mean of all 10 random lacunarity curves and is plotted along with the upper and lower 95% confidence intervals in Fig. 5.3a. When compared to the lacunarity values as a function of log *r* for model E, the $\langle L(r) \rangle$ curve for the randomized scanlines has smaller values of lacunarity at

all scales. This result demonstrates that the spatial clustering of fractures with respect to aperture values in model E can be identified using lacunarity. The narrow range between the upper and lower 95% confidence intervals around $\langle L(r) \rangle$ indicates that 10 random realizations can be safely assumed to be sufficient for our purpose.

The lacunarity-ratio for model E was determined by comparing its $L(r)$ curve to that of the $\langle L(r) \rangle$ curve for the random realizations (equation 2). The upper and lower 95% confidence intervals and their corresponding lacunarity ratios were also computed by comparing their $L(r)$ curves to that of the $\langle L(r) \rangle$ curve. Plotted as a function of scale, the lacunarity ratio for model E shows a broad peak substantially higher than the upper 95% curve and spanning the entire range of scales (fig. 5.3b). It is thus statistically more clustered (at the 95% confidence level) than the average curve generated from model E by randomizing the sequence of apertures. This clearly demonstrates that at all scales of observation, model E has large apertures that are present in clusters. This happens because large and small apertures are completely partitioned between the clusters and the inter-cluster regions respectively, along the scanline.

The broad peak in the curve as described above drops off to a local minima at r = 237 ($\log r \sim 2.38$). This value is approximately equal to the sum of the cluster width and average inter-cluster distance, 81 and 162 units respectively, totaling to 243 units. In other words, the $LR(r)$ curve also provides information about the fracture spacing that was not evident from the raw lacunarity curves.

3. APPLICATION TO NATURAL DATA

The lacunarity-ratio technique described above was applied to natural data from two scanlines, each consisting of spacing and aperture values, collected from the Monterrey salient, Sierra Madre Oriental, NE Mexico (Gomez, 2007). These fracture data are from veins in carbonate layers of the Lower Cretaceous Cupido Formation. The scanlines were obtained from layers 11 and 13 in the Palmas canyon and are henceforth referred to as P11 and P13 respectively (fig. 4a and b). The former is a 21 m long scanline with 257 recorded

fractures of apertures larger than 0.95 mm in fourteen 22cm wide clusters spaced at about 110 cm. P13 is a 5.5 m long scanline with 459 randomly-arranged fractures of apertures greater than 0.5 mm.

The first part of this research used only the spacing values from these data sets for identifying presence of fracture clusters (Roy et al., 2013). For our present analyses we include both spacing and aperture values. The data were discretized on the millimeter scale following the scheme of Priest and Hudson (1976), where 1 mm spacing is represented by a 0 and a fracture by 1. Given that the data contain a unique value for each aperture, the fracture was represented by its normalized aperture value, i.e. its aperture width divided by the sum of all aperture widths for that scanline (Belfield, 1994). Since the normalized aperture is a fraction, the discretization yields a sequence of zeros and fractions, i.e., a 1-dimensional non-binary data set. Our discretization scheme is thus a combination of the approaches of Priest and Hudson (1976) and Belfield (1994).

Figure 5.5a shows the lacunarity-ratio, $LR(r)$, curve of P11 generated by comparing its $L(r)$ curves to that of the averaged random $L(r)$ curve as was done for model E in the previous section. Again 10 random realizations were used to construct $\langle L(r) \rangle$. The results may be considered as somewhat of a variation of model E. The major difference being that large and small fractures aren't completely partitioned between the clusters and inter-cluster spaces, such that large and small apertures can be found both within the clusters and in the inter-cluster regions, as may be expected with a natural example. Therefore, the degree of clustering of the apertures is less, producing a peak at a value of LR = 1.09 as compared to LR = 1.71 for model E. This means that compared to their respective averaged random counterparts P11 is 9% more clustered whereas model E is 71% more clustered at its maximum.

Furthermore, as opposed to model E, for P11 the scale of observation over which the clustering is statistically significant is quite limited. This is defined by the points where the P11 LR-curve crosses the upper 95% confidence interval curve. These are log $r \sim 2.37$ and 3.03 i.e. $r \sim$ 23cm and 107 cm (fig. 5.5a). As seen from the analysis of Gomez (2007), these values are very close to that of the average values of the cluster width and inter-

cluster distance, respectively. This means that at scales of observation less than the cluster width it is difficult to ascertain if the observed fractures are part of a cluster, or if they populate the entire scanline. On the other hand, if the window of observation coincides with an inter-cluster region, which may happen if r is equal to the average inter-cluster width, it will not be possible to determine if there are clusters with large fractures present in other regions of the scanline. In other words, the presence of large fractures occurring next to each other can be best observed between scales corresponding to the cluster width and inter-cluster distance, respectively, since large fractures are statistically found within the clusters.

At scales greater than $\log r \sim 3.6$, i.e. $r \sim 4$m, the *LR*-curve crosses the lower 95% confidence bound. This is so because the clusters in which these large apertures occur are regularly-spaced themselves (Roy et al., 2013), such that at an observation window larger than 4-m wide, fractures will appear to be anti-clustered. Finally, just as in model E, the peak in this curve is followed by a minimum at $\log r \sim 3.1$ ($r \sim 126$cm). This value is almost equal to the sum of the average cluster width and the average inter-cluster distance, 23 cm and 107 cm respectively (totaling to 130 cm), reported previously by Gomez (2007).

Fig. 5.5b is the lacunarity-ratio curve for P13. For most scales this curve lies within the upper and lower 95% confidence intervals. The *LR*-curve never crosses the upper 95% confidence interval indicating that there is no clustering of apertures i.e., large fractures are not statistically found to be occurring next to each other. Therefore P13 is a sequence of randomly-spaced fractures (Roy et al., 2013) with no preferential arrangement of fracture apertures. Our technique therefore yields results in agreement with Gomez (2007) that P11 has fracture clusters with large apertures preferentially occurring within such clusters, and that P13 is a sequence of randomly-arranged fracture apertures.

4. DISCUSSION AND CONCLUSIONS

There are a number of techniques available for characterizing fracture spacing and attributes like aperture or length. While most of these techniques consider aperture and

spacing data separately, Gillespie et al (1999) plotted the cumulative aperture against spacing, known as "staircase plots", for differentiating between stratabound and non-stratabound fractures. Tran (2004) used the cross-variogram to relate two independent fracture attributes as a function of scale. Belfield (1994) integrated fracture spacing and aperture by treating the dataset as a multifractal. Gomez (2007) documents a method based on the technique developed by Belfield (1997) that creates subsets of the data by placing artificial thresholds on fracture aperture. This method then determines the clustering of fractures in these subsets pertaining to various aperture size ranges and finds whether large ones are more clustered than smaller ones. It is however, always desirable that there should be minimum alteration of data while running any statistical analysis.

We have devised a new technique for characterizing the clustering of fractures in terms of spacing and one other attribute at different spatial scales based on lacunarity. Our approach involves finding the lacunarity-ratio, *LR* of a 1-dimensional sequence of apertures and spacing values to that of its average random counterpart created by randomizing the ordering of the aperture values while maintaining the original fracture spacing's. This approach is equally applicable to any data set that contains values of a single parameter that is either spatially or temporally distributed. In fracture analysis, spatially-distributed aperture values may be replaced by length or orientation data and it may be determined if long fractures or fractures along any specific direction are statistically found next to each other. In the case of time series such as, for example, rainfall data, this technique could be used to delineate trends in pH within individual precipitation events.

The technique developed here has been used to essentially address the question: "*do large fractures occur statistically within clusters*?" It has been demonstrated in this research that the technique returns similar results when compared to that of Gomez (2007), the advantage being that it does not require taking artificial subsets of the original data. In addition, this technique can identify the cluster width and the intercluster distance in a scanline. Therefore, it is seen that adding a size attribute to spacing values, thus creating a non-binary data set, and analyzing it for lacunarity represents a significant advance with respect to our earlier research (Roy et al, 2013) that calculated the lacunarity

of spacing-only (binary) data. As stressed throughout this document, not only can this technique identify fracture clusters in a scanline but it can also statistically evaluate if the larger fractures occur preferentially within those clusters.

REFERENCES

Allain, C. and Cloitre, M., 1991, Characterizing the lacunarity of random and deterministic fractal sets, *Phys. Rev. A.* vol. 44, no. 6, 3552-3558

Belfield, W.C., 1994. Multifractal characteristics of natural fracture apertures, *Geophysical Research Letters,* vol. 21, no. 24, 2641-2644

Belfield, W.C., 1997. Optimization of horizontal well spacing based on stochastic fracture modeling, p. 209-216 in *Fractured Reservoirs: Characterization and Modeling Guidebook*, Rocky Mtn. Ass. Geologists

Belfield, W.C., 1998. Incorporating spatial distribution into stochastic modeling of fractures: multifractals and Levy-stable statistics, *Journal of Structural Geology,* vol. 20, no. 4, 473-486

Chiles, J. P., 1988. Fractal and geostatistical methods for modeling of a fracture network, *Math. Geol*., vol. 20, no. 6, 631-654

de Joussineau, G., and Aydin, A., 2007. The evolution of damage zones with fault growth in sandstones and its multifractal characteristics, *Journal of Geophysical Research*, B12401, doi:10.1029/2006JB0045711

Gillespie, P.A., Howard, C.B., Walsh, J.J., Watterson, J., 1993. Measurement and characterization of spatial distributions of fractures, *Tectonophysics,* vol. 226, 113-141

Gillespie, P., Johnston, J.D., Loriga, M.A., McCaffrey, K.J., Walsh, J.J. and Watterson, J., 1999. Influence of layering in vein systematics in line samples; in *Fractures, Fluid Flow and Mineralization*

Gillespie, P.A., Walsh, J.J., Watterson, J., Bonson, C.G. and Manzocchi, T. 2001. Scaling relationships of joint and vein arrays from The Burren, Co. Clare, Ireland, *Journal of Structural Geology,* vol. 23, 183-201

Gomez, L., 2007. Characterization of the Spatial Alignment of Opening-mode Fractures, PhD Dissertation, The University of Texas at Austin, 844 pp.

La Pointe, P.R. and Hudson, J.A., 1985. Characterization and interpretation of rock mass joint patterns, *Geological Society of America*, Special Paper 199.

La Pointe, P.R., 1988. A method to characterize fracture density and connectivity through fractal geometry, *Int. J. Rock Mech. Min. Sci. & Geomech. Abstr.*, vol. 25, 421-429

Marrett, R., Ortega, O., and Kelsey, C., 1999. Extent of power-law scaling for natural fractures in rock, *Geology* vol. 27, 799-802

Narr, W. and Suppe, J., 1991. Joints spacing in sedimentary rocks, *Journal of Structural Geology*, vol. 13, no. 9, 1037-1048.

Ouillon, G., Castaing, C. and Sornette, D., 1996. Hierarchical geometry of faulting, *Journal of Geophysical Research,* vol. 101, no. B3, 5477-5487.

Plotnick, R.E., Gardner, R.H., O'Neill, R.V., 1993, Lacunarity indices as measures of landscape texture, *Landscape Ecology*, vol. 8, no. 3, 201-2011

Plotnick, R.E., Gardner, R.H., Hargrove, W.W., Prestegaard, K., Perlmutter, M., 1996, Lacunarity analysis: A general technique for the analysis of spatial patterns, *Phys. Rev. E.* vol. 53, no. 5, 5461-5468

Priest, S.D. and Hudson, J.A., 1976, Discontinuity spacings in rock, *Int. J. Rock Mech. Min. Sci. & Geomech. Abstr.*, vol. 13, 135-148

Roy, A., Perfect, E., Dunne, W.M and McKay, L.D. 2007, Fractal characterization of fracture networks: An improved box-counting technique, *Journal of Geophysical Research* vol. 112, B12201

Roy, A., Perfect, E., Dunne, W.M., Odling, N. and Kim, J. 2010, Lacunarity analysis of fracture networks: Evidence for scale-dependent clustering, *Journal of Structural Geology*, vol. 32, 1444-1449

Roy, A., Perfect, E., Dunne, W.M. and McKay, L. D. 2013, A technique for revealing scale-dependent patterns in scanline data: I. Fracture spacing, *Journal of Geophysical Research*

Tran, N.H., 2004, Characterisation and modeling of naturally-fractured reservoirs. Doctoral dissertation, School of Petroleum Engineering, University of New-South Wales, Sydney, Australia, 255 pp.

Velde, B., Dubois, J., Touchard, G., Badri, A.,1990, Fractal analysis of fractures in rocks, *Tectonophysics,* v. 179, 345-352.

APPENDIX IV: FIGURES

(a)

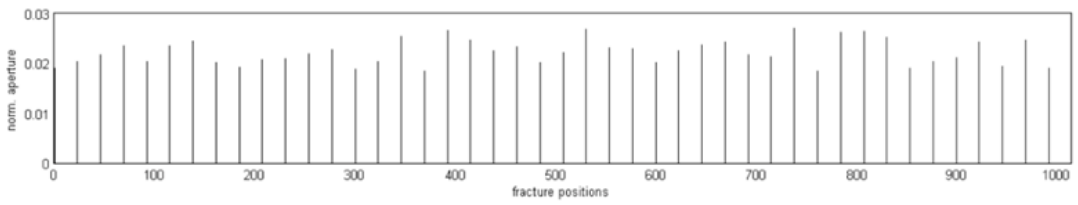

(b)

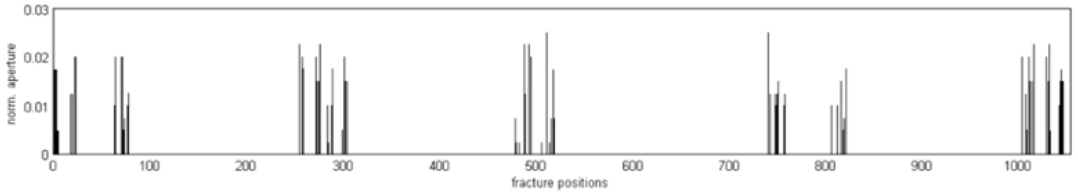

Figure 5.1. Model non-binary scanlines with uniformly-distributed apertures, where the x-axis denotes positions of fractures along a line, and the y-axis denotes normalized aperture: (a) model A1: uniformly spaced fractures, spacing = 22 units, and (b) model C1: regularly-spaced clusters, avg. spacing = 162 units

(a)

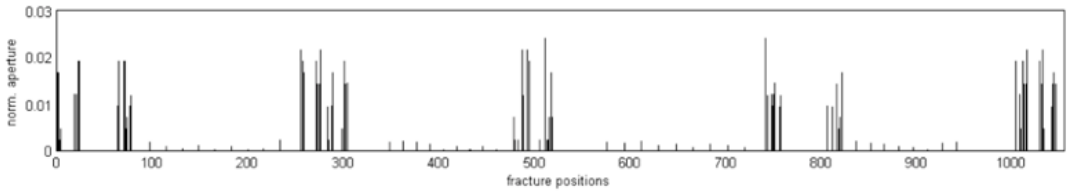

(b)

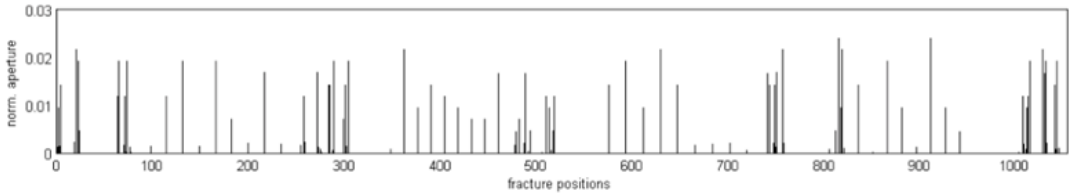

Figure 5.2. (a). Model non-binary scanline E generated by combining models A1 and C1 in fig 1 and scaling down the apertures in A1 by 1 order of magnitude, (b) one realization of the randomized model, E*, with random ordering of apertures but unaltered spacing

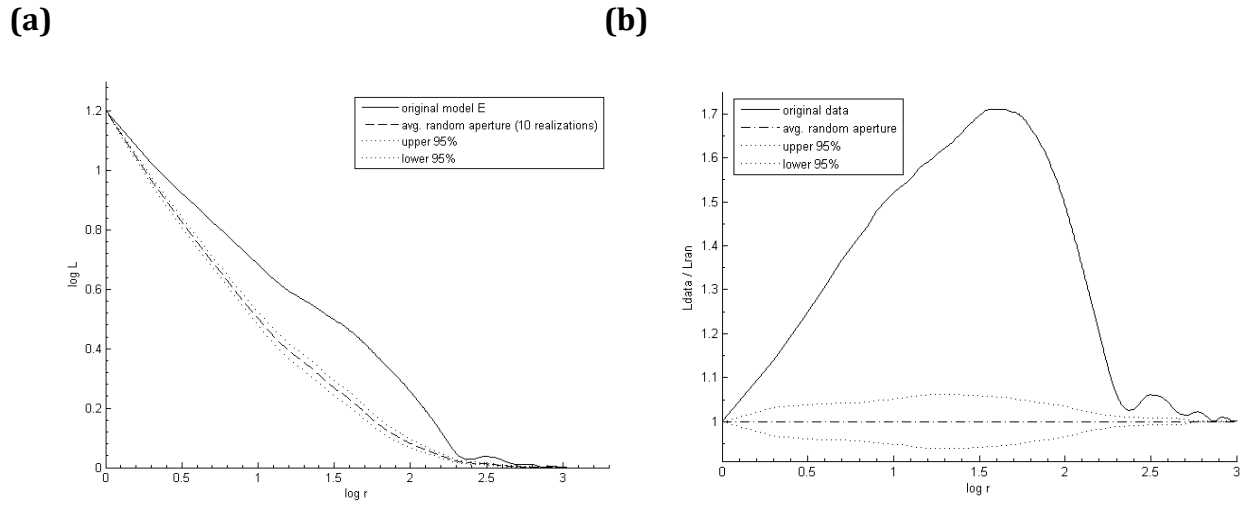

Figure 5.3. (a) Lacunarity curves for model E and its counterpart with random ordering of apertures (average of 10 realizations), (b) Lacunarity-ratios for model E with respect to the average of its random counterparts showing extreme clustering of large apertures.

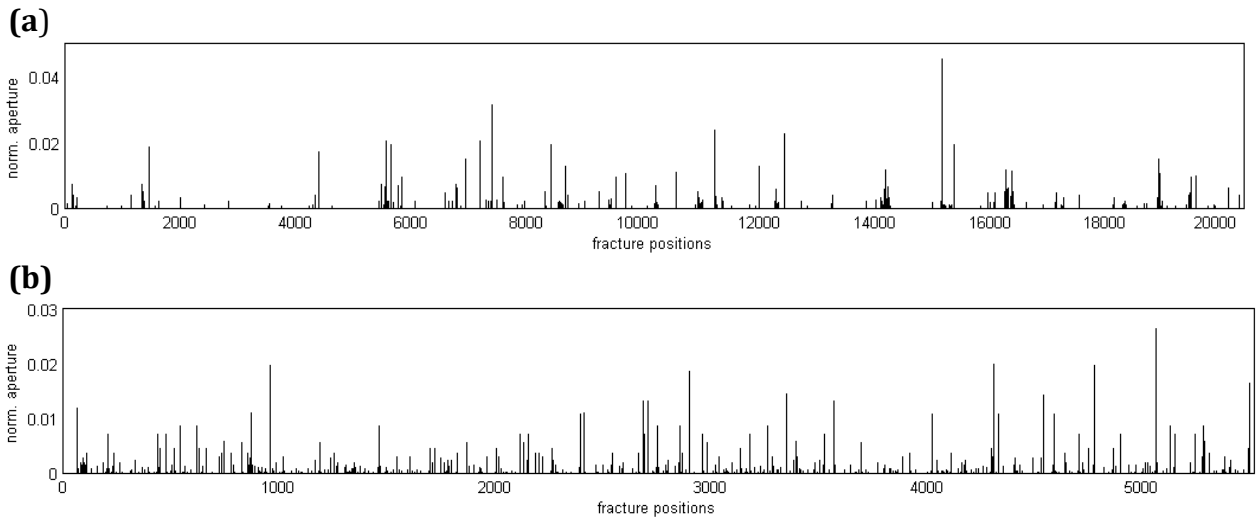

Figure 5.4. Natural non-binary scanline data: (a) P11: 20 m scanline with fracture clusters: note larger fractures occur within clusters, (b) P13: 5.5 m scanline with random fractures. In both cases, spacing units are in mm, while normalized fracture aperture has no units

(a)

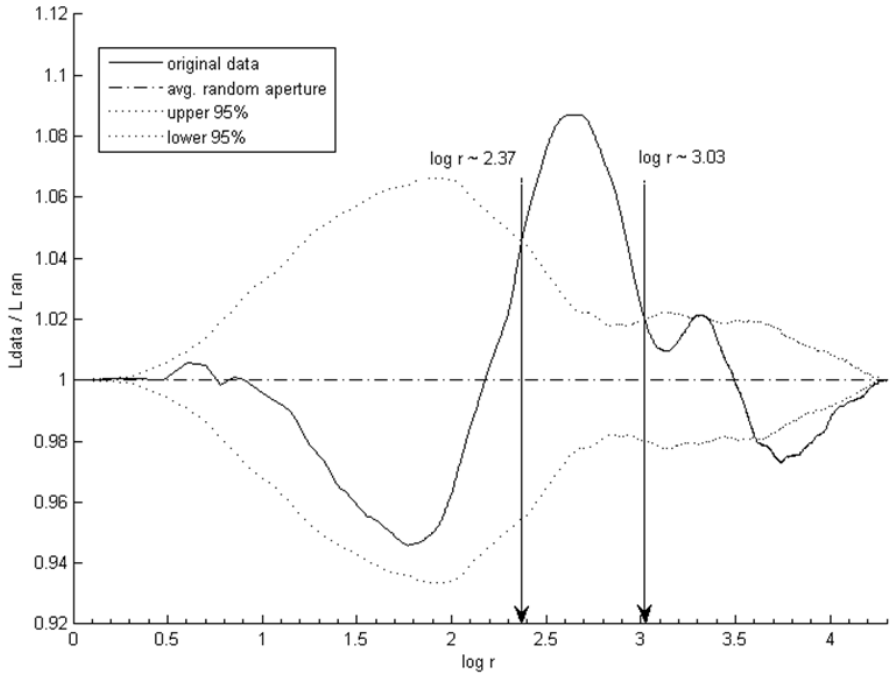

(b)

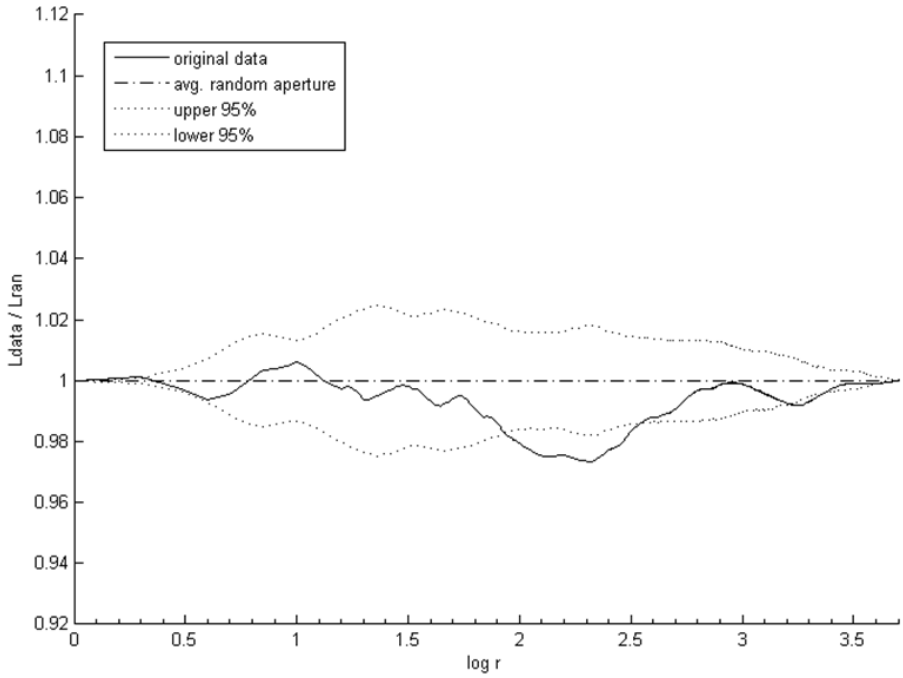

Figure 5.5. (a) Lacunarity-ratio of P11 with respect to its counterpart with random ordering of apertures (avg. of 10 realizations). Large apertures occur within clusters between scales of r = 234mm [log r ~ 2.37] and r = 1072mm [log r ~ 3.03]. (b) Same plot as (a) for P13 data. Large apertures do not occur next to each other

Anisotropy in Fracture Clustering: A Lacunarity Study

Chapter VI: A manuscript for submission as a short note to Tectonophysics / Journal of Structural Geology

Ankur Roy & Edmund Perfect
Potential Co-authors: Noelle E. Odling, William M. Dunne

ABSTRACT

The quantification of anisotropy is important in fracture networks because it controls directionality of fluid flow. Although the use of rose diagrams is common, they do not fully capture directional variations in fracture clustering. Consequently, it becomes difficult to predict connectivity and preferential flow paths within a network. Quantifying anisotropy in fracture clustering is a possible solution because clustering leads to connectivity that creates flow paths in networks. Lacunarity, L, is a parameter that has been used to quantify scale (r) dependent clustering, thus identifying heterogeneities in fracture patterns. Here we apply lacunarity to investigate the clustering anisotropy of fracture maps by rotating scanlines incrementally and computing the lacunarity at each orientation. This rotation changes the length of the scanline and so the scale was normalized to r^* with respect to the total scanline length and a weighted mean, $\langle L \rangle^*$ was computed from the log-transformed lacunarity values, log L, the weights being the log-transformed normalized scale, log r^*. For any given map, the computed $\langle L \rangle^*$ values are plotted along the radius of a circle, in this case every 5°, to delineate the clustering anisotropy. This technique was applied to two natural fracture maps at the scales of 18 m and 720 m from the Devonian Sandstone, Hornelen Basin, Norway. The results showed that $\langle L \rangle^*$ plots can delineate fracture sets that are more clustered than others, thus identifying potential preferential flow pathways. They also indicate that clustering anisotropy decreases at larger scales suggesting that smaller scale fracture networks are more anisotropic.

1. INTRODUCTION

Considerable research in the last 25 years has focused on quantifying the heterogeneity of fracture networks. Various techniques, ranging from semi-variograms (LaPointe and Hudson, 1985; Chiles, 1988) to fractal descriptors (La Pointe, 1988; Berkowitz and Hadad, 1997; Roy et al., 2007), have been applied to this problem. Since fractures result from deformation processes that are inherently directional (Kruhl, 2013), it is to be expected that, in addition, to being heterogeneous, fracture networks will also display some form of anisotropy.

Although the use of rose-diagrams to identify fracture sets with different orientations within a network is common practice (Ouillon et al., 1996; Eyal et al., 2001; Dunne et al., 2003) only a limited number of studies have focused on delineating the anisotropy of heterogeneity in fracture patterns. These studies all employed the technique of finding the fractal anisotropy of fracture networks as documented in Volland and Kruhl (2004) and Perez-Lopez and Paredes (2006). This was done by taking scanline samples from maps at different orientations and determining the fractal dimension of each sample line. A limitation of this approach is that it is strictly applicable to only those networks that are fractals.

Lacunarity is a technique that is based on a multiscale analysis of spatial dispersion and is applicable to all kinds of patterns, fractals or otherwise (Plotnick et al., 1996). Stated simply, lacunarity characterizes the distribution of spaces or gaps in a pattern as a function of scale. For a fracture pattern therefore, it can be employed to quantify the degree of fracture clustering at a given spatial resolution. In a previous study, we focused on analyzing the overall clustering of fractures in a 2-dimensional network by using a modified lacunarity parameter (Roy et al., 2010). In the present chapter, this technique is extended to directional variations in clustering based on lacunarity evaluated in different directions, thus testing a fracture network for its clustering anisotropy. Since clustering of fractures somewhat controls connectivity (Manzocchi, 2002), quantifying clustering anisotropy can potentially help in predicting anisotropy in the flow properties of a fracture network.

2. QUANTIFYING CLUSTERING ANISOTROPY

2.1 The Rotating Scanline

Lacunarity is considered a scale-dependent measure of textural heterogeneity and can be quantified by employing the gliding-box algorithm (Allan and Cloitre, 1991; Plotnick et al., 1996). The details of the notion of lacunarity and the gliding-box algorithm as applied to a 1-dimentional sequence of 0's and 1's can be found in Roy et al. (2010) and in chapter 3 of this dissertation, respectively. Roy et al. (2012) documented a simple technique for finding clustering anisotropy by laying a series of scanlines every 10 pixels along x and y axes of a fracture map and computing the average lacunarity in each direction. The present research is based on a more robust sampling technique where a scanline passing through the center of a square map is rotated every 5° (fig. 6.1). Each such sample scanline produces a sequence of 0's (spacing) and 1's (fractures) and the lacunarity at every orientation is calculated using the gliding-box technique.

Comparing the lacunarity of scanlines at different orientations involves 3 parameters – log $L(r)$, log r, and the scanline orientation, θ. For creating simple 2-dimensional plots, it is therefore important to collapse the log L vs. log r curve into a single number. Chapter 3 describes a method of taking the weighted mean of log L values as:

$$< L >= \frac{\sum \log L \cdot \log r}{\sum \log r} \quad \text{.....(1)}$$

Rotating the scanline however, changes its length (fig. 6.1). While this method works for comparing lacunarities of sequences of equal length, e.g. in case of a circular sampling area, it however, does not work for sequences that are unequal in length.

2.2 Comparing Lacunarity of Sequences with Varying Lengths

Figure 6.2a is a series of Cantor-bars that are scale-independent fractal sequences. These are generated by iterating the same sequence i.e. 1 0 1 0 0 0 1 0 1 (here 0's represent spacing and 1's are fractures) over different scales such that they have the same clustering attribute, hence equal lacunarity irrespective of the length of the sequence. Figure 2b

shows the log-transformed lacunarity curves of cantor-bars at iteration levels i = 3, 5 and 7. Table 6.1 and fig. 6.2b demonstrates that differences in the lengths and intensity (no. of elements per unit length) influence the lacunarity curves and that <L> values calculated from equation (1) are thus different for Cantor-bars at various iteration levels.

Normalizing the scale, r, with respect to the total length of a given scanline, r_{max}, as in equation 2, eliminates differences in the lacunarity curves due to variations in scanline length / intensity (fig. 6.2c). A new weighted mean, <L>* can then be calculated based on the r*-values (i.e., equation 3):

$$r^* = \frac{r}{r_{\max}} \quad \text{.....(2)}$$

$$< L >^* = \frac{\sum \log L \cdot \log r^*}{\sum \log r^*} \quad \text{.....(3)}$$

It is clear from Table 6.1 that all three Cantor-bars with different lengths and intensities now have the same <L>* value as is expected.

2.3 Clustering Anisotropy of Fracture Maps

Odling (1997) documented a nested set of seven maps from the Devonian sandstone of Hornelen Basin, Norway. They are based on imagery collected from different heights where the sampling resolution changed with the map scale by varying the height of the camera. The maps range from a size of 18m x 18 m (map 1) to 720m x 720m (map 7). Each map represents a scale window on the fracture system and contains a range of fracture lengths, the shortest being dictated by the resolution of the image and the longest by the area mapped. When analyzed as fractals, the fractal dimensions for each map were statistically similar (Bour et al., 2002; Roy et al, 2007). However, 2-dimensional lacunarity analyses showed that these maps have different clustering attributes. Maps at larger scales were less clustered than maps at smaller scales (Roy et al., 2010). The technique developed in the present research was applied to the smallest and largest of Odling's (1997) maps, i.e. map 1 and map 7 (fig 6.3a & c).

For this analysis the original fracture maps of Odling (1997) were converted to 1042 x 1042 pixel bitmaps. The $\langle L \rangle^*$ values for maps 1 and 7 were then calculated from scanlines oriented at 5° intervals using eq. 3 as shown in figures 6.3b & d. The scanline orientations are plotted in degrees around the circumference while the $\langle L \rangle^*$ values are along the radius of the circular graph. It may be noted that since the sampling algorithm implemented here changes the length of the scanline we have used normalized scales for calculating the $\langle L \rangle^*$ values. Any other sampling technique where the scanline length remains unaltered upon rotation, e.g. a circular window instead of a square map, may use non-normalized scales and calculate values for the $\langle L \rangle$ parameter from equation (1).

The results bring forth two important observations. A visual comparison of figures 6.3a & b shows that while there are three main fracture sets in map1, E-W, NE-SW and NW-SE (Odling, 1997), there is a distinctly long "spike" in the $\langle L \rangle^*$ plot approximately in the NW-SE direction and another much smaller (but still distinct from the others) spike in the E-W direction. This may be interpreted as the NW-SE spike reflecting the highly clustered NE-SW set while the E-W spike may be related to the NW-SE set which is almost periodic, hence the lower $\langle L \rangle^*$ values. Secondly, it is also seen that in going from map 1 to map 7, i.e. with increasing scale the "spikes" become less distinct as the anisotropy decreases. The anisotropy of map 1, as quantified by the ratio of the largest and smallest $\langle L \rangle^*$ values, was 2.44, while that of map 7 was 2.07. This suggests that large-scale fracture networks are less anisotropic with respect to clustering. This outcome is expected because these fractures tend to become more random at larger scales.

It should also be noted that map 7 has $\langle L \rangle^*$ values that are generally smaller than those for map 1 (Fig. 6.3). A paired t-test between the 1-D $\langle L \rangle^*$ values for the two maps indicated that they were significantly different at the 95% confidence level. This difference is because map7 is less clustered than Map1 in 2-D, as was discussed in Roy et al. (2010)

3. DISCUSSION & CONCLUSIONS

Determining clustering anisotropy using lacunarity can delineate fracture sets that are more clustered than others. For the specific examples of maps at different scales as used here, this technique can additionally identify changes in clustering of entire fracture populations and anisotropy with scale. Clustering anisotropy appears to decrease at larger scales suggesting that large-scale fracture networks are more isotropic. This outcome is because fractures become more randomized at these scales.

It is seen from map 1 that the NE-SW fractures are tightly clustered whereas the NW-SE fractures are almost regularly spaced. The $<L>^*$ plot is sensitive to this trend as reflected in the NW-SE spike that is caused by the clustering of the NE-SW trending fractures. On the other hand, the near periodic distribution of the NW-SE fractures is manifested in the smaller E-W spike in the $<L>^*$ plot. The NE-SW fractures might potentially provide a preferential flow pathway as compared to the other sets. Since the $<L>^*$ plot picks up this trend, this technique may be valuable for delineating possible flow paths in fracture networks. Therefore, comparing such $<L>^*$ plots to permeability anisotropy plots similar to those in Odling and Webman (1991) may help resolve questions about the nature of the relationship between fracture clustering and equivalent permeabilities.

REFERENCES

Allain, C. and Cloitre, M., 1991, Characterizing the lacunarity of random and deterministic fractal sets, *Phys. Rev. A.* vol. 44, no. 6, 3552-3558

Berkowitz B., Hadad, A., 1997, Fractal and multifractal measures of natural and synthetic fracture networks, *Journal of Geophysical Research*, vol. 102, no. B6, 12,205-12,218

Bour O., Davy, P., Darcel, C., Odling, N., 2002, A statistical scaling model for fracture network geometry, with validation on a multiscale mapping of a joint network (Hornelen Basin, Norway), *Journal of Geophysical Research*, vol. 107, no. B6, 4-1 – 4-12

Chiles, J. P., 1988, Fractal and geostatistical methods for modeling of a fracture network, *Math. Geol.*, vol. 20, no. 6, 631-654

Dunne, W.M., Ferril, D.A., Crider, J.G., Hill, B.E., Waiting, D.J., La Femina, P.C., Morris, A.P., Fedors, R.W. 2003, Orthogonal jointing during coeval igneous degassing and normal faulting, Yucca Mountain, Nevada, *GSA, Bulletin*, vol. 115, no. 10, 1492–1509

Eyal, Y., Gross, M.R., Engelder, T., Becker, A. 2001, Joint development during fluctuation of regional stress field in southern Israel, *Journal of Structural Geology*, vol. 23, 279-296

Kruhl, J.H., 2013, Fractal-geometry techniques in the quantification of complex rock structures: A special view on scaling regimes, inhomogeneity and anisotropy, *Journal of Structural Geology*, vol. 46, 2-21.

La Pointe, P.R. and Hudson, J.A., 1985, Characterization and interpretation of rock mass joint patterns, *Geological Society of America*, Special Paper 199.

La Pointe, P.R., 1988. A method to characterize fracture density and connectivity through fractal geometry, *Int. J. Rock Mech. Min. Sci. & Geomech. Abstr.*, vol. 25, 421-429

Manzocchi, T. 1996, The connectivity of two-dimensional networks of spatially correlated fractures, *Water Resources Research*, vol. 38, no. 9, 1-1 – 1-20

Ouillon, G., Castaing, C. and Sornette, D. 1996, Hierarchical geometry of faulting, *Journal of Geophysical Research*, vol. 101, no. B3, 5477-5487

Odling, N. E., 1997, Scaling and connectivity of joint systems in sandstones from western Norway, *Journal of Structural Geology,* vol. 19, no. 10, 1257-1271

Odling, N. E. and Webman, I. 1991, A conductance mesh approach to permeability of natural and simulated fracture paterns, *Water Resources Research,* vol. 27, no. 10, 2633-2643

Perez-Lopez, R. and Paredes, C. 2006, On measuring the fractal anisotropy of 2-D geometric sets: Application to the spatial distribution of fractures, *Geoderma*, vol. 134, 402-414

Plotnick, R.E., Gardner, R.H., Hargrove, W.W., Prestegaard, K., Perlmutter, M. 1996, Lacunarity analysis: A general technique for the analysis of spatial patterns, *Phys. Rev. E.* vol. 53, no. 5, 5461-5468

Roy, A., Perfect, E., Dunne, W.M and McKay, L.D. 2007, Fractal characterization of fracture networks: An improved box-counting technique, *Journal of Geophysical Research*, vol. 112, B12201

Roy, A., Perfect, E., Dunne, W.M., Odling, N. and Kim, J. 2010, Lacunarity analysis of fracture networks: Evidence for scale-dependent clustering, *Journal of Structural Geology*, vol. 32, 1444-1449

Roy, A., Perfect, E., Kumar, J. and Mills, R.T. 2012, Does Anisotropy in Fracture Clustering Translate into Anisotropy in Intrinsic Permeability, *Abstract 1235622*, *AAPG Annual Convention & Exhibition*, Long Beach, CA

Volland, S. and Kruhl, J.H. 2004, Anisotropy quantification: the application of fractal geometry methods on tectonic fracture patterns of a Hercynian fault zone in NW-Sardinia, *Journal of Structural Geology*, vol. 26, 1489-1500

APPENDIX V-A: TABLES

Table 6.1. Weighted mean lacunarity values <*L*> compared to weighted mean normalized lacunarity values <*L*>* for Cantor-bar models (fractal dimension = 0.631 and scale factor = 3) at three iterations, *I* = 3, 5 and 7 with variable sequence lengths and intensities

i	length	intensity	<*L*>	<*L*>*
3	27	0.30	0.04	0.18
5	243	0.13	0.05	0.18
7	2187	0.06	0.06	0.18

APPENDIX V-B: FIGURES

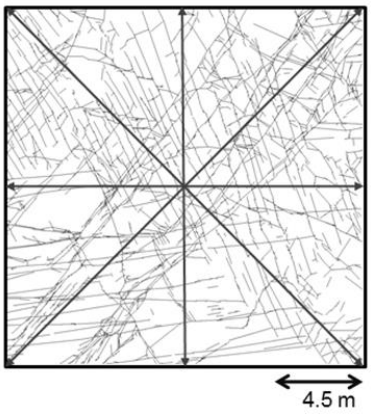

Figure 6.1. 1-D samples are obtained from a 2-D network by systematically rotating a scanline every 5°; for clarity only 4 out of the 36 scanlines analyzed are shown.

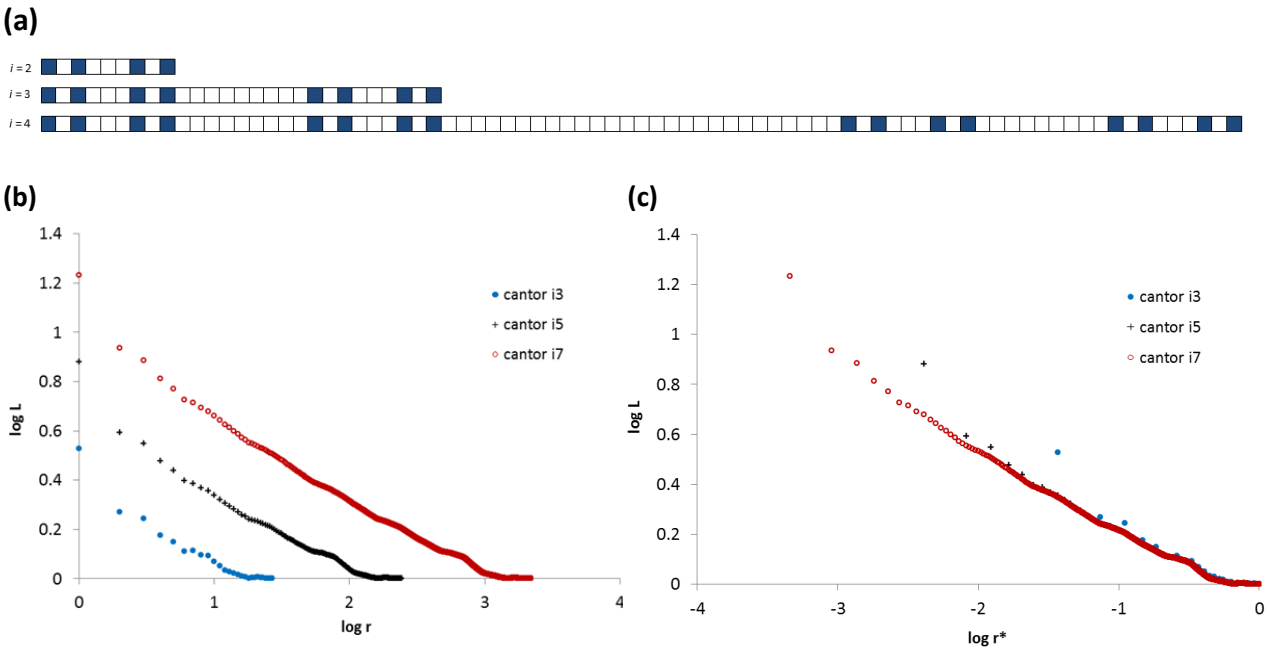

Figure 6.2. (a) Cantor-bars at iterations i = 2, 3 and 4 with differences in length and number of elements between models; (b) log L vs. log r curves for cantor-bars at iterations i = 3, 5 and 7 – curves are offset showing that lacunarities are unequal for different iterations; (c) log L vs. log r^* curves for same cantor-bars as in (b) where r^* is normalized r

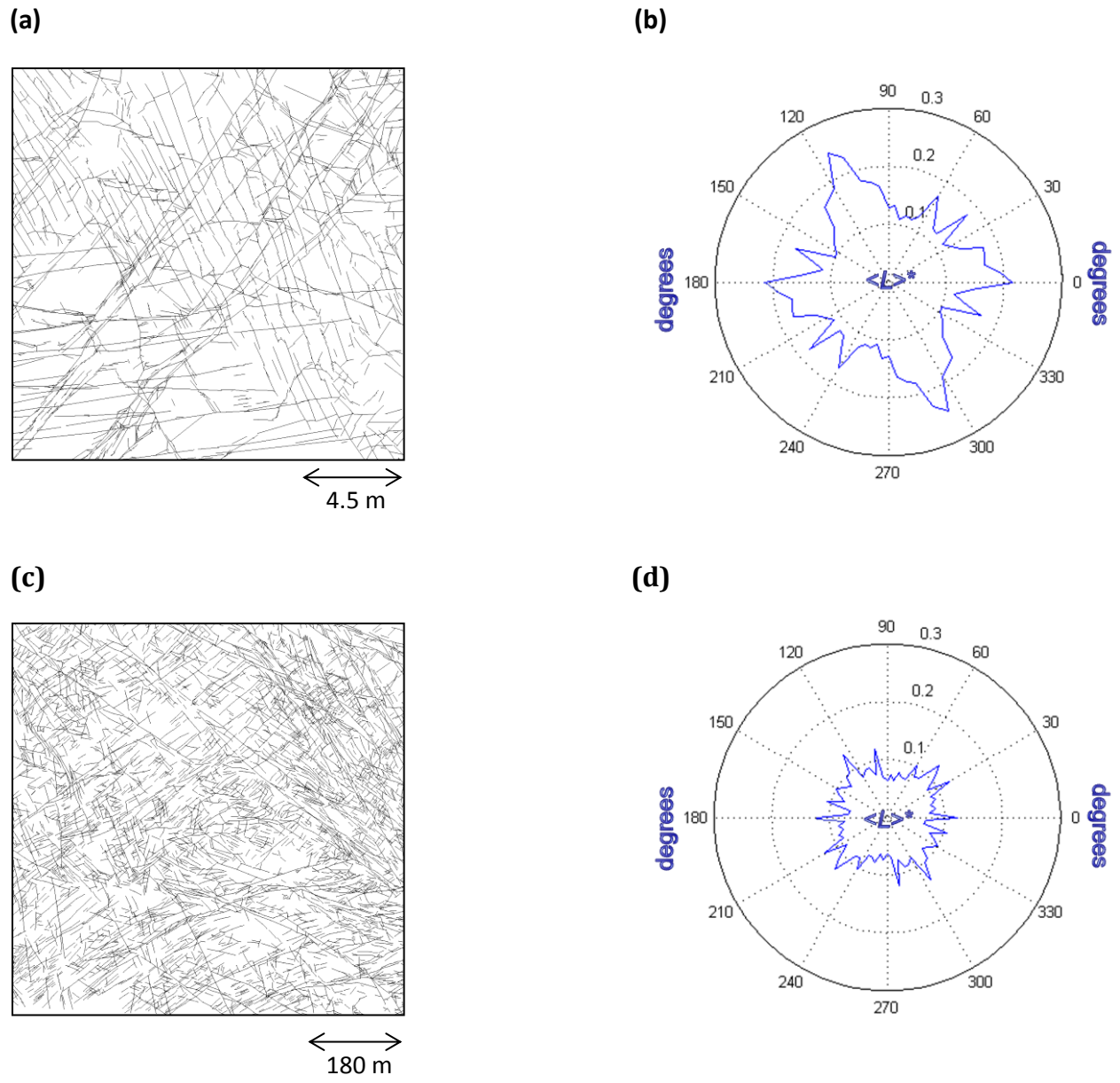

Figure 6.3. (a) Map 1, (b) plot for *<L>** values for map 1, (c) map 7, and (d) plot of *<L>** values for map 7. Comparison between *<L>** plots for maps 1 and 7 shows that the "spikes" become less pronounced with increasing scale, and that the absolute clustering also becomes smaller.

Conclusions & Future Research

Chapter VII

Ankur Roy

This dissertation essentially builds around the concept of *lacunarity* which has been shown to be a versatile tool for analyzing different data types. Various kinds of fracture data have been used in all of the chapters except for chapter 3 which deals with grayscale soil images. Most fracture patterns are created from superimposition of two or more deformational episodes that introduce heterogeneity and anisotropy in the rock structure. Lacunarity, being essentially a measure of heterogeneity, is an ideal tool that has been demonstrated to capture the complexity of fracture patterns. It can characterize fracture geometry at *different* scales within the *same* dataset thereby delineating fracture clusters and organization within them such as possible fractal or random behavior and can even identify anisotropy in clustering of fractures from 2-dimensional networks.

There are a number of possible research avenues that can follow from this research. Three examples of such future research possibilities are discussed in the rest of this section. These pertain to estimating the clustering of fractures in maps from analyzing 1-dimensional samples, forward modeling of fracture networks, and using lacunarity as a tool for delineating shapes of geologic features other than fractures.

The research in chapters 2 and 6 may be combined to test if the clustering ($<L>^*$ value) of a fracture network computed from 2-dimensional lacunarity analysis can be estimated from the $<L>^*$ values of 1-dimensional scanline samples from the same map. This may be achieved by laying scanlines at random orientations and positions and averaging the resulting $<L>^*$ values. The best form of averaging (i.e., arithmetic, geometric, harmonic) will need to be investigated empirically. It is hypothesized that increasing the number of sample scanlines will give a closer average estimate of the $<L>^*$ value computed from the 2-dimensional lacunarity analysis.

It has been shown in the present research that lacunarity can delineate scale-dependent trends in patterns and the range of scales over which a pattern displays fractal, multifractal (for non-binary data) and uniform or random behavior. This information can be used to build forward models honoring the scale-dependent distribution of natural fractures. For example, a model can be built that is random over a certain range of scales and fractal (or multifractal) over another range based on the lacunarity values for those

scales. In creating a model with a given fractal dimension, a number realizations can be built stochastically with the one that most closely matches the observed lacunarity distribution being considered ideal. Since lacunarity is simply a linear function of the mean and variance of the data at a given scale, it is possible to create a spatial distribution of fracture elements at that scale from the lacunarity curve of a natural dataset. Models at different resolutions (scales) based on the distributions of elements can thus be created that will have similar clustering attributes as the original dataset. Finally, 2-dimensional (and possibly, 3-dimensional) realizations can be built if data from wells drilled in different directions are integrated. Such realizations can help populate geocellular grids in building synthetic fracture models.

Notwithstanding the fact that this dissertation has focused on delineating the heterogeneity of fracture patterns, lacunarity is a tool that can also be potentially used to quantify shapes of other geo-patterns. The sinuosity of a river channel for example can be quantified by running the gliding-box algorithm both in two and three dimensions. Shapes of other types of geo-patterns (e.g. tidal bars) may be characterized in 3-dimensions by modifying the shape and/or orientation of the “gliding-box” in space.

SELECTED MATLAB CODES

Appendix VI

Ankur Roy

CODE #1: Compute lacunarity of 2-dimensional data

```
%   Lacunarity (2-Dimension)
%   evalculate clustering of either 0's or 1's or fractions
%   OUTPUT: *.out file containing box-size & lacunarity
%   INPUT mat: *.dat file, original image (binary/non-binary), map etc
%   written and updated by Roy (2011)

matnew=dlmread('b7n9_a_trumulti_i4.dat')
%matnew=imread('hornsd_red.bmp')

% to turn 0's to 1's / invert colors of an image/matrix

disp('****************************************');
orz = input('turn zeros to ones etc [y/n]? ', 's');
if isempty(orz)
    orz = 'n';
end
if orz ~= 'y' && orz ~= 'n'
     disp('!!!!! you need to make a choice between y and n !!!!!');
     return
end

 if orz == 'y'
[br bc] = size(matnew);
A =rand(br, bc);
    for i=1:br
      for j=1:bc
           A(i,j)= 1-matnew(i,j);
      end
    end
 elseif orz == 'n'
     A=matnew;
 end

tic;
%N is total no. of window sizes used - for best results N = ncol/2
[nrow, ncol] = size(A);
N=ncol
lac=rand(N,1);box_size=(1:N)';
for wind = 1:N
    imax = nrow-wind+1;
    jmax = ncol-wind+1;
    tot = imax*jmax;
    mom1 = 0;mom2 = 0;v=0;
    s = rand(imax,jmax);
    for i = 1:imax
    for j = 1:jmax
        s(i,j) = sum(sum(A(i:i+wind-1,j:j+wind-1)));
    end
    end
mom1 = mean(s(:));
v=var(s(:),1);
mom2 = mom1^2+v;

lac(wind) = mom2/(mom1^2);
end
toc

L = [box_size,lac]
dlmwrite('lacunarity.out',L);
```

CODE #2: Plot lacunarity and its slope

```
% plot log-log lac and its slope:
% written by Roy (2011-12)

A=dlmread('lacu_soil1_flip.out'); l=length(A)
r=A(1:l,1); L=A(1:l,2);
logR=log(r);logL=log(L);figure
plot(logR,logL,'m.'); title('lacunarity curve'); xlabel('log r'); ylabel('log
L');
c=0;
w=input('averaging window...')
for i=w+1:w:l
    c=c+1;
end
delL=rand(c,1);
for i=w+1:w:l
    delL(i)=(logL(i)-logL(i-w))/(logR(i)-logR(i-w));
end
delL;
figure
plot(logR(w+1:w:l),delL(w+1:w:l),'r-'); title('lacunarity slope');
xlabel('log r'); ylabel('d(logL)/d(logr)');
```

CODE #3: Generate 2-dimensional multifractals based on truncated binomial distribution

```
%   random and deterministic multifractals
%   Based on truncated binomial distribution (Perfect et al.,2006)
%   modified by Roy (Feb,2012)
%   INPUT: scale factor, iterations, probability
%          'mass-fractions map' for creating generator (determisitic)
%   OUTPUT: image and *.dat file of generated multifractal

clear all;

disp(' ');
disp('****************************************');
b = input('Scale factor (default = 3) [Integer] ... ');
maxit = input('Iteration number (default = 5) [Integer] ... ');
pb = input('Numerator of probability (default = 8)  [Integer] ... ');

if isempty(b) == 1
    b = 3;
end
if isempty(maxit) == 1
    maxit = 5;
end
if isempty(pb) == 1
    pb = 8;
end

n = b^2;     % total number
p = pb/n;    % probability

%   binomial distribution
for k = 1:n
    bidi(k) = binopdf(n-k+1,n,p);
end

%   truncated binomial distribution
tbidi = bidi/sum(bidi);

%   average mass fraction in multifractal
f(1) = tbidi(1)/n;
for k = 2:n
    f(k) = f(k-1)+tbidi(k)/(n-k+1);
end

% flipping f to match Dr Perfect's excel sheets
ff=fliplr(f)

%   deterministic or random
disp(' ');
disp('****************************************');
disp('1. Random multifractal (default)');
disp('2. Deterministic multifractal');
dor = input('Choose type of generator ... ');
if isempty(dor) == 1
```

```
    dor = 1;
elseif dor ~= 1 & dor ~= 2
    disp('!!!!! Wrong selection ...  Try it again ... !!!!!');
    return
end

if dor == 2    %   deterministic location (using progression)
       disp('input a matrix that maps the ff-values onto a generator e.g:');
       genn = input('[9 8 6; 7 5 3; 4 2 1] where 1 maps the max ff and 9 the
min...');
    if isempty(genn) == 1
        for i = 1:b
            for j = 1:b
                lgen(b-i+1,j) = (1+(i-1)*(i+2)/2) + (j+(i-1)*2)*(j-1)/2;
                ugen(i,b-j+1) = (b^2-(i-1)*(i+2)/2) - (j+(i-1)*2)*(j-1)/2;
            end
        end
        genn = tril(lgen,-1)+triu(ugen);
    elseif size(genn) ~= [b b]
        disp('!!!!! Wrong Generator Input ...  Try it again ... !!!!!');
        return
    end
    % it may be important to look at gen: so if, remove ";" in line71
    for i = 1:b
        for j = 1:b
            gen(i,j) = ff(genn(i,j));
        end
    end
end

%   multifractal
matold = 1;
for it = 1:maxit

    [nrow ncol] = size(matold);
    matnew = zeros(nrow,ncol);
    for i = 1:nrow
        for j = 1:ncol

            if dor == 1       %   random location; NOTE: NOT changing f to
ff; original code not tampered with!
                rndf = randperm(n);
                for ii = 1:b
                    for jj = 1:b
                        gen(ii,jj) = f(rndf((ii-1)*b+jj));
                    end
                end
            end

            matnew((i-1)*b+1:i*b,(j-1)*b+1:j*b) = matold(i,j)*gen;
        end
    end
    matold = matnew;
end
```

```
%   normalize

mat = (matold - min(min(matold))*ones(size(matold))) ...
    / (max(max(matold)) - min(min(matold)));

%   data file output

    save multifractal.dat mat -ascii;

%   visualization

figure
imagesc(mat);
set(gca,'XTick',[],'YTick',[])
set(gca,'Box','on','Position',[0 0 1 1]);
set(gcf, 'NumberTitle','off','Name','Multifractal','pos',[200 100 500 500]);
colormap;
```

CODE #4: Generate fractal-fracture scanlines and their non-binary counterparts

```
%   generates cantor bars like 1 1 0 1 1 0 0 1 1 & their non-binary cousins
%   OUTPUT: *.dat file
%   INPUTS: maxit = maximum iteration number
%           b     = scale factor
%           pb    = probability (cells to be taken out)
%   calls function randht for generating random number from a power-law dist
%   modified by Roy (2012) from a fractal-fracture map generator by Kim(2005)

clear

b = input('scale factor b ')
maxit = input('no. of iterations ')
pb = input('no. of element removed n ')
if maxit ~= abs(fix(maxit)) | b ~= abs(fix(b)) | pb ~= abs(fix(pb))
    disp('!!!!! Wrong Input...  Try it again... !!!!!');
    return;
    end
matold = 0;
for it = 1:maxit
    nrow  = length(matold);
    matnew = ones(1,b^it);
    for i = 1:nrow

            if matold(i) == 0
                odr = zeros(1,b);
                rnd = randperm(b);
                for k = 1:b
                    if rnd(k) <= pb
                        odr(k) = 1;
                    else
                        odr(k) = 0;
                    end
                end
                matnew((i-1)*b+1:i*b) = odr;
            end

    end
    matold = matnew;
end
matnew;

l=length(matnew); ERAN=[];MRAN=[];
for i = 1:l

% generating a random number between 1 and 10 from a power-law distribution

 randomnum=randht(1,'xmin',1,'powerlaw',0.3);
    while randomnum < 10
        r=randomnum; break
    end
```

```
if matnew(i)==0
        ERAN(i)=r; MRAN(i)=1;
        else ERAN(i)=0;MRAN(i)=0;
        end
end

sumERAN=sum(ERAN);

for i = 1:l
    ERAN2(i) = ERAN(i)/sumERAN;
end

dlmwrite('multi.dat',ERAN2); dlmwrite('mono.dat',MRAN);ERAN2
```

CODE #5: Digitize scanline data from *.xls files with spacing and aperture/length values

```
% digitize scanline data
% OUTPUT: *.dat files SCAN(all lengths or apertures = 1), SCANM
% written and updated by Roy (2012)

clear;
X=xlsread('p13_alt2.xls','Sheet2','A3:c454')
S=X(:,1); A=X(:,3);
n=length(S);
Z=[]; ZNA=[];SCAN=[];ZA=[];SCANM=[];
for i=1:n
 Z = zeros (1,S(i));
 ZNA = [Z,1]; ZA = [Z,A(i)];
 SCAN = [SCAN, ZNA];
 SCANM = [SCANM, ZA];
end

SCANM'
save p13_bin.dat SCAN -ascii;
save p13_gr.dat SCANM -ascii;
disp('done with digitizing scanline')
```

CODE #6: Generate model E in chapter V

```
% generates a model with large fractures in 5 clusters
% uniformly spaced small ones in inter-cluster regions
% written by Roy (2013)

A1=load('multi1.dat');
A2=load('multi2.dat');
A3=load('multi3.dat');
A4=load('multi4.dat');
A5=load('multi5.dat');
Araw=[A1,zeros(1,172),A2,zeros(1,142),A3,zeros(1,182),A4,zeros(1,152),A5];
ap=Araw(Araw~=0);
ap_small = [];
for i = 1:36
    ap_small(i)= unifrnd(0.1,1);
end

c=0;
for i = (81+17):17:(81+172-17)
    c=c+1; Araw(i)= ap_small(c);
end
for i = (81+172+81+14):14:(81+172+81+142-14)
    c=c+1; Araw(i)= ap_small(c);
end
for i = (81+172+81+142+81+18):18:(172+81+81+142+81+182-18)
    c=c+1; Araw(i)= ap_small(c);
end
for i = (172+81+81+142+81+182+81+15):15:(172+81+81+142+81+182+81+152-18)
    c=c+1; Araw(i)= ap_small(c);
end
A=[];
for i = 1:length(Araw)
    A(i) = Araw(i)/sum(Araw);
end
A
     dlmwrite('largeapclsts_n_smallap.dat',A);
```

CODE #7: Compute average spacing and coefficient of variation (Gillespie et al., 1999)

```
% find spacings, avg. sp. and coefficient of variation of a binary scanline
% written by Roy (2013)

A=load('clusters5.dat');
A(1)=1;
A(length(A))=1;
dsig=diff(A);
startindex=find(dsig<0);
endindex=find(dsig>0);
spacings=endindex-startindex; n = length(spacings);
spacings(n)=spacings(n)+1
mean_spacings = mean(spacings)
stdv_spacings = std(spacings)
gillespie_cv = stdv_spacings/mean_spacings
```

CODE #8: Randomize scanline data with respect to aperture/length values

```
%original data to original spacing +random aperture/length
% written by Roy (2013)

S=load('p13_gr.dat')
l = length(S);

AP=S(S~=0)
lap=length(AP)

c2=0;
APran=AP(randperm(lap));
for i = 1:l
if S(i)~=0 c2=c2+1;
S(i)=APran(c2);
end
end
dlmwrite('p13gr_ranap##.dat',S);
```

CODE #9: Compute and plot lacunarity ratio

```
%compute and plot lacunarity ratios from *.out lacunarity files
% written by Roy (2013)
clear;

data=load('lac_p11_gr.out');
random=load('lac_p11gr_ranap_avg.out');
random_u=load('lac_p11gr_ranap_upper.out');
random_l=load('lac_p11gr_ranap_lower.out');

Ld=data(:,2);Lr=random(:,2);
Lru=random_u(:,2);Lrl=random_l(:,2);
Ldiv=Ld./Lr;
Ldiff=Ld-Lr;

for i = 1:length(Ldiff)
        if Lr(i)==0 Ldiv(i)=0;
    end
end

hold on; %figure;
plot(log10(data(:,1)),Ldiv,'b-')
xlabel('log r(mm)'); ylabel('Ldata / Lran');title('normalized clustering
scanline-#: wrt ##')
```

CODE #10: Lay scanlines every 5 degrees on a map and find *<L>**

```
%   lacunarity of 1D scanline through fracture map: rotate map every 5 deg
%   OUTPUT: separate *.out files of lacunarity and box-size for each scanline
%           *.out file for <L>* and orientation values
%   INPUT: image
%   matnew=matnew1(1:1042,1:1042) used for map5 - last row & col = zeros
%   calls the function deg2rad for changing degrees to radians
%   written and updated by Roy (2013)

clear; matnew=imread('hornsa_red.bmp'); %matnew=matnew1(1:1042,1:1042);

% to turn 0's to 1's / invert colors of an image/matrix

disp('****************************************');
orz = input('turn zeros to ones etc [y/n]? ', 's');
if isempty(orz)
    orz = 'n';
end
if orz ~= 'y' && orz ~= 'n'
     disp('!!!!! you need to make a choice between y and n !!!!!');
     return
end

 if orz == 'y'
[br bc] = size(matnew);
A =rand(br, bc);
    for i=1:br
      for j=1:bc
           A(i,j)= 1-matnew(i,j);
      end
    end
 elseif orz == 'n'
     A=matnew; [br bc] = size(A);
 end
 t1=tic;
if rem(length(A),2)==0
    Atrim=A(1:br-1, 1:bc-1);
else Atrim = A;
end
    [row, com] = size(Atrim);
datapts=length(0:5:180-5)
a=(row+1)/2
count_r=0;circ_lac=rand(datapts,1);
for r=0:5:180-5
count_r=count_r+1;
AA=imrotate(Atrim,r); aa=floor((length(AA)+1)/2);

if (r>45)&&(r<90)rr=90-r;
else if (r>=90)&&(r<135)rr=r-90;
    else if (r>=135)&&(r<180)rr=180-r;
        else rr=r;
        end
    end
end
```

```
radius=floor(a/cos(deg2rad(rr)));
A1D=AA(aa,aa-(radius-1):aa+(radius-1));ncol = length(A1D);

str = ['laying scanline #', num2str(count_r), ' along ', num2str(180-r) , '
degrees']; disp(str)

por=length(find(A1D==1))/length(A1D);

lacunarity=rand(ncol,5);
for wind=1:ncol
    mom1=0; v=0; mom2=0;
jmax = ncol-wind+1;

sA1D=rand(1,jmax);
    for j = 1:jmax
                        sA1D(1,j) = sum(sum(A1D(j:j+wind-1)));
    end

mom1A1D = mean(sA1D);
vA1D=var(sA1D,1);
mom2A1D = mom1A1D^2+vA1D;
lacA1D = mom2A1D/(mom1A1D^2);

rn=wind/ncol;logrn=log10(rn);
logL=log10(lacA1D);
product = logL.*logrn;

lacunarity(wind,:)= [wind lacA1D logrn logL product];
end
lacufile = sprintf('lac-log_m1_05deg_%d.out', 180-r);
dlmwrite(lacufile,lacunarity);
wmlnl=sum(lacunarity(:,5))/sum(lacunarity(:,3));
circ_lac (count_r,1)=180-r;circ_lac(count_r,2)=wmlnl;
end
disp('****************************************');
toc(t1)
circ_lac
dlmwrite('map4_05deg_circwmlnl.out',circ_lac);
```

CODE #11: Create a circular plot for $\langle L \rangle^*$ values

```
%   plot weighted mean lacunarity around a circle
%   written by Roy (2013)

circ_lac=load('map1_05deg_circwmlnl.out')
circ_lac_whole1 = [circ_lac(:,1); 180+circ_lac(:,1)];
circ_lac_whole2 = [circ_lac(:,2);circ_lac(:,2)];
circ_lac_whole = [circ_lac_whole1, circ_lac_whole2];
figure;
polar(0,0.3,'-k')
hold on
polar(deg2rad(circ_lac_whole(:,1)), circ_lac_whole(:,2),'-b');
hold off
anisotropy = max(circ_lac(:,2))/min(circ_lac(:,2))
```

VITA

Ankur Roy was born in Calcutta, India in the year 1977 to parents Mr. Deb Kumar Roy and Mrs. Dipali Roy. He attended The Frank Anthony Public School, Calcutta from where he took the Indian School Certificate Examination (ISCE) in the year 1996. Thereafter, following his family's tradition of pursuing science related careers, he enrolled in the prestigious Presidency University (then known as Presidency College) with major in Geology from where he graduated with a BSc degree. He then moved on to obtain a master's degree in Applied Geology from the Indian Institute of Technology at Kharagpur, India where he concentrated in the study of modern sediments that finally led to his MSc thesis titled "*Ripple Mark Characteristics of Intertidal Regions*". He furthered his education and completed a thesis based MS from The University of Tennessee, Knoxville in 2006 where his research focused on improving fractal characterization of fracture networks. His MS thesis is titled "*A Quantitative Study of Scaling Properties of Fracture Networks*" part of which was published in *Journal of Geophysical Research* in 2007. With two master's degrees to his credit, Ankur started working as an oil & gas professional with Shell Technology India but his continued interest in research in geostatistics and fractures led him to come back to the University of Tennessee, Knoxville to start a PhD in the year 2009. During his stay at UTK as a PhD student Ankur has published a research paper in the *Journal of Structural Geology* in 2010 and has produced several conference abstracts. He hopes to continue his research interest in fractures and also diversify his work in other directions such as building new modeling tools that may be implemented in the study of not only fractures but other geologic features as well.